The Little Pistol's Guide to HF Propagation

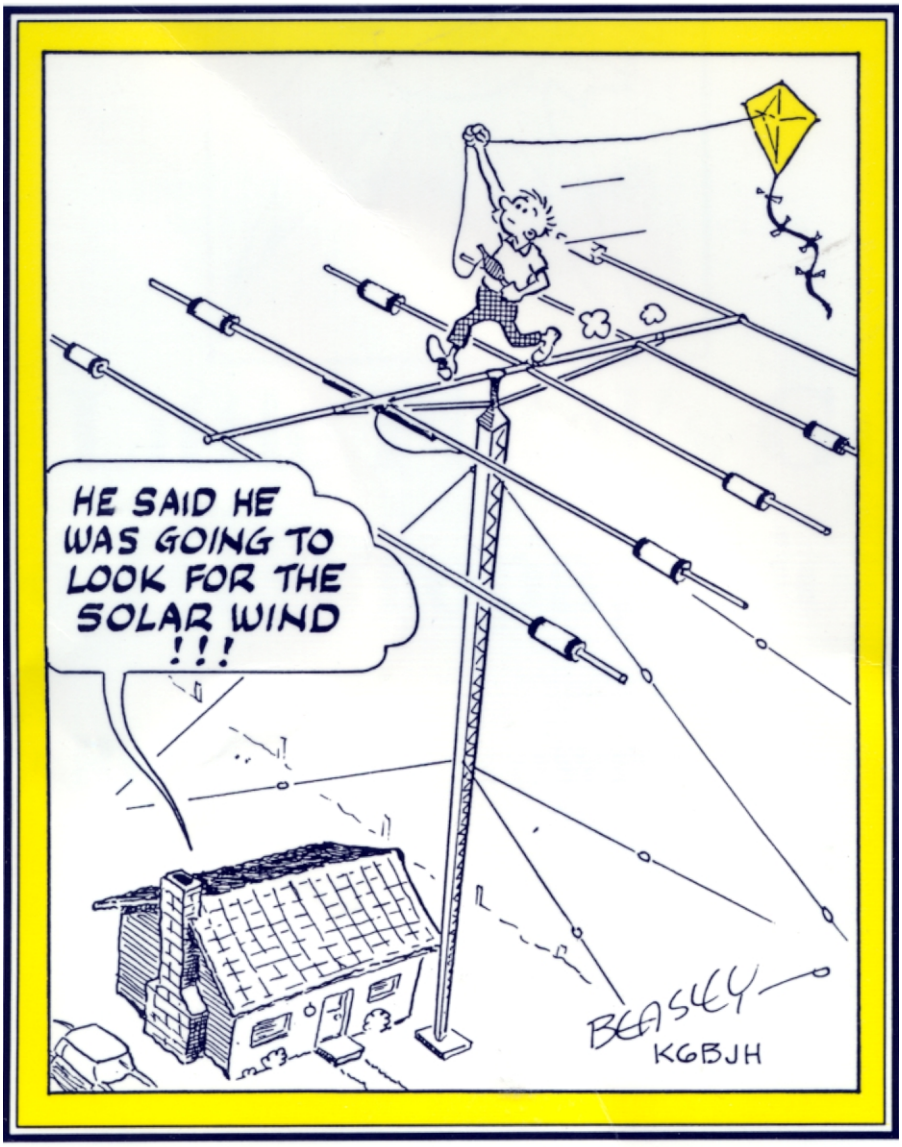

by Robert R. Brown, NM7M

$10.00

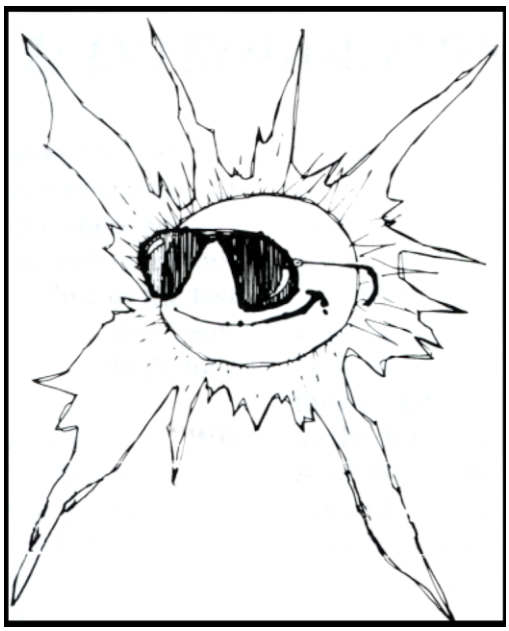

The Little Pistol's Guide to HF Propagation

by Robert R. Brown, NM7M

Published by
WORLDRADIO BOOKS
P.O. Box 189490
Sacramento, CA 95818

The Little Pistol's Guide to HF Propagation

Robert R. Brown, NM7M

Copyright March, 1996

WORLDRADIO BOOKS
P.O. Box 189490
Sacramento, CA 95818

Publisher's note

Radio signals — in the air everywhere.....sometimes.

As we drive home from work, the thought that comes to mind is, "I hope the band is open tonight."

It may turn out to be a night of great signal reports, or you might wonder if the receiver is broken.

When I was a small child, I came across some pre-WWII copies of *QST*. In the DX column were pictures of amateurs in exotic locales of the world. It seemed we could *talk* to people who lived in those lands that Lowell Thomas presented in theaters, and that the *National Geographic* wrote about.

I was hooked! I still am. The adrenaline level jumps a little when a "rare" country is on the air. With a child's imagination back then I could picture those radio waves striking the ocean on the way to Sumatra. Others hit and were reflected from a moonlit Iowa cornfield on the way to Europe.

I'm older now, and I still think of radio waves that way.

Worldradio is very pleased to present the writings of a true expert (who writes so we can understand it) regarding the when, why and how radio waves really get from one spot to another. Bob Brown, NM7M, brings to this task the knowledge of a true scholar and the ability to communicate.

— Armond Noble, N6WR, Publisher

CONTENTS

PREFACE

When it comes to DXing, it is my firm opinion that a person can contact any place on the face of the earth with just a 100-Watt rig and a tri-bander. Having said that, let me admit I haven't worked all the countries in the world myself, but I do sport a WAZ certificate on the wall of my shack and think it supports my statement. But if that's not enough to convince you, I have a friend who made the DXCC Honor Roll with just 5 Watts QRP. That was Dan Walker, WG5G; his accomplishment is a matter of public record. So, being a Little Pistol can have its rewards, but it takes operating skills and an ability to take best advantage of what the bands have to offer in the way of HF propagation.

I can't help you with the former; that comes with experience. But I think I can shed some light on the latter. In that regard, I have my own way of introducing and developing the subject. And since DXing is an intellectual pursuit, I like to think my approach has the kind of logical framework needed to guide a DXer from simple beginnings up to the present understanding of the ionosphere and HF propagation. So if you want to know and understand what's going on "upstairs" when you're in the pursuit of DX, read on.

Please don't think I'm putting you "on hold" in the early sections dealing with solar and geomagnetic data. I do that just to make sure you're aware of where to get the information you"ll need to take a measure of current conditions, anywhere from quiet to stormy. That done, you can judge when it's best to retreat from the bands and read on in what I've written or, with promising indicators and well-founded hope, push ahead and go for another "New One," leaving your reading to another day.

Now since DX is synonymous with distance, the logic of my approach in the discussion takes you along, one ionospheric hop at a time, out to about 10,000 km distance, a quarter of the way around the globe.

But those efforts, often aimed at reaching into inaccessible zones, are affected by the state of the high-latitude ionosphere, and that brings the discussion into the Space Age, with the new model of the earth's magnetic field. From there, it goes on to the solar wind, solar flares and coronal streams, holes and mass ejections, the emphasis being their role in disturbing HF propagation rather than the theory and intricacies of solar physics.

When you're finally done with what I've written, I think you'll see better how HF propagation really works and it won't seem quite so puzzling. And you'll quickly recognize the elements of order (or chaos) in what's going on at any given time. Once that's true, you're on your way to being able to deal appropriately with the circumstances, knowing better when to "go for it" or when to retreat from the bands and regroup for another day.

But more to the point, you'll be in a position to do some real sharpshooting — DXing with a specific target in mind. That's the ultimate intellectual side of DXing and when successful, you can not only point with pride at the QSL on your wall, just like a Big Gun would, but also offer a critique of the propagation conditions that were involved. With that, you can show how reason triumphs, even in DXing, and never be mocked for mindless pursuit of DX, blasting away with disregard of conditions and others on the band.

At this point, having said all the above, I'd suggest you read up through the sections on solar and geomagnetic data. When that's done, you can figure out what to do next, read on or get on the bands and chase some DX. But whatever your choice, see it through; it pays.

Guemes Island, WA
January 1995

PART ONE

1: INTRODUCTION

In writing about propagation for the Little Pistol, I'm really writing about two different subjects, the first being the ionosphere and the other DXing. So I'll have to deal with those topics, perhaps just one at a time, but in the last analysis, the emphasis will be on the ionosphere and how it relates to the Little Pistol's DXing.

Now I started in ham radio before WWII and I don't recall that term, "Little Pistol," being used back then. True, there was great interest in DXing in the late '30s, DXCC getting its start in '37. But I don't remember people strutting around, being pointed at as being a "Big Gun," or anyone feeling sheepish for being just a Little Pistol. Perhaps my own personal sphere of interaction was too small or too local. On the other hand, I did know of some operators who'd qualify now as being a Big Gun, say Reg Tibbetts, W6ITH, in the San Francisco Bay Area and the late Don Wallace, W6AM, in Southern California.

When you come right down to it, the difference between a Little Pistol and a Big Gun is one of degree, not interests. So I would have to think that the operative term in describing a Little Pistol is "modest," say one having a modest station or modest accomplishments when it comes to DXing. But modest is not the term to use in talking of the Little Pistol's ambitions; they're larger and grander than that, even to the point of wanting to become a Big Gun in the future.

Before getting to what the Little Pistol needs to know about the ionosphere to make that transition, let's look at his modest station and see what's typically involved. First, the Little Pistol usually operates on the upper bands at the "barefoot" level, running about 100 Watts RF output from a transceiver with some "bells and whistles." And the antenna system would be something like a triband Yagi with three elements, up there between 30 and 50 feet above ground. A 40-Meter antenna would be included in the setup, say a trapped vertical or a single inverted-V with its apex up around 35 feet.

By contrast, a Big Gun would have a stout linear amplifier after a flashy transceiver, with bells and whistles galore. As for power levels, they could be from 100 Watts output right up to the full legal limit, at the flip of a switch. And antennas would be monoband Yagis, stacked or otherwise, on several towers at 50 ft. or more above ground. There might be a 40-Meter Yagi included as well but certainly 80-Meter and 160-Meter dipoles, well up off the ground, for low-band DXing. So I think you can see there's nothing modest about a Big Gun's setup.

As for accomplishments, the Little Pistol has the "DX Bug" and may already have gone beyond the first step, getting the DXCC Award, and is looking to eventually have enough DX in the log to qualify for the DXCC Honor Roll. That takes "a heap of doing," as the saying goes, but every Little Pistol knows of a Big Gun up there in "Honor Roll Country" and usually has a role model close at hand. So it becomes a numbers game for the Little Pistol, the difference between the number of DXCC countries actually confirmed and the number needed currently to qualify for the Honor Roll. How that game is played out is another matter, in part related to our main topic, HF propagation. But there's another important side related to paperwork.

In that regard, no matter what job I've had, it seemed like I always had to push a broom at one time or another and I also had to keep records. So it is for the Little Pistol, keeping the shack in good order and maintaining an accurate log of stations worked, QSLs received or outstanding, and following the DX scene, perhaps from reading a DX bulletin or monitoring the DX packet cluster. To those chores, I'd

have to add another — keeping tabs on the current state of solar/geomagnetic conditions. When taken with the knowledge of the ionosphere that I'll be laying out next, those will be vital to the Little Pistol's advancement toward becoming a Big Gun.

As for what information about the ionosphere will help the Little Pistol in reaching his goals, I plan to offer a full and serious discussion of the subject for the Little Pistol to think about and study. However, I will I assume the Little Pistol has gone through the basic ideas, as presented in the ARRL Handbook, to get to his present position in the DX hierarchy. That spares me going through what I'd term "introductory material." Since DXing is truly an intellectual pursuit, my task is to build on that kind of fundamental discussion and bring out additional, finer points that will help in DXing.

2: ELEMENTARY CONSIDERATIONS

The Little Pistol knows that RF is really electromagnetic waves, time-varying electric and magnetic fields which can propagate through a vacuum with the speed of light. But in the LP's efforts at DXing, those waves are actually propagated through a material medium, the weakly ionized portion of the upper atmosphere, termed the ionosphere. Indeed, with good fortune, the LP's signals go up into the ionosphere and then returned to earth at a great distance from where they started.

In some circles that's called ionospheric reflection but a better term is refraction, or bending of the ray path followed by the waves. All that results from the waves going through a medium which consists of free electrons and whose number density, so many electrons per cubic meter, increases with increasing altitude. And the Little Pistol knows there are several regions that make up the ionosphere, the F-region being the highest and peaking in number density around 300-400 km, then the E-region around 110 km and finally the D-region below 90 km.

The present knowledge of a complex ionospheric structure is in contrast to the idea of one region of ionization developed by Chapman in the early '30s. Then, as shown in Figure 2.1, it was assumed that ultraviolet (UV) quanta from the solar spectrum would encounter an increasing number of ionizable atoms and molecules on penetrating the atmosphere and would produce ionization at an increasing rate.

But solar quanta would suffer absorption in the process and the radiation intensity would decrease closer to the earth's surface. As a result, a peak in the production rate of ionization would be reached and then decline at lower altitudes.

Actually, UV photons in the solar spectrum have enough energy to not only ionize molecules of nitrogen and oxygen, as mentioned above, but also to dissociate them into

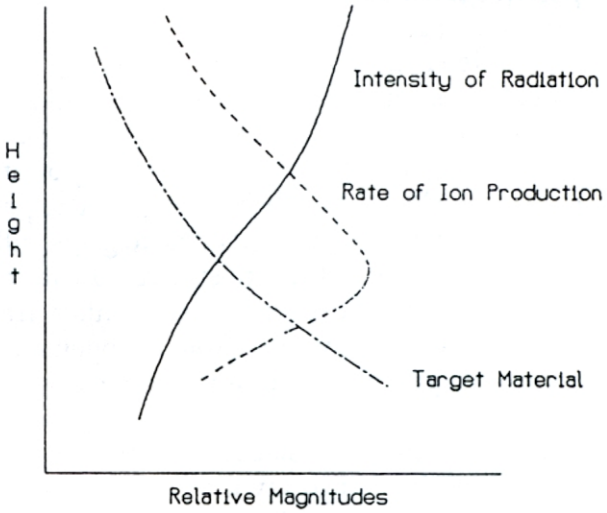

Figure 2.1 A schematic representation of the production of ionization in the atmosphere.

their constituent atoms. That last statement wouldn't involve too much of a stretch of the Little Pistol's imagination but to get into the various chemical reactions which might take place is another matter. Needless to say, "Whatever can happen will happen" in the part of the upper atmosphere reached by solar UV and the LP shouldn't be surprised at the result, an atmosphere whose chemical composition varies with altitude.

More specifically, from ground to the 100-km level, the atmosphere is well mixed by convection and turbulence and has a rather homogeneous composition of the major constituents, nitrogen (78%) and oxygen (21%), but with some trace constituents (such as water vapor, carbon dioxide and ozone) which are not homogeneously distributed. But above the 100-km level, atomic oxygen, resulting from dissociation of molecular oxygen by the solar UV, assumes greater relative importance with increasing altitude.

All this discussion of the neutral atmosphere may seem strange to the Little Pistol. "After all, radio propagation involves charged

particles — electrons — right?" I won't say "Wrong!" But how about "Not exactly?" It turns out that ionospheric electrons find themselves in the middle of a great big chemistry laboratory up there with all the electrons, positive ions, atoms and molecules mixing it up, as it were.

Indeed, under the right (or wrong) circumstances, some of the atoms, molecules or ions can affect the electron density adversely, to the detriment of propagation so important to the Little Pistol. So it behooves the LP to pay attention to those ideas and come to grips with the current view of the ionosphere; to wit, the higher reaches of the ionosphere contain free electrons and positive ions from nitrogen molecules, oxygen molecules and atomic oxygen and as well as minor, but important, positive ions formed by ion-molecule interactions.

I think it's fair to say the Little Pistol understands that the density number of electrons in the ionosphere varies with altitude but the LP probably doesn't know that the height variation of the electrons depends on a competition between rates of their production and loss. But the LP could understand that the rates for those processes vary with altitude, with solar illumination (for production) and changes in chemical composition (for loss).

Now the Little Pistol understands the matter in our atmosphere and ionosphere are parts of our environment, held to the earth by its gravitational field. And the LP's DXing probes the ionosphere, showing changes in the degree of ionization from time to time. But the changes in the neutral atmosphere escape the LP's attention as it's not directly responsive to HF radio signals. Again, imagination takes over and the LP knows that both parts of the environment vary as a result of changes in solar illumination.

But what the LP probably doesn't understand is that the ionosphere is also controlled, even influenced, by the earth's magnetic field and its variations. In the static circumstance, geomagnetic control of the ionosphere may be a new one for the LP, at least when discussed in any detail. The LP is far more likely to have heard of, even experienced, the effects of ionospheric storms which go along simultaneously with geomagnetic storms and affect HF propagation. Those circumstances are not beneficial to LP's DXing and their explanation will turn out to be rather complicated. So the LP had best pay attention to those discussions as becoming a Big Gun may depend heavily on dealing with those occasions.

I want to conclude this section on elementary considerations by having the reader note that so far, everything has all been qualitative in nature. Of course, some quantitative aspects have been implied — the LP's operating frequencies, changing seasons and times of day, transmitter powers and antenna gains. Those are all characteristic of operations at the Little Pistols's QTH.

Now what needs to be added to the discussion are the quantitative aspects, particularly those which go with DX paths across the earth's surface, their location relative to the geomagnetic field and the effects of solar illumination, rapid on a daily basis and slow over a solar cycle. That additional discussion will turn knowledge of the ionosphere into a quantitative decision-making tool and, I believe, serve the Little Pistol well so let's get to it, starting with the sun.

3. THE SUN AND ITS RADIATION

The solar radiation that we're all familiar with is in the visible portion of the spectrum, with wavelengths from 400-700 nanometers (1 nm = 1E-9 Meter), in going from violet to red. Using more classical units, the visible spectrum lies between 4,000 and 7,000 Angstroms (1 A = 1E-8 cm). The fact that the frequency of radiation is the speed of light (300,000,000 meters/sec) divided by the wavelength allows one to find the frequency for visible radiation, around 1E+14 Hz or almost a billion times greater than typical HF Amateur Radio frequencies (3-30 MHz).

While the visible spectrum goes through the "atmospheric window," the radiation responsible for creating the ionosphere does not, being absorbed at high altitudes as it ionizes and dissociates atoms and molecules in the upper atmosphere. For our purposes, dealing with HF radio propagation, the amazing thing is that only a tiny fraction, about .001%, of the solar radiation incident on the earth's atmosphere is the source of energy for ionospheric processes. Ponder that for a moment or two! One-thousandth of one percent — simply amazing!

That energetic part of the spectrum lies below the visible spectrum, in the extreme ultraviolet (EUV) and X-ray range. And for the radiation to ionize or dissociate constituents in the atmosphere, its energy must be equal to or greater than the ionization potential or binding energy of the atoms or molecules. But those are atomic and molecular processes and so we have to digress a moment to give the energy unit that's appropriate to use, the electron-Volt or eV, instead of the Joule, the unit for mechanical energy in the M.K.S. system.

Now an electron volt is the energy that an electron gains in going through a potential difference of 1 Volt, that is to say it's equal to the electron's charge Q (1.6E-19 Coulomb) multiplied by the potential difference V, 1 Volt or 1 Joule/Coulomb, so 1 eV equals 1.6E-19 Joule. Going to the energy associated with photons in the solar spectrum, we use the Planck's Law, the energy of a photon being given by Planck's Constant h (6.6E-34 Joule-sec) multiplied by its frequency f in cycles per second (or Hz). And rewriting that expression to use eV for units of energy, Planck's Law would give the energy of a photon in eV as the product of 4.1E-15 and the frequency in Hz or 1240 divided by the wavelength in nanometers.

Now a quick look at one's high school chemistry text shows that the ionization potential for hydrogen, the simplest atom of all, is 13.6 eV. As you might expect, the ionization potential of atomic oxygen, found in the upper atmosphere, is about the same and that for atomic nitrogen is about 1 eV higher. For the important diatomic molecules in the upper atmosphere, those of oxygen, nitrogen and nitric oxide (NO), their ionization potentials are 12.5 eV, 15.5 eV and 9.5 eV, respectively. On that basis, the part of the solar spectrum that's effective in creating the ionosphere is wavelengths of about 100 nm (1000 A) or shorter. And the same energy range would apply to the photodissociation of oxygen and nitrogen molecules into their constituent atoms.

At this point, the discussion has become quantitative, dealing with the parts of the solar spectrum which ionize and dissociate atoms and molecules in the upper atmosphere. But it should be noted that the "quiet sun" not only emits EUV photons in the 100 nm range, as was discussed above, but also X-rays at shorter wavelengths, say 10 nm or even 1 nm. So, they, too, contribute to ionizing the upper atmosphere but to degrees in accordance with their relative strength in the solar spectrum and the abundance of targets in the upper atmosphere.

All those remarks apply to what is termed the "quiet sun" but as the Little Pistol well knows, there are times when the sun is rather disturbed, sending out bursts of radiation

across the spectrum, say radio noise, light, and X-rays. Obviously, the energetic photons in such outbursts may change the amount of ionization in the ionosphere, affecting the LP's DXing. So the question comes up, "Does the Little Pistol himself have any way of knowing about variations of the flux of photons, energetic or otherwise, from the sun?"

The answer to that question is a qualified "Maybe!" and depends on the part of the spectrum under discussion. So if the Little Pistol is operating at the top of the HF spectrum, say on the 10 Meter band, solar noise bursts might be heard, sort of a "whooshing" sound, and if strong enough, "solar QRN" could even interfere with the LP's pursuit of DX. Another possibility is when the LP is in a contact where the path goes across the sunlit part of the earth; then, increases in the EUV and X-ray flux that go with solar flares could make signals fade, maybe even to the extent of being the victims of a blackout. As for increases in visible light, as an indication of a disturbed state for the sun, that is extremely unlikely. The light output of the sun is remarkably constant and only a few solar flares have been seen in white light; much more sophisticated optical devices are needed to observe changes in the visible portion of the solar spectrum.

The above response to the question of variations in the flux of solar photons assumes that the Little Pistol is the only observer. Of course, that's not the case as there's a whole industry, as it were, just watching and listening to the sun. And the information that's collected is disseminated promptly and widely so if the LP misses some activity on the sun, it'll be available as part of the solar data for the day. So if the LP wants to know about any changes in the solar radiation which might affect DXing, it's just a matter of getting hold of the solar record and looking at it. And that's the record keeping that I alluded to earlier; in the LP's case, it'll be part of the discipline that goes with DXing, keeping tab of solar/terrestrial conditions.

Before getting to those matters, we have to start the discussion of propagation and then bring forth some its finer points for the Little Pistol. When that is done, we can get to how it is affected by changes in the various physical parameters that go to make up an appraisal of solar/terrestrial conditions.

4: ELEMENTS OF PROPAGATION

There's no need to tell the Little Pistol what goes to make up HF propagation as LP has been practicing that already. Thus, LP knows signals are brought back to earth, hop after hop, by ionospheric refraction. More to the point, as far as the LP's DXing goes, is to show more about how ionospheric hops take place and the factors which influence them. Some of the factors are right here at ground level — signal loss and polarization changes with ground reflections — while others are at higher altitudes, up in the regions that go to make up the ionosphere.

Now the Little Pistol's RF leaves ground level as expanding waves, the vertical distribution of signal intensity depending on the type of antenna the LP is using and the ground surface nearby. The usual representation of antenna patterns, both vertically and horizontally, gives the signal strength in various directions, along ray paths which are perpendicular to the advancing wave fronts. At this point antennas and their patterns are not our concern; rather, it's the ray paths of RF through the ionosphere and how they're affected in going through or approaching regions of the ionosphere.

To begin that discussion, the Little Pistol needs to understand that ionospheric refraction depends on the reradiation of RF by the electrons that go to make up the ionosphere. In the simplest terms, radiation by the LP's antenna results from oscillatory or accelerated motions of electrons in his antenna. As the RF waves expand outward and encounter free electrons in the ionosphere, they're set in motion at the same frequency by the electric field E associated with the wave. Like the electrons in the LP's antenna, the free electrons radiate RF because of their oscillatory motions. In short, ionospheric electrons reradiate RF passing by, resulting in an advancing wave front whose direction depends on the spatial distribution of the electrons.

Now if the density of free electrons in the ionosphere did not vary with height, there'd be no refraction, i.e., no bending or change of the ray directions that describe the advance of the RF wave front. There's an optical counterpart to that; light advancing in a straight line in going through a transparent substance with a constant index of refraction. In the ionospheric case, the electron density increases with altitude and unless the frequency of signals is too high, the RF is continuously (but not constantly) refracted back toward earth.

It should be noted that statement applies whether the ray path is ascending or descending through the ionosphere and results from the fact that the electron density increases with altitude above the earth. A crude way of saying the same thing is that RF is always being bent away from regions of higher electron density. The optical counterpart, involving a medium of atoms and molecules with bound electrons, is just the opposite, light always being bent toward regions of higher index of refraction.

Returning to the ionosphere, Little Pistol has enough experience to know that hops are not always the same, say day and night or at different times of the year, or even in the course of a solar cycle. But that's all anecdotal information and what the LP needs is something more quantitative to go on, what factors affect the numbers that are associated with the ionosphere.

The place to start, of course, is with the vertical profile of the electron density, so many electrons per cubic meter, as a function of height above ground. Two such profiles are shown in Figure 4.1, one for daytime conditions at the maximum of a solar cycle and the other at the minimum. Of importance to the Little Pistol are the heights of the various regions — from below 100 km to above 300 km for the D-, E-, F1- and F2-regions, respectively — and the magnitudes of various electron densities,

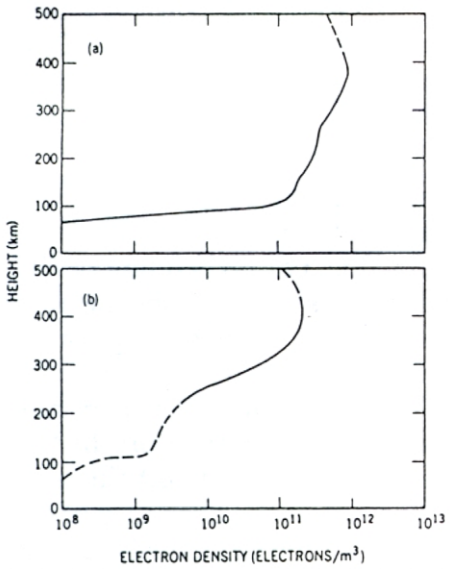

Figure 4.1 Sample electron density profiles: (a) daytime and (b) nighttime. From Davies [1990]

from a thousand electrons per cubic centimeter down in the D-region to a few million electrons per cubic centimeter at the F-region peak.

Those profiles apply during daytime conditions at mid-latitudes. At night, the F1- and F2-regions coalesce, the E-region density falls and the D-region disappears. Different profiles are found in the polar and equatorial regions but they need not concern the Little Pistol at this point. And looking at those profiles, it might be added that LP's experience is primarily with the hops below the F-region peak. That's because the LP has been prudent, using operating frequencies which did not penetrate the F-peak and, as a result, the hop lengths of the LP's RF were determined by the radiation angle of the RF and the height of the highest ionospheric region called into play.

But one cannot control all the RF radiated by antennas so some high-angle rays from LP's antenna might penetrate the F-region peak and venture into the topside of the ionosphere. That brings up the idea of critical frequencies, the highest frequencies which are returned by the ionosphere when probed by RF at vertical incidence. That technique, ionospheric sounding, was used in the late 1920s to explore the main features of the ionosphere, the various regions and their critical frequencies, say foE, foF1 and foF2.

In that regard, theoretical considerations show that if RF is sent vertically upward toward a region with a number density of N electrons per cubic meter, the highest frequency fc (in MHz) that is returned from that level as an echo is given by the following equation

fc = (9•E-6)• SQRT(N)

With that as a guide, ionospheric sounders probed the electron density overhead by directing RF pulses vertically upward and simultaneously sweeping the sounder frequency from about 0.5-20 MHz. The time of flight of echoes was displayed on the Y-axis of an oscilloscope and the instantaneous frequency on the X-axis. When a critical frequency is exceeded, say for the E-region, the RF pulses pass through it toward the next region, and is shown by a sudden increase in the time for an echo to return as the RF pulses go on to higher altitudes.

As the technique was developed, the various regions of the ionosphere were established, along with representative values of critical frequencies and altitudes. For example, the E-region is present during daylight hours and the critical frequency foFE ranges from 0.5 MHz to 4.5 MHz, depending on local time and latitude. And the F1-region is also present during daylight and its critical frequency foF1 ranges similarly from about 0.5 MHz to 6 MHz. The F2- region is more important for LP's DXing but its critical frequencies are quite variable and do not show any simple relation to the degree of solar illumination.

To go on, as the sounding technique was perfected, geographic mapping of the critical frequencies was begun and expanded after WWII to show on a global scale how illumination affects the ionosphere, with the time of day and the seasons. In addition, vertical soundings were carried out during different phases of solar cycles and that dimension was added to the database of ionospheric characteristics.

To illustrate those points, consider Figures 4.2 and 4.3 which show global maps of the F2-region, with contours of the critical frequency foF2 in MHz, at two levels of solar activity. Figure 4.2 shows the foF2 map for 0600 UTC at

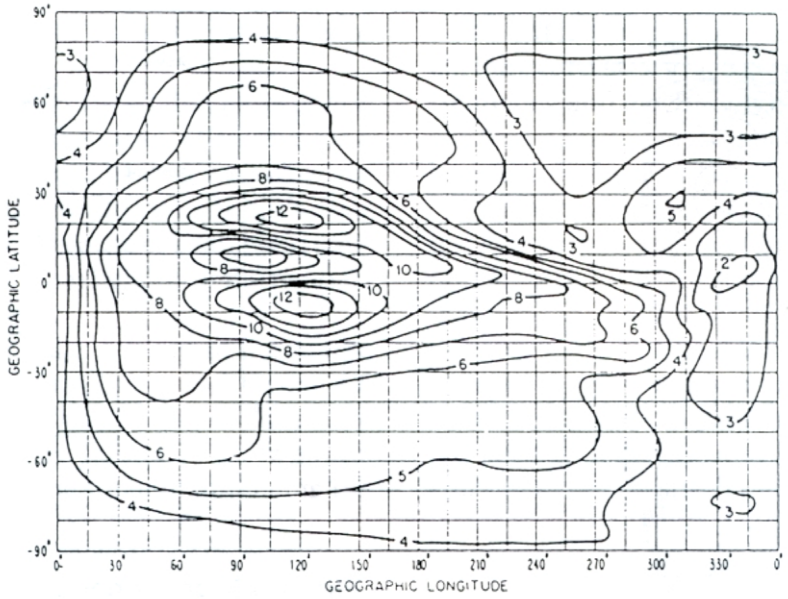

Figure 4.2 Global foF2 map for 0600 UTC, March 1976. (SSN=12) From Davies and Rush [1985]

the spring equinox of 1976 when the sunspot number was 12 and Figure 4.3 gives a similar map for 1979 when the sunspot number was 137. For that time of day, the subsolar point is on the geographic equator at 90° East longitude and the illuminated portion of the earth is between 0 and 180° E while that in darkness is between 180° E and 360° E.

It is of importance to note the foF2 map lacks symmetry about the geographic equator even though solar illumination is symmetrical at the equinox. In addition, it is of interest to see that F2-region critical frequencies do not drop to vanishingly small values in the dark regions beyond the sunset terminator, lying at 180° East longitude. Both the lack of symmetry of the foF2 map across the equator and the presence of ionization in the dark ionosphere result from geomagnetic control of the ionosphere and will be discussed in a later section.

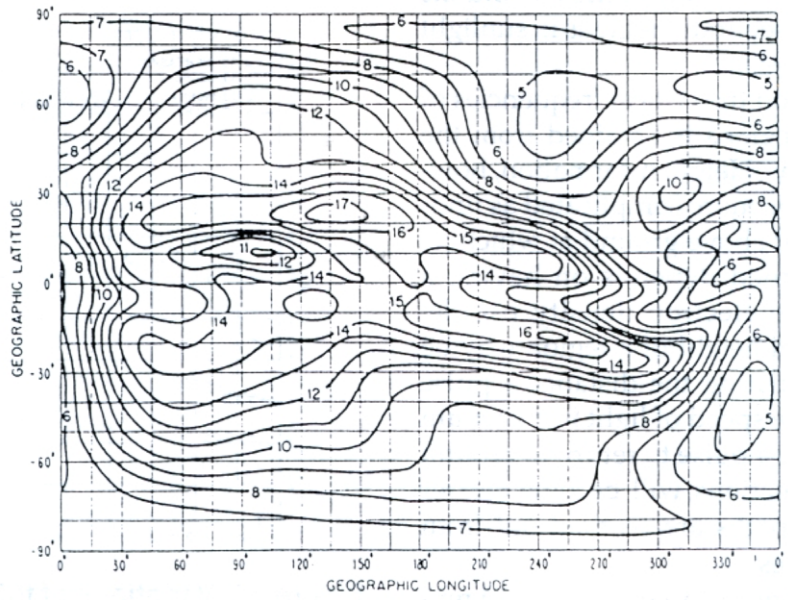

Figure 4.3 Global foF2 map for 0600 UTC, March 1979. (SSN=137) From Davies and Rush [1985]

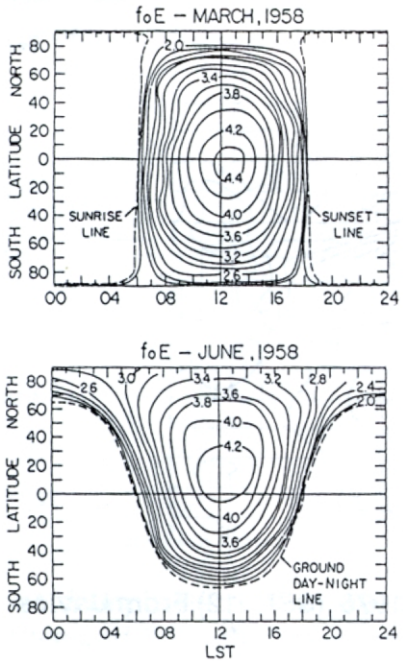

Figure 4.4 Map of foFE, March and June 1958. From Davies [1965]

As noted above, the E-region is present during daylight hours and examples of the latitude and local time variations of its critical frequency foFE are shown in Figure 4.4, the upper portion of the figure for the equinox and the lower portion for the summer solstice when the subsolar point is at 23.5° N latitude. It is seen that foFE goes to small values beyond the terminator which separates regions in sunlight and those in darkness.

Information on the critical frequencies of the ionospheric regions is obtained from the study of ionograms. Height information, however, turns out to be more complicated as finding the true height above ground at which an RF pulse is returned depends on having a knowledge of the electron density profile. However, a virtual height of a region may be obtained by calculating the distance a pulse would travel at the speed of light in a vacuum in half the time for a pulse to return to ground level. These distinctions will become clearer when actual ray paths are worked out from ionospheric profiles.

And that brings us to a more detailed representation of the main structure of the ionosphere, from the ground to just below the peak

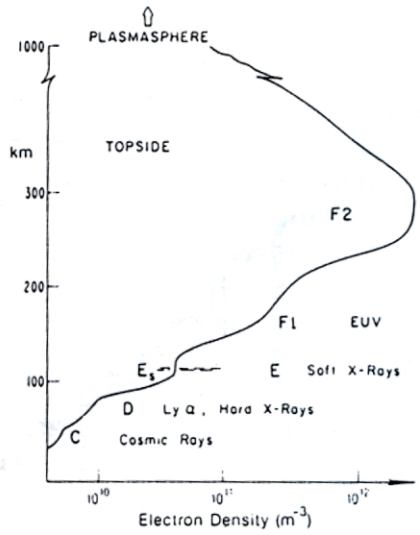

Figure 4.5 Ionospheric structure for daytime conditions at mid-latitude. From Davies [1990]

of the F2-region, in Figure 4.5. Ionospheric profiles like that involve a combination of electron densities derived from critical frequency data and heights of the peaks and ledges from studies of iono-grams. Of particular importance is that the data are brought together in a smooth fashion using mathematical models. The lack of discontinuities or sudden changes in electron density makes it possible to follow ray paths through the ionosphere without having

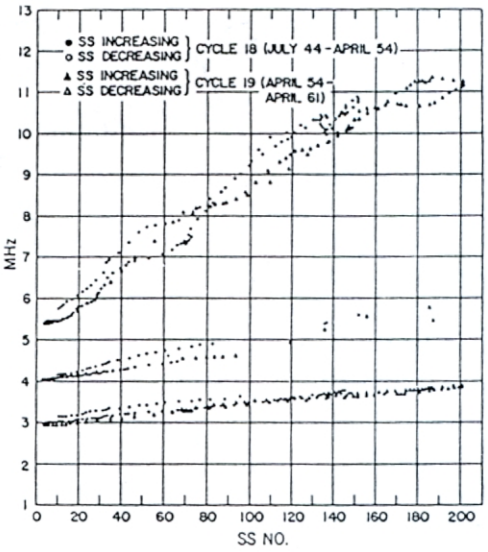

Figure 4.6 Variations of foFE, foF1 and foF2 with sunspot number for midday conditions at middle latitudes. From Davies [1965]

any abnormal kinks or sudden deviations in ray directions.

Earlier it was mentioned that ionospheric hops are not always the same, changing for a number of reasons. Now, having seen close up what an ionospheric profile looks like, it's clear that hops may differ because of changes in critical frequencies and even heights of the regions, say the F-region peak.

Changes with solar activity, in the course of a solar cycle, are one cause and Figure 4.6 shows how foFE, foF1 and foF2 at midday vary with sunspot number. Taking 11 MHz as the value for foF2 when the sunspot number is 180 and 6 MHz for foF2 for a sunspot number of 20, the expression given earlier relating critical frequency and electron density shows that the electron densities between the extremes differs by a factor of about 3.4.

When we get to tracing ray paths through the ionosphere, it will become apparent how hop lengths differ for those two extremes. But that is in the abstract and the Little Pistol needs to know more practical things, say what is the sunspot number and just where that value fits in the solar cycle in progress. So at this point we need to look into the means that LP can employ to obtain solar data.

5: SOLAR DATA

Here in the USA the principal source of solar data, as it relates to HF propagation, is through NOAA in Boulder, CO. It comes in three different forms: (1) WWV broadcasts at 18 minutes after each hour, (2) mailed weekly as "The Preliminary Report and Forecast of Solar Geophysical Data" or (3) by telephone at any time, just by calling the NOAA/SESC PBBS at (303) 497-5000 and downloading the Solar Report file. But before we look at those sources, let's look at the information itself.

The solar data that will interest the Little Pistol in the first instance is that which is given daily through one of those means. Confining ourselves to the electromagnetic spectrum, NOAA provides daily information on the solar radio noise flux at 10.7 cm, the count of sunspots visible on the solar disk facing the earth and the average background X-ray flux in the 1-8 Angstrom range, as recorded by the GOES-7 satellite at synchronous altitude.

The 10.7-cm solar noise flux is broadcast hourly by WWV on 2.5, 5, 10, 15 and 20 MHz and is given as a number which expresses intensity in solar radio flux units (1 s.f.u. = 1E-22 Watts per square meter per Hz bandwidth). Typical values of the 10.7-cm flux are anywhere from 65- 350, depending on the level of solar activity.

At this point a word of warning is called for. Solar photons with a wavelength of 10.7 cm have an energy of only 1.1E-5 eV, falling below the energy required to ionize any atmospheric atom or molecule by a factor of one million (!). Thus, 10.7-cm radiation contributes nothing to ionizing the upper atmosphere. Knowledge of its current value comes from the fact the atmosphere is transparent to 10.7-cm radiation. With the radiation passing freely through the atmospheric window, any changes in its value in s.f.u. shows the growth or decay of active regions on the sun or their passage across the solar disk facing the earth, no matter what the terrestrial weather conditions.

That word of warning was given, as uninformed operators often think inappropriately about increases in the daily value of the 10.7-cm solar flux, taking them to represent significant changes in the solar ionizing flux and thus improvements in propagation conditions. That is just not the case as the relationship between solar EUV radiation and the nonionizing 10.7-cm flux is a statistical one, and a very loose connection at that.

In addition to the 10.7-cm noise flux, the count of sunspots, seen as dark regions on the solar disk, also serve as an indicator of solar activity. In that regard, the occurrence of a number of terrestrial phenomena have been found to be correlated with sunspot numbers: magnetic storms, visual aurora, and long-distance radio communication, to mention those of direct interest to the Little Pistol. All of those are what might be termed "gross phenomena" and when more detailed observations are made, other correlations are found. We'll get to them in due time. Since both the 10.7-cm solar noise flux and sunspot number provide measures of solar activity, they may be plotted as daily values, giving a graphical representation of changes in solar activity and a means of anticipating future activity. By way of illustration, Figure 5.1 shows daily values of the 10.7-cm solar flux and the sunspot count during a period of recurrent activity in mid-1990. Examination of that figure shows the sunspot number has more irregular variability than does the 10.7-cm solar flux.

Another way of representing long-term changes in solar activity is to plot monthly averages of the two quantities. The monthly averaging process serves to smooth the data, at least compared to a plot of daily values; even smoother representation involves a 13-month averaging process. By way of illustration, the 13-month smoothed average value of the sunspot number (140) for July 1990 is obtained by adding the monthly average sunspot numbers

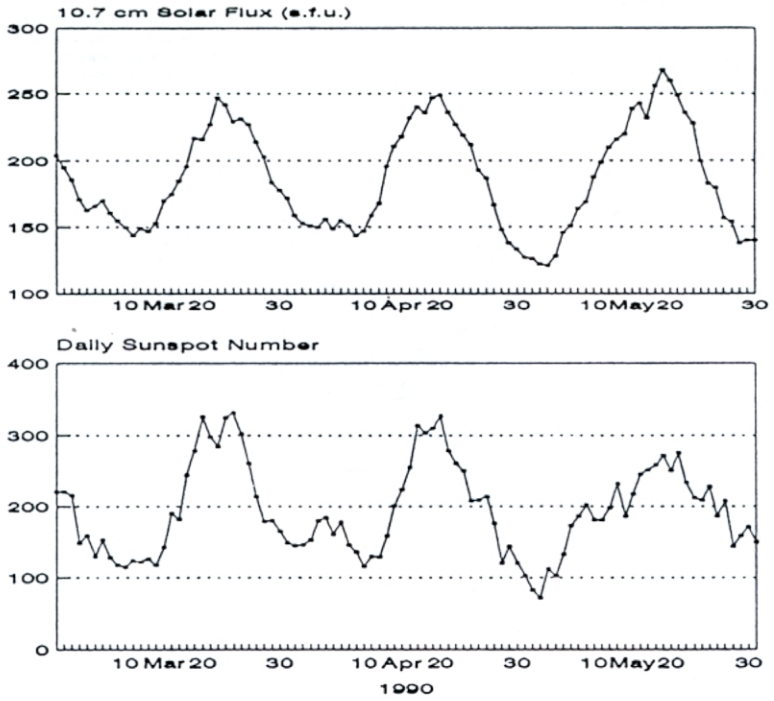

Figure 5.1 Variations of the 10.7-cm solar flux and daily sunspot count in 1990, showing 27-day recurrences. Data from NOAA/SESC.

from February 1990 to December 1990 and one-half the average sunspot numbers for January 1990 and January 1991. That sum is for the 11 months centered on July 1990 and one-half of the first and last months of a 13-month period. Finally, the smoothed sunspot number for July 1990 is obtained by dividing the full sum by 12, for the effective number of months used in the smoothing process.

The smoothing obtained by using the 13-month running averages is seen in Figure 5.2, comparing the smoothed sunspot numbers (SSN) with monthly averages for the period starting in 1900. Needless to say, that type of smoothing is not limited to just sunspot data, also being used now in connection with solar flux values. However, in contrast to sunspot data which goes back to the middle of the 18th Century, 10.7-cm radio observations are limited to the period following WWII.

In that connection, the Little Pistol knows about solar cycles, the sunspot number changing in a cyclical manner with about 11 years periodicity. Back in February 1990, the weekly Boulder Report summarized the features of Solar Cycles 1-22, dating from March 1755 to the present. Of the 21 cycles already completed, the average value of the smoothed sunspot number was 111.7, the average length of the cycles was 11.0 years (132.3 months), the average time to the maximum was 4.29 years (51.5 months) and from the maximum to the end of the cycles 6.73 years (80.8 months), respectively.

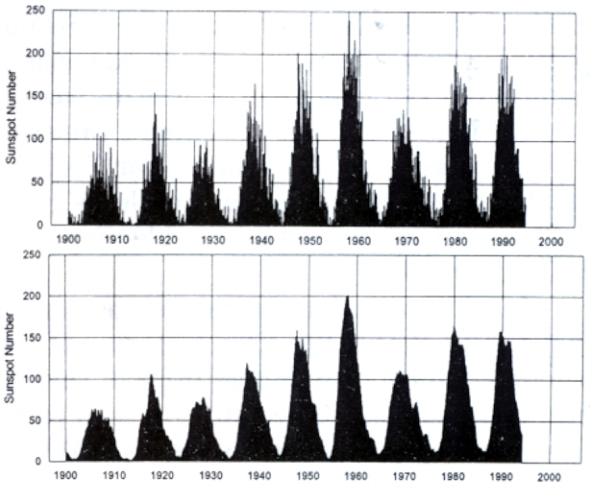

Figure 5.2 A comparison of monthly averages and smoothed sunspot numbers starting in 1900. From NOAA/SESC Report 25 October 1994.

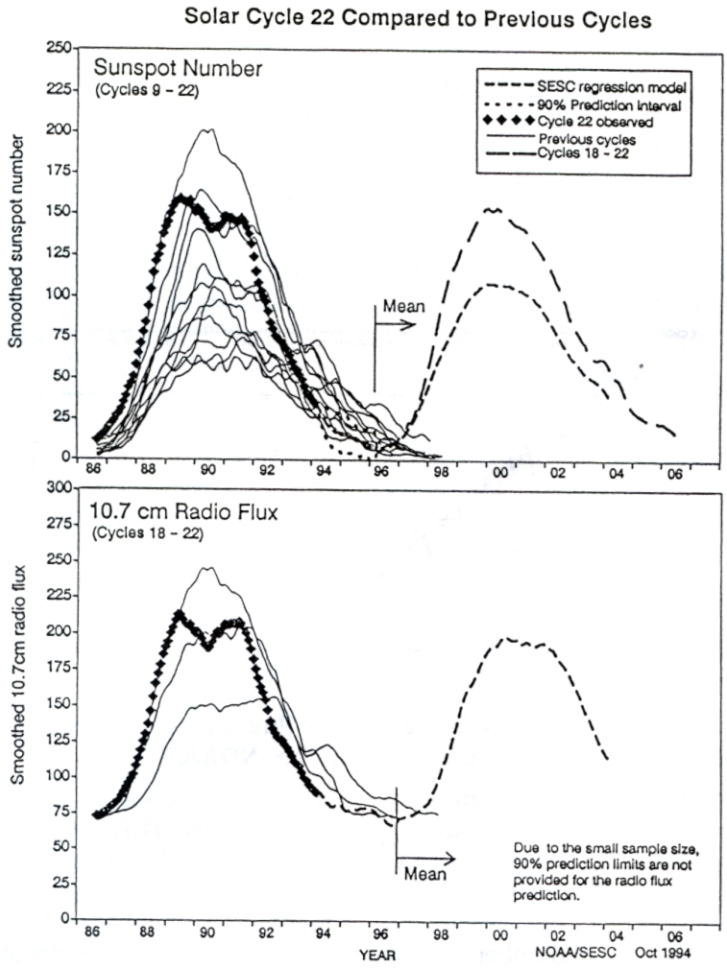

Figure 5.3 A comparison of smoothed sunspot numbers and 10.7-cm solar flux for Cycle 22 with previous cycles.

At the moment, we're nearing the end of Cycle 22 which started in September 1986 and peaked in July 1989 with a smoothed sunspot number of 158.5. Every month or so the weekly Boulder Report updates the current values of the smoothed data. A summary for Cycle 22 and the features of recent solar cycles is given in Figure 5.3, taken from the Boulder Report of 11 October 1994.

In addition to data from the current cycle, that figure shows the time histories of the smoothed sunspot numbers (top) in several past cycles and smoothed 10.7-cm solar radio flux (bottom) for the few cycles since WWII. Beyond data from the past cycles, those figures also show predictions for the coming solar cycle.

The last type of solar data that's available from NOAA is the background X-ray flux in the 1-8 Angstrom band. It's given on a daily basis in the solar data file on the NOAA PBBS and expressed on a logarithmic scale in Watts per square meter, a number being used for the multiplier and a letter (A, B, C, M and X) for the power of 10, starting at 1E-8 for the letter A. Daily values for the background X-ray flux are also included in the Solar Data Summary in the weekly Boulder Report, along with daily values for the 10.7-cm flux, sunspot number, and sunspot area. Also included in the weekly Boulder Report is a figure which shows five-minute averages of the X-ray flux, the example in Figure 5.4 showing how the X-ray flux varies on that time scale and as well as an X-ray burst.

X-ray data, whether from background or a flare outburst, gives a better indication of the geophysical importance of solar conditions

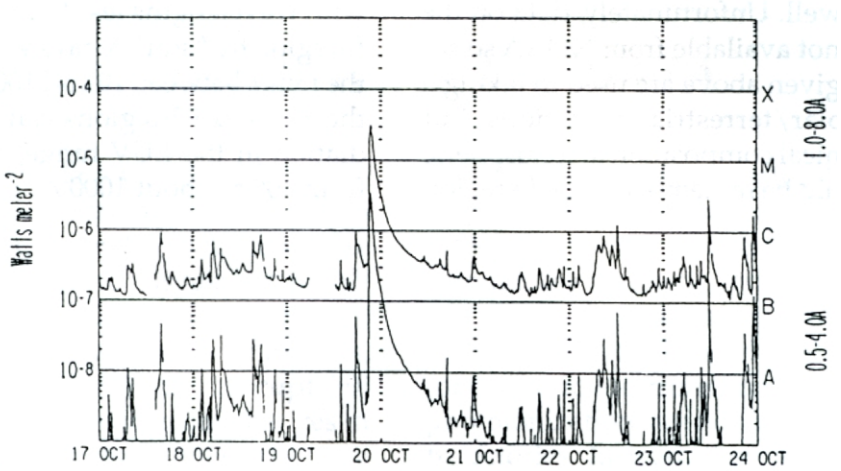

Figure 5.4 Five-minute averages of the X-ray flux from the GOES satellite. Units are Watts per square meter. Data from NOAA/SESC Report 11 October 1994.

than observations taken in the visible range of the solar spectrum. And it gives a measure of ionizing radiation coming from the solar disk. Unfortunately, the X-ray data in the Boulder Report is not accompanied by measures of solar radiation in the EUV range. However, the energy of X-ray photons in the 1-8 Angstrom band exceeds the energy needed to ionize atmospheric constituents by about a factor of 100 instead of falling short by a factor of 1,000,000 as is the case in the 10.7-cm range.

As a result, one can take the X-ray flux as a better measure of the rate of ionization in the ionosphere from solar activity. And it is of interest to compare the range of the X-ray flux in a solar cycle with the ranges for the other indicators of solar activity, the 10.7-cm flux and smoothed sunspot numbers. In that regard, the 1-8 Angstrom X-ray flux varied by about a factor of 100 in going from solar minimum to the maximum of Cycle 22, the background flux rising from the A category to the C category. Over that span of time, the smoothed 10.7- cm flux rose by a factor of three, from about 70 to about 200 s.f.u., and sunspot numbers rose by a factor of 15, going from about 10 to 150.

The variations of the X-ray flux during the period used in Figure 5.1 are now shown in Figure 5.5. As expected, they go along with the changes in 10.7-cm flux and sunspot count although they show a larger dynamic range.

All three variables characterize solar activity on the side of the sun facing the earth. However, it should be noted that sunspots are at the solar surface (photosphere) while X-rays and the 10.7-cm photons are created in the solar atmosphere. Indeed, X-ray bursts can originate, even be detected, from high above active regions which are behind the solar limb and the same is true of radio emissions associated with bursts of solar activity.

The solar spectrum includes not only the

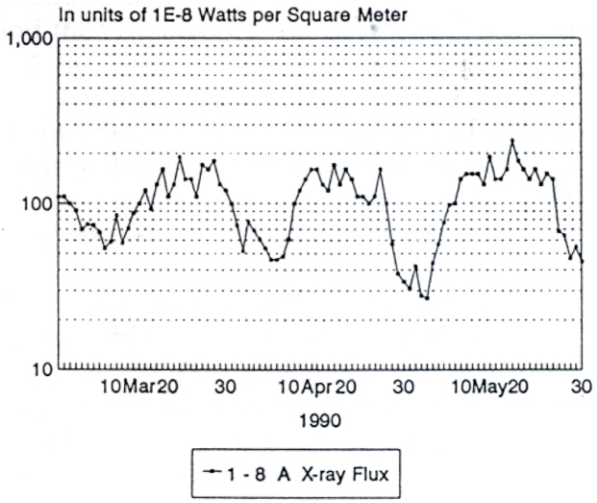

Figure 5.5 Variations in the 1-8 Angstrom X-ray flux from the GOES satellite. Units are in Watts per square meter. Data from NOAA/SESC Reports.

portions mentioned in the reports from NOAA but others as well. Unfortunately, data on the EUV range is not available from NOAA so solar indicators given above are used in taking a measure of solar/terrestrial conditions. But given the chemical composition at ionospheric heights, it should be remembered the D-region is produced by what is termed "hard" X-rays with wavelengths less than 10 Angstroms, the E-region by "soft" X-rays with wavelengths in the range between 10 and 100 Angstroms while the F1- and F2-regions can be ionized by radiation in the EUV range, with wavelengths from 100 to about 1000 Angstroms.

6: GEOMAGNETIC DATA

In turning from data for the 10.7-cm visible or X-ray parts of the radiation coming from the sun to data for magnetic conditions here on earth, the shift in the discussion of HF propagation is from slowly varying changes of the ionosphere, over days, weeks or months, to more rapid ones which can disrupt HF propagation and result from major changes in solar activity. Of course, that's not to say there can't be any rapid changes in solar radiation which result in disturbances of the ionosphere for an hour or so, say from outbursts of solar X-rays. Dellinger discovered events of that nature in 1937, shortwave fade-outs (SWF) or sudden ionospheric disturbances (SID) associated with flare outbursts on the sun.

But that was back in what might be termed the "photochemical era" when both the steady and disturbed states of the ionosphere were thought to result largely from "action at a distance," solar photons going across the vast empty space between the sun and earth until encountering the earth's atmosphere. With the coming of the Space Age, spacecraft observations showed that empty space or void actually contains a weak and disordered magnetic field from the sun, the interplanetary field, as well as streams of solar particles, electrons and protons, spewed out by the sun. This is called the "solar wind" — sometimes in a fairly steady flow, other times in gusts and even as shock waves.

Ionospheric disturbances associated with geomagnetic activity result from changes, namely increases in speed, in the solar wind (or solar plasma) which propagate through the interplanetary medium until encountering the outer reaches of the geomagnetic field. The fact that geomagnetic variations induced by that sort of encounter will disturb or distort the ionosphere results from ionospheric electrons being under geomagnetic control. That was pointed out earlier from the fact that foF2 maps for equinoctal periods are not symmetrical about the geographic equator. As a result, geomagnetic disturbances from such interactions affect the spatial distribution of ionization through the magnetic control.

While that may have come as a surprise to the Little Pistol, it merely reflects the fact that ionospheric electrons, on being released by photoionization, are not free to follow ballistic trajectories. Instead, they move in their local environment and experience a magnetic force which influences their motions. As for details, the magnetic force depends directly on the electron's velocity and the geomagnetic field strength it finds itself in.

If the electron's velocity is perpendicular to the geomagnetic field, the magnitude of the force is given by the product of the electron charge (e), its speed (v) and the magnetic field strength (B), when those quantities are expressed in M.K.S. units. The direction of the magnetic force is perpendicular to the plane of the velocity and field vectors. The electron goes in a circular path around the field line with an angular velocity equal to the product of the electron's charge (e) and the field strength (B), and then divided by the electron's mass (m), e•B/m.

The magnitude of that angular velocity is about 8.8•E+6 radians per second for a typical value of the geomagnetic field strength. When changed to the number of rotations or cycles of motion per second around the field line, it's called the electron gyrofrequency and is about 1.4 MHz. That number should be kept in mind for later reference as the effect of the geomagnetic field on propagation becomes important when the radio frequency (f) of a signal approaches or is comparable to an ionospheric electron's gyrofrequency.

Of course, the velocity of an ionospheric electron at its time of release by a photoionization process need not be perpendicular to the local geomagnetic field. In that case, the electron spirals around the field line at a rate which

depends on the component of its velocity perpendicular to the field. In addition, the electron advances along the field line, spiralling up or down it, with a speed equal to the component of the electron's velocity along the field direction. Indeed, if its velocity is parallel to the field direction, it will not spiral nor experience any magnetic force, simply sliding along the field line.

To go any further in this discussion, more information is needed about the geomagnetic field, its shape and how it can be disturbed. As for shape, the Little Pistol surely remembers high school physics and the fact that the earth's field resembles that of a bar magnet. That sort of description is termed a "dipole field" and has magnetic field lines as shown in Figure 6.1.

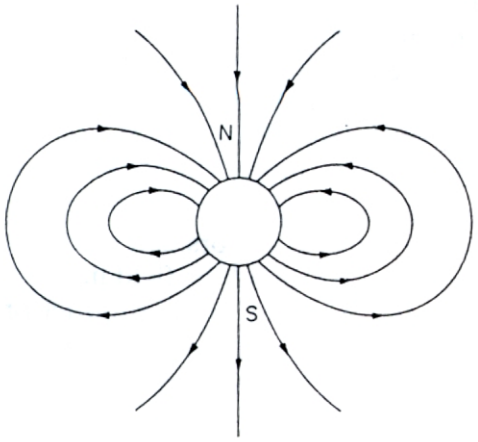

Figure 6.1 A sketch of dipole magnetic field lines.

In the earth's case, the magnetic axis of symmetry of the dipole field and that of the earth's rotation do not coincide. As a matter of fact, both the dipole and rotation axes are known to wander over the earth's surface. At the moment, the dipole axis is tilted about 11.5 degrees with respect to the axis of the earth, passing through the earth's surface near 78.5° N, 69.0° W and 78.5° S, 110.0° E. That means the geomagnetic equator is tilted 11.5 degrees with respect to the geographic equator and crosses the latter at 21° E and 159° W longitude.

All that is well and good but in reality, it only gives a rough approximation to the actual field of the earth. So, for the Little Pistol's sake, let me say what's wrong with the dipole model that's been around so long. First, it was based on an analysis of surface data, largely from populated areas, and had gaps over the vast oceans and the polar regions. And the old data was collected slowly, taking years to assemble before performing the mathematical analysis. As a result, it was incomplete and missed the variability that is so characteristic of the polar regions.

Having said the dipole model is only an approximation, the next question is where it has validity and to what degree. There, the good news is that it's a fairly good approximation at low and middle latitudes. For the moment, let's put off the rest of the discussion but keep in mind that there's much more to the story than such a simple model, especially at high latitudes and the effects of solar plasma streaming by the earth.

With that discussion put on hold, let's get into the geomagnetic data, principally with regard to disturbances of solar origin, that are available here in the USA. As with the solar radiation data, the principal source is NOAA in Boulder, CO. And again, the information comes in the same ways: the WWV radio broadcasts 18 minutes after each hour, by mail in the weekly Boulder Report and any day by telephone from the NOAA PBBS.

All three of those sources of data give the same sort of information, values of the daily 24-hour A-index and three-hour K-indices for geomagnetic disturbances. Those indices are based on data from magnetic sensors, termed magnetometers, which continuously follow the strength and direction of the geomagnetic field at a number of locations on the earth. Thus, they develop information on the quiet level for the geomagnetic field, say in its components to the north, toward the east and vertical direction, as well as observe departures from those levels due to disturbances.

Each observatory develops its own scale for variations above or below the quiet-day levels but they've been normalized so that all sta-

tions report on the same basis. So, in terms of averages, the three-hour K-indices range go from 0 for very quiet to 9 for extremely disturbed and the 24-hour A-indices range from 0 (very quiet) to 400 (extremely disturbed).

On the WWV broadcasts at 18 minutes after each hour, the most recent value of the three-hour K-index is reported from the magnetometer at Boulder, CO. In addition, either a 21-hour estimate of the Boulder A-index is given from 2100 UTC until 2400 UTC for that day or the past 24-hour A-index is given from 0000 UTC until 2100 UTC when the next 21-hour estimate is reported. In addition, a verbal description is given for the level of current geomagnetic activity, using terms like quiet, unsettled, active, minor storm, major storm and severe storm, as well as a forecast in those same terms.

Turning to the weekly Boulder Report, it gives a summary of the Daily Geomagnetic Data from two observatories, Fredericksburg, VA and College, AK, as well as estimates for the planetary 24-hour A-indices and eight 3-hourly K-indices for days in the past week. It should be noted that Fredericksburg data is from a mid-latitude station while that from College is from a high-latitude site. A close look at both sets of data will show that the K-indices from the high-latitude site tend to be greater than those from mid-latitudes, an important fact which will be discussed later.

The estimated planetary A- and K-indices are obtained from a group of five magnetic observatories in the Western Hemisphere, extending from Alaska to England. Those values are used as an approximation to the planetary indices, Ap and Kp, which are derived each month from an analysis of data from 13 observatories, 11 in the Northern Hemisphere and two in the Southern Hemisphere. The estimated planetary A- and K-indices are derived in real time whereas the actual planetary indices, Ap and Kp, are derived at the end of a month, when the data from the widespread network of observatories has been collected.

Geomagnetic data on the NOAA PBBS is found in two files, the Solar Report and the Propagation Report. The Solar Report gives the A-indices for the previous day, AFR from Fredericksburg and AP, as obtained from observations at the five observatories mentioned earlier. In addition, the Solar Report gives estimates of AFR and AP for the day in question as well as predicted values for the next three days. The Propagation Report, on the other hand, only gives the values of the KP- and AP-indices for the day in question as well as the forecast of their values for the next three days.

The Solar Report and Propagation Report from the PBBS differ from the weekly Boulder Report in that they offer predictions for the 10.7-cm solar flux as well as probabilities of geomagnetic activity or storminess at both middle and high latitudes for the next three days. Those two reports do include discussions of solar and geophysical activity as well as forecasts of activity.

Further explanation of the details in those reports will have to wait until propagation has been discussed more fully. But in the short run, following solar and geomagnetic data would be helpful to the Little Pistol in understanding solar/terrestrial conditions and in anticipating changes which might have an adverse effect of propagation, particularly increases in magnetic activity to minor and major storm levels.

7: MORE ON PROPAGATION

Now that the origin of the ionosphere and the possibility of its disturbance by solar activity have been discussed, the ground has been laid for a fuller treatment of HF propagation. The discussion will be broken down into three parts: (1) critical frequencies, (2) signal strength and (3) noise. Such an elaboration is necessary as any communication on the HF bands depends on a path being open as well as adequate signal strength and low noise at the receiver.

The role of critical frequencies will be dealt with first in a plane or flat-earth geometry and then extended to include earth's curvature. That discussion will begin with idea of the highest possible frequency on a path in a simple, plane ionosphere, then make use of ray-tracing to show results for a curved ionosphere and finally determine the geometry for more realistic propagation paths.

So let's begin with a one-layer, plane ionosphere with a maximum electron density Nmax at its peak, a height Hmax above the earth's surface, as shown in Figure 7.1. That sort of model would serve to illustrate conditions at night when the E-region ionization has fallen to low levels and only the F2-region remains. From the discussion in the first section on propagation, the highest frequency that can be sent vertically upward from a transmitter and still returned to the ground as an echo is termed the critical frequency (fc) of the layer and given by

$$fc = (9 \bullet E\text{-}6) \bullet SQRT(Nmax)$$

where Nmax is the electron density at height Hmax.

Now consider a transmitter sending RF upward at an angle above the horizon or, more appropriately, an angle Z with the vertical or zenith direction. The RF enters the bottom of the ionospheric layer at the angle Z but follows a curved path because of refraction. In that case, theory shows for oblique incidence the highest frequency fmax returned to the ground from the peak of the layer is greater than fc by a factor 1/cosZ. As an example, take fc as 4 MHz and angle Z as 60 degrees. In that case, the electron density Nmax is 2E+11 per cubic meter and the frequency fmax returned at that angle of incidence is 8.0 MHz, twice the critical frequency for vertical incidence.

That simple example shows how HF propagation works, the return to ground level of an 8.0-MHz signal at oblique incidence and involving a smaller deviation of its path, 60 degrees instead of 180 degrees for the 4-MHz signal at vertical incidence. And that results from the higher frequency signal encountering a greater number of electrons along the oblique path than for RF at vertical incidence at the critical frequency (fc).

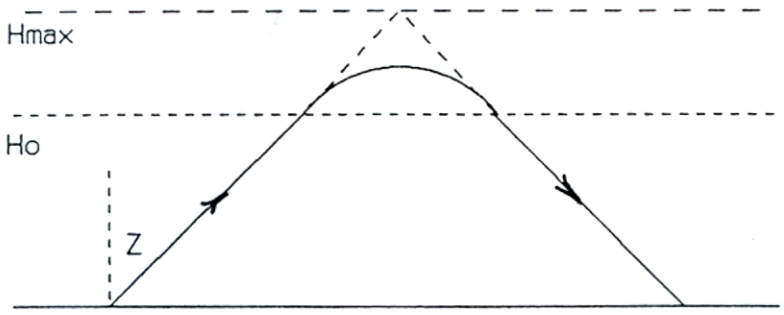

Figure 7.1 Ray refraction in a single-layer plane ionosphere.

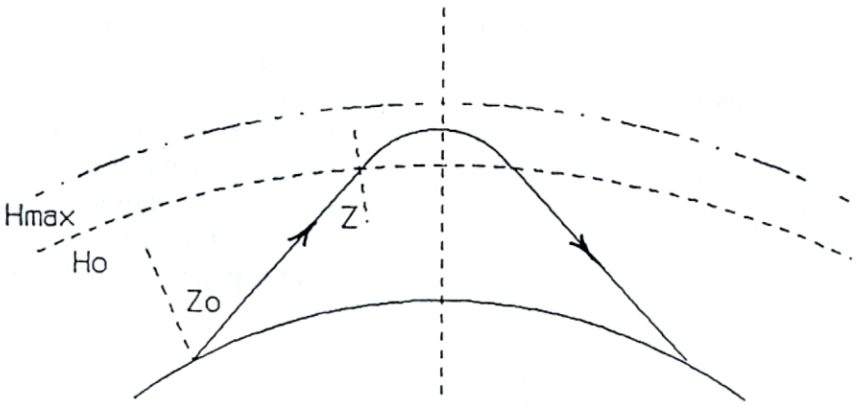

Figure 7.2 Ray refraction in a single-layer, curved ionosphere.

Thus, HF communication is possible at frequencies well beyond the critical frequencies found by sounding the ionosphere and the limits are set by the electron density overhead and the radiation patterns of antennas. Of course, lower frequencies (f) will also propagate at oblique incidence, the main difference being that they won't penetrate as far into the ionospheric layer. Since radiation at a frequency fmax given by

$$fmax = fc/\cos Z$$

propagates at a zenith angle Z and reaches the top of the layer at height Hmax where the electron density is Nmax, it's clear that its effective vertical frequency is fmax•cosZ. By that token, radiation of a lower frequency (f) will have a lower effective vertical frequency, f•cosZ, and be returned from a lower altitude, where the electron density N may be found from the fact that

$$f \bullet \cos Z = (9 \bullet E\text{-}6) \bullet SQRT(N)$$

and the physical height found from the electron density profile.

Beyond that important result, Figure 7.1 shows the ground range or hop distance for that angle of incidence on the ionosphere. And a diagram like that points out the difference between the actual height from which RF is refracted downward and the virtual height for return of RF by reflection from an ionospheric "mirror."

While the idea of mirror reflection finds further application in the discussion of propagation, it should be remembered that it is more symbolic than physical. The reason, of course, is that a mirror has no refractive properties and thus fails to represent the principal feature of the ionosphere, that propagation paths vary according to frequency. A better way to deal with ionospheric problems, whether by refraction or reflection, is to include the earth's curvature and calculate the details of paths in spherical geometry, using 6,378 km for the earth's radius.

Under those circumstances, the one-layer ionosphere problem works out much like the plane case done before except that the angle Z for incidence at the height Ho, where the curved ionospheric layer begins, has to take into account the spherical geometry of the problem. From the geometry shown in Figure 7.2, the zenith angle Z at height Ho will be different (smaller) than the zenith angle for the RF at launch from ground level.

In addition to that adjustment, there is a correction (k) that has to be applied to the factor $1/\cos Z$ because of curvature effects in the ionosphere itself. The correction factor then becomes $k/\cos Z$, where k varies linearly with distance, from 1.05 for a 1,000- km path to about 1.20 for a 3,000-km path. With those changes, one can make a good estimate of the maximum frequency fmax returned to ground level by a curved ionosphere with a critical frequency (fc) and electron density profile peaking at height Hmax.

As indicated earlier, frequencies lower than fmax will not penetrate as far into the ionospheric layer shown in Figure 7.1 nor have

as great hop lengths. The next figure will show those results but before getting to it, a few words of explanation are needed. In particular, ray-path calculations can be carried out easily using a curved ionosphere but it is not convenient to display the results in spherical coordinates. Instead, a rectangular format is used, the horizontal axis showing the distance along the curved earth and the vertical axis the height above ground level. And quite frequently the distance scales along the two axes will differ. Those features should be borne in mind in reviewing the following figures.

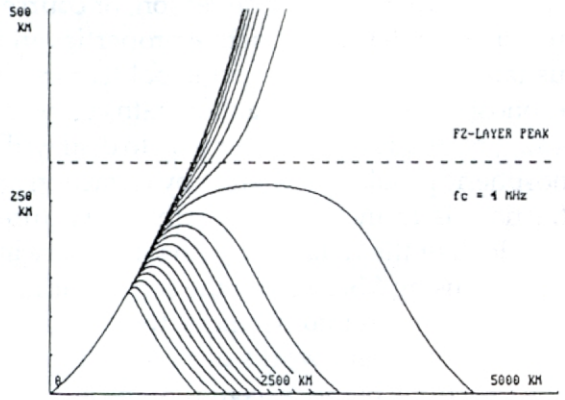

Figure 7.3 Ray traces for launch at 5° elevation, 2-20 MHz in 1-MHz steps.

With those remarks, look at Figure 7.3 which shows the result when rays launched at 5 degrees above the ground horizon go into a curved ionosphere with properties like that shown in Figure 7.1 (fc=4 MHz, Hmax=300 km, Ho=125 km). The paths were traced out in small steps by means of a computer program and to obtain that display, the lowest frequency was taken as 2 MHz and the frequency then stepped upward 1 MHz at a time to 20 MHz. The ray traces first show the bending or refraction at the bottom of the layer for the lowest frequency and show deeper penetration of the layer as the frequency in increased. The 13-MHz ray comes close to the electron density peak at 300 km altitude and then rays from 14 MHz to 20 MHz pass up through the F-layer peak and go into the topside ionosphere.

The ray traces in Figure 7.3 also show how hops at a given launch angle increase in length due to greater penetration with increasing frequency. Next look at Figure 7.4 where the launch angle has been increased to 15 degrees above the ground horizon. It is seen that the hop lengths are shortened by almost a factor of 2 at the steeper launch angle and the highest frequency for which the F-region supports forward propagation dropped from 13 MHz to 10 MHz.

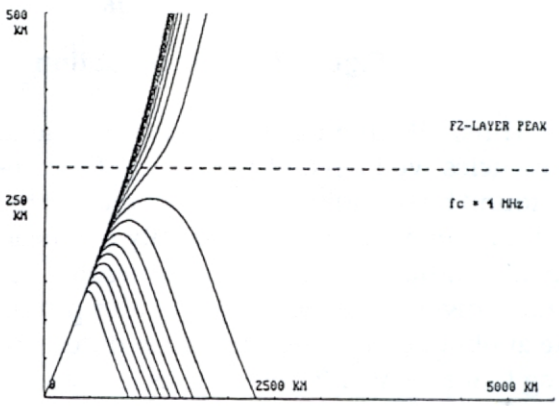

Figure 7.4 Ray traces for launch at 15° elevation, 2-20 MHz in 1-MHz steps.

As indicated above, that simple ionosphere was used to represent a nighttime F-region. If one turns to the foF2 maps in Figures 4.2 and 4.3, it is seen that a 4-MHz value for foF2 would be more appropriate for nighttime during a period of low sunspot number. One could use higher values for foF2 to explore the matter but at this point, it's more appropriate to make the discussion more realistic by including the E-region and showing the role it plays in daylight.

To that end, turn to Figure 7.5 which shows ray traces for a mid-latitude ionosphere around daybreak and now includes ionization in the E-region around 115 km altitude. For that circumstance, the profile used for electron density in the E-region rose quickly from 90 km to a plateau around 115 km, with a foFE value of 2.5 MHz; from there, the electron density rose smoothly to the F-layer peak at 285 km, with an foF2 value of 8.0 MHz. In this case, the launch angle was set at 5 degrees above the

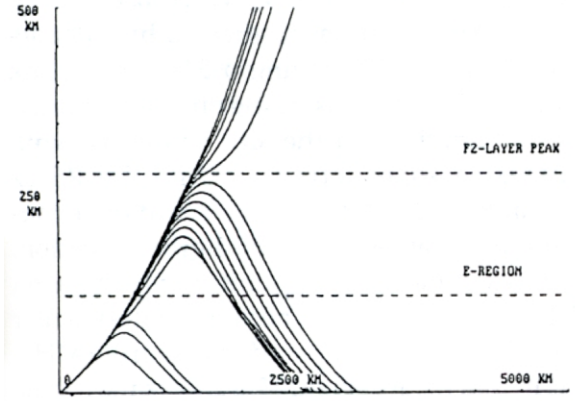

Figure 7.5 Ray traces in a mid-latitude ionosphere, showing effects of the E-region, for 3-48 MHz in 3-MHz steps.

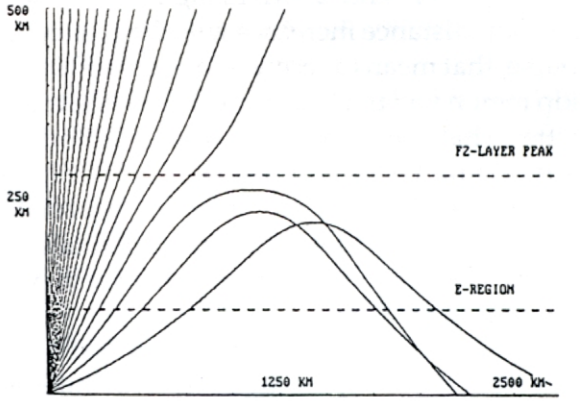

Figure 7.6 Ray traces for 21 MHz. The launch angle starts at 5° and is increased in 5-degree steps to 90°.

ground horizon while the lowest frequency was taken as 3 MHz and the frequency then stepped upward 3 MHz at a time to 48 MHz.

Inspection of that figure shows low frequency rays (3-9 MHz) which are returned by the E-region, then 12-33 MHz rays which are returned to earth before the F2-peak is penetrated and finally the 36-MHz and higher frequency rays go through to the topside of the F-region. A careful examination of that figure shows some deviation of the 12-MHz ray as it goes through the E-region on ascent and descent. That has to do with changes in the rate of refraction or bending on going through a region where the electron density begins to level off, as below the E-region ledge, and then begins to increase with height again.

Using the same model ionosphere again, now consider the frequency being held constant and the radiation angle above the horizon varying. First, take the case of a frequency of 21 MHz and the radiation angle going from 5 degrees to 90 degrees in 5-degree steps. Ray traces for that case are shown in Figure 7.6. The first ray trace at 5 degrees elevation goes out to about 3,000 km distance but the next two fall around 2,250 km distance. Then the ray at 20 degrees elevation and all others at higher angles penetrate the F-layer peak and pass into the topside of the F-region.

Now consider the same ionosphere again but ray tracing for 14 MHz instead. The results are shown in Figure 7.7 and we should note the similarities and differences between the two cases. First, the horizontal range at 5 degrees elevation is about the same. Next, it is seen that rays converge again, now around 1,125-km range, before then starting to penetrate the F-layer peak. That convergence of rays is a form of focussing and results in stronger signals. The distance between the transmitter and those converging rays is called the "skip distance" and the ray convergence illustrates "skip focussing," a form of signal gain of ionospheric origin.

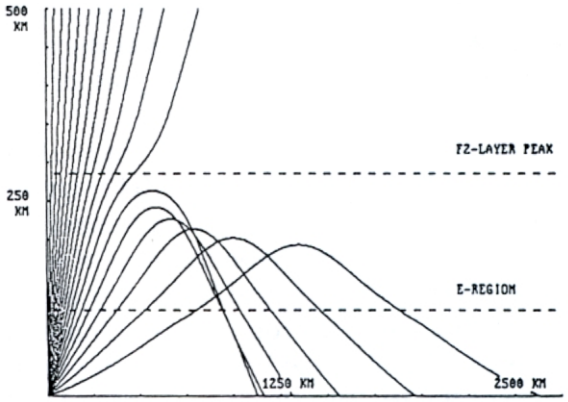

Figure 7.7 Ray traces for 14 MHz. The launch angle starts at 5° and is increased in 5-degree steps to 90°.

By comparing the skip distances for those two cases, 14- and 21-MHz signals, one sees that skip distance increases with frequency. Of course, that means a receiver located within the skip region will not hear signals from the transmitter. That is not an uncommon situation but as the Little Pistol will testify, it proves quite annoying when trying to work DX, especially on 10 and on 15 Meters, as one often fails to hear nearby stations in a pileup that are in contact with the DX station.

Another aspect of propagation that's evident from those ray traces deals with antenna patterns. In particular, high-angle rays from antennas may not return to earth, depending on the frequency and the state of the ionosphere. For the ionosphere under discussion, the limiting radiation angle for RF penetrating the ionosphere is around 20 degrees for 21 MHz signals and 30 degrees for 14 MHz signals. By that token, a lower limiting angle would be expected on 28 MHz and antennas for that band should be as high as possible to keep the radiation pattern low, thus minimizing power wasted by high-angle radiation going off to infinity. But I'm sure the Little Pistol already knew that!

On that same subject, RF going through the ionosphere, it should be noted that ray direction or signal travel may be reversed and the results obtained above may be used to consider reception of signals coming in from space, from satellites or as cosmic radio noise. In either case, it is seen that signals coming from the topside of the ionosphere pass down through what is called an "iris," after the stop in a camera lens aperture or the part of the human eye.

For the cases discussed above, the iris has a radius of about 750 km for 21-MHz signals and 500 km for 14-MHz signals. Of course, the size of the iris will depend on the level of solar activity and the local critical frequency of the F-layer, being larger at around solar minimum and smaller at solar maximum. In any event, the size of the iris shrinks to zero at the local critical frequency (fc) of the F-layer and signals at lower frequencies from outer space are not heard coming through the peak of the F-layer.

The Little Pistol knows about the Russian satellites, RS-10 and RS-12, which use HF signals and how their use is affected by solar activity. Thus, RS-12, having a 21-MHz uplink and 29-MHz downlink, is the one most vulnerable to variations in the size of the iris with changes in solar activity. While the RS-12 downlink on 29 MHz may be heard over considerable distance or time by a ground station, the access time to the uplink transponder on RS-12 may be much less because of the smaller iris on 21 MHz as compared to that on 29 MHz.

In that regard, Figure 7.8 shows the results of some calculations made for a particular RS-12 pass back in 1992. Since the satellite covers about 440 km distance per minute in its orbit up at 1,000 km altitude, one cannot use just one critical frequency to characterize the F-region below it. So instead of thinking of the satellite as overflying an iris of fixed size or opening centered over the receiving station, the calcu-

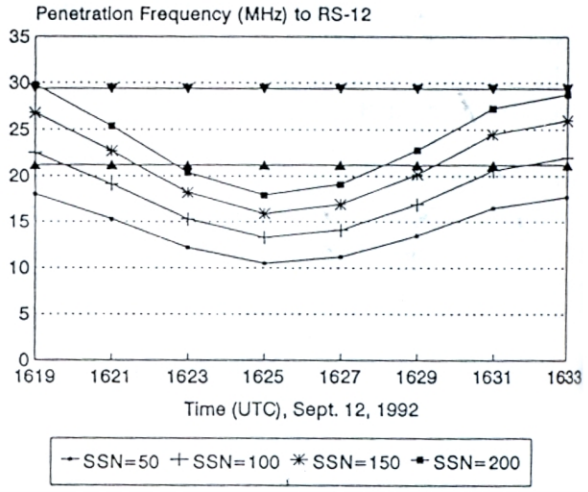

Figure 7.8 F-region penetration frequency for the RS-12 satellite at different levels of solar activity.

lations for access to the satellite's uplink are done in terms of the F-layer penetration frequencies along the line of sight to the satellite's flight path.

While that sounds more complicated, it's really nothing but an iris effect and the results show what one would expect from the elementary considerations developed above: the frequency for F-region penetration falling below

the satellite's uplink frequency for longer periods of time, i.e. greater access to the uplink transponder, when solar activity is low than when high. If one wants to retain the idea of an iris over the receiving antenna, that means the iris would take on a more complicated shape because of the N-S orientation and extent of the satellite's path, not just the simple conical one that goes with a constant F-layer over the antenna.

Another aspect of the same idea, signals going through the iris, is found when trying to make contacts via the RS-12 satellite, one hears "strange voices" on SSB calling "CQ Contest" on the downlink. That can happen when 21-MHz signals inadvertently reach the satellite through the iris of a transmitting antenna while normal 15-Meter operation is in progress. Even more strange and curious is hearing Novice signals from the 15-Meter CW band right on the 29-MHz downlink frequency of RS-12's Robot. That comes from Novices accidentally operating right on the 21-MHz frequency of the Robot's uplink receiver.

Finally, solar and galactic radio noise signals can reach the earth at the upper end of the HF range and over VHF/UHF frequencies. Those signals are monitored by receivers with beam antennas pointed upward. For propagation purposes, galactic noise signals around 30 MHz may be used to indicate times when the ionosphere is disturbed by auroral electron and solar proton bombardment at high latitudes, as well as the occurrence of geomagnetic storms. In those circumstances, cosmic noise signals penetrating the F-region are attenuated because of greater absorption in the lower ionosphere, the D-region. That brings us to the next subjects in our discussion, signal strength and absorption.

8: NOW TO SIGNAL STRENGTH

Oddly enough, we begin our reality check on the ability of the Little Pistols of the World to make their DX contacts by using simple, idealized methods. But that's the way one starts to make sense out of the complicated radio world they operate in. So we begin our task by thinking of one Little Pistol who lives in Boulder, CO, the mecca for those interested in radio. Then we'll use one of the hops just discussed earlier, off toward St. Louis, MO around daybreak, say the 14-MHz ray trace in Figure 7.7 that goes out to 1,300 km distance. On the 20-Meter band, that hardly qualifies as DX but we have to start simply now; we'll get to real DX in due course.

The problem we have to work out now is the strength of Little Pistol's signals at that distance after going through the ionosphere that was specified earlier, with an foF2 value of 8.0 MHz and foFE of 2.5 MHz. I didn't mention it at the time but that was for a day in mid-January and with a smoothed sunspot number (SSN) of 100.

The first step in the process is to consider the loss of Little Pistol's signal strength due to signal spreading over the distance between Boulder and St. Louis. We begin with a grossly unrealistic representation of the situation by thinking of LP using one of those mythical isotropic radiators in free space. So if the 100 Watts from LP's rig were radiated equally in all directions, we can find the RF power per square meter at 1,300 km distance by simply dividing the 100 Watts radiated by the area of a sphere of 1,300 km radius. That result is 4.7E-12 Watts per square meter, certainly a small number.

In the radio world, both large and small numbers are dealt with using logarithms (to base 10). If we use 1 Watt per square meter as a reference value, then the power ratio of LP's RF power (P1) at 1,300 km distance to the reference power level (P2) is 4.7E-12. That power ratio can be expressed in decibels (dB) by using the definition

$$dB = 10 \bullet \log(P1/P2)$$

and one obtains –113 dB for the power ratio, meaning that LP's RF is 113 dB below 1 Watt per square meter at that distance.

As a step in improving the calculation, let's say now that LP's isotropic radiator is not in free space but a half-wavelength above a perfectly conducting ground. That means that all the RF that went down below LP's original horizon is now reflected upward by the ground plane and adds to the RF going out above the horizon.

But that addition is done using the amplitudes and phases of the electric field strength E of the rays, both direct and reflected. In the directions where the field amplitudes add constructively, signal amplitude would be doubled or the intensity quadrupled. Thus, LP's signals would be 6 dB greater in intensity in those directions where the direct and reflected rays are in phase, bringing the LP's signal strength up to –107 dB Watts per square meter in the direction of strongest signals.

If the Little Pistol's antenna were a dipole, it would have a gain of 2.1 dB over the isotropic radiator and if placed a half-wavelength above a perfect ground plane, its strongest signals would be at 30 degrees elevation. But we said LP's antenna is a 3-element Yagi so, instead, we'll take its gain over an isotropic radiator to be 6 dB, bringing LP's signals up to –101 dB Watts per square meter. But since the rays going off to St. Louis are somewhat below that elevation angle, the vertical radiation pattern for the Yagi indicates that signal strength should be corrected downward by about 1 dB, bringing it to –102 dB Watts per square meter.

At the outset, it was indicated that idealized methods would be used in embarking on a reality Check, so at this point we have to pause and look where approximations were made, as well as whether they could be improved on and then taken into account in arriving at Little Pistol's signal strength at St.

Louis. The first place to start is with the signal spreading calculation. There the ground range covered by LP's signals was used instead of the actual distance along the ray path in the ionosphere. By going back to the computer program, one finds that a more realistic distance would be closer to 1,400 km, making loss due to signal spreading about 0.6 dB greater.

That correction is one where a geometrical calculation is improved on by considering the ionospheric path in more detail. There are other such corrections which can be enumerated, in two and three dimensions, but which are difficult to evaluate in magnitude. For example, there is the question of where the receiving station is located relative to the skip distance. Thus, any increase in the height of the F-layer peak could shift the skip distance further toward 1,300 km ground range and, as noted earlier, contribute gain because of skip focusing. If the height decreased, the effect would be just the opposite.

In three dimensions, there's the question of how the ionosphere's spherical shape or curvature affects signal intensity. After all, there's some focusing or ray convergence obtained from a concave spherical mirror and one can expect that the same would be true for the ionosphere. The trouble is that it's difficult to calculate without resorting to huge efforts with ray tracing programs.

That's in contrast to the case in geometrical optics for light. There, the geometry is fairly simple as all rays travel in directions which are close to the axis of symmetry of the mirrors and admit the use of straight lines in ray diagrams dealing with the problems. For the ionospheric case, however, RF rays are off axis in the extreme, and elementary methods are just not available. With those remarks, we can suggest there's some positive gain from ionospheric focusing but we'll have to pass when it comes to estimating it, at least for the Little Pistol's situation.

Now it wasn't said in so many words at the time but the values of foF2 and foFe used to characterize the path between Boulder, CO and St. Louis, MO were really for the midpoint of the path, close to Belleville, KS. Thus, in reality, around daybreak the sun is higher in the sky over St. Louis than over Boulder. That suggests that there is more in the way of ionization, and ionospheric refraction, on the eastern half of the path than the western half. That point needs no testing but the effect could be examined by making new ray-tracing calculations which take into account the variation of the solar elevation angle for an hour difference in local time, from 90° E to 105° E longitude. But it seems fair to say that when it comes to the dB of signal loss from path length or spreading, it would be a very small effect. So we'll just leave it there, being aware of the fact the ray path is an approximation, for those reasons.

But those very reasons do affect the Little Pistol's signal strength at the St. Louis end of the path. Here, the matter is that of signals' absorption in the D-region of the ionosphere. That region was mentioned early in the discussion and the fact is its electron density was the lowest of the ionospheric regions. In addition, it was pointed out the D-region is present only when the atmosphere is illuminated around the 60-90-km level and then with at most 1,000 electrons per cubic centimeter.

That electron density is too low to give rise to any refraction of HF signals passing through the D-region. However, in the daytime, it can weaken signals, low frequencies more than higher ones. Essentially, the D-region electrons are excited into oscillatory motions by passing RF but at those depths, the D-region electrons collide with atmospheric constituents and transfer energy to them. That means the atmosphere is heated by a beam of RF passing through and, given the conservation energy, that results in the loss of signal strength.

The transfer of energy from the wave to the atmosphere takes place in two steps, the first part when the D-region electron gains energy from the passing wave and the second part when it undergoes a collision and transfers energy to a molecule. Deep in the atmosphere, where ionospheric electrons have a high collision frequency (fcoll) with atoms and molecules (about two billion or 2E+9 collisions per second), RF waves have little chance to impart any energy to the electrons before a collision

occurs. So the absorption of RF energy is very low for all HF frequencies down around 30 km.

But higher in the D-region, say around 90 km, the collision rate is much lower (about 300,000 or 3E+5 collisions per second), even below typical amateur operating frequencies. As a result, an ionospheric electron makes many oscillations, reradiating RF energy from the incident wave, before it finally makes a collision and transfers some energy to the atmosphere.

In between those two extremes, the absorption of energy from the passing waves goes through a maximum, essentially when the collision and operating frequencies are about the same. For that circumstance, both the first and second steps of the absorption process are working at comparable rates. The numerical details of D-region absorption can be worked with the aid of laboratory experiments which simulate the electron collisions and a model for the atmospheric region. From that, one can find the *absolute* efficiency for energy absorption per electron and how it varies with height in the D-region and wave frequency.

In that regard, the *relative* absorption efficiency per electron at D-region heights and for the five harmonically-related amateur bands in the HF spectrum is shown in Figure 8.1. In a qualitative sense, the Little Pistol is aware of those results, knowing it's tough to work real DX on the 7-MHz band in broad daylight but much easier at night. Under nighttime conditions, the D-region electron population falls to low levels as the main source of ionization, the flux of "hard" solar X-rays, is no longer incident and the only sources of ionization are scattered sunlight and the low flux of galactic cosmic rays passing through the region.

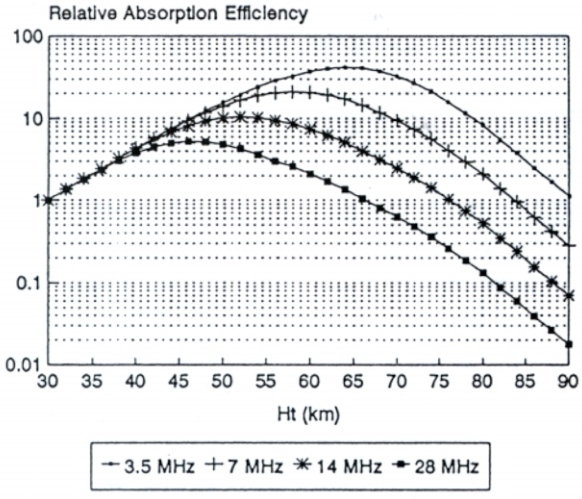

Figure 8.1 The relative absorption efficiency per electron as a function of height in the D-region and at different frequencies.

As for working out the absorption loss for the LP's path in Figure 7.7, it's just a matter of following the ray path through the D-region, on ascent from Boulder and descent to St. Louis, and then weighting the number of electrons encountered in a square-meter column along the way according to their absolute absorption efficiency at each altitude and adding up the losses. When that's done, the result is another 1.7 dB loss, bringing LP's signal strength to –103.7 dB Watts per square meter. If we add in the 0.5 dB correction for signal spreading, LP's signal strength would be –104.3 dB Watts per square meter.

It should be noted, however, that the absorption result noted above was not obtained with the ray tracing program but another, separate calculation which took into account the fact that the actual D-region illumination differed in the vicinity of those two sites separated by 15 degrees of longitude or one hour of local time. Thus, no further adjustment is needed, say along the lines suggested earlier for the F-region, and we can go on to the next item related to the Little Pistol's signals, the antenna at the other end of the path which determines the signal strength reaching the input of the distant receiver.

Let's assume the receiving antenna is a half-wave dipole at a half-wavelength over a perfect ground and oriented so that its axis (or wire direction) is perpendicular to the direction of LP's incoming signals. There are hard ways and easy ways to find how much of LP's RF power arrives at the input of the receiver. The hard way is to find the electric field strength of LP's signals at the dipole and then find the voltage induced. The easy way, and the one we'll use, is to think of the receiving

antenna as a collector of RF that's passing by; in that approach, one merely has to know the collecting area or aperture for the dipole.

Again, we start simply and ideally and work our way up toward reality. So if the receiving antenna were an isotropic radiator, electromagnetic theory shows its collecting area would be 0.079 times the square of the wavelength. That idea is not new, dating back to work by Friis in 1946 and you'll even find it in the ARRL Antenna Book. So for the LP's 14-MHz signals, the effective collecting area would be 36.3 square meters if the isotropic receiving antenna were in free space. If we express the collecting area in logarithms, then the RF power collected by that isotropic receiving antenna would be the sum of –104.3 dB for the radiation flux (Watts per square meter) and the antenna area (15.6 dB square meters) or an RF power of –88.7 dB below 1 Watt at the antenna feedpoint.

Now we make some additional corrections, +6 dB for the receiving antenna being over a ground plane and +2.1 dB for it being a dipole instead of an isotropic radiator. That brings the signal power at the feedpoint up to –80.6 dB Watt or –80.6 dBW. Finally, the last correction, for the fact that the radiation is coming in below the 30-degree angle, the most favorable direction of a dipole; for the ray from Boulder to St. Louis, that amounts to a correction of –0.5 dB, bringing the RF power to –81.1 dBW.

All of the discussion above has been on a lofty plane, using the results for idealized situations and assuming the ionosphere can be considered as a stable, smooth distribution of ionization. But, as the saying goes, we have to "get down to earth" in the discussion, putting in a correction for the fact that both the transmitting and receiving antennas are not over perfectly conducting ground planes. In order to do that, we have to resort to the effects of real ground on vertical antenna patterns, both the LP's 3-element Yagi and the receiving antenna.

Each type of real ground has its own electrical conductivity and a dielectric constant and in terms of quality, they range from excellent (sea water) to poor (sand or ice) when it comes to simulating the ideal ground that was used in the discussion above. There'll be more on the subject of ground when the discussion turns to the surface reflections that contribute to multi-hop paths. At this juncture, the important point is that the finite conductivity of a ground surface leads to losses on wave reflection in the vicinity of an antenna, whether used for transmitting or receiving purposes.

So, for the moment, a correction of –2 dB, taken from the *ARRL Antenna Book,* will be used for the effect of an average ground on radiation coming from a dipole and also on the LP's 3-element Yagi. That brings the RF power available at the feed point of the receiving antenna to -85 dBW, on rounding to the nearest integer value. Assuming no other losses, that power at the receiver must be compared with noise power from atmospheric and man-made sources to see if LP's signals are readable.

So now we should turn to a discussion of noise. Before doing that, however, it should be noted that the ideas expressed above are the outline of how longer, more complicated paths would be analyzed for signal strength. It's just a matter of taking the hops one at a time and adding up the results. Of course, the degree of solar illumination will vary along a path and that will have to be taken into account.

9: NOISE

We've already considered two of the aspects needed for successful communication — signals getting through the ionosphere and their strength. Now the question is whether the signal strength is great enough to compete with the noise at the receiving end. That is an important question but before turning to it, one should bear in mind that the analysis to this point has been for an ionosphere whose critical frequencies, foFE and foF2, were specified, not derived or predicted quantities.

In reality, those characteristics of the ionosphere will change in the course of a day as the sun goes across the sky. That being the case, one would think that the specified quantities would be of value for some limited period of time or, if used for an hour, be considered to have some variability. But if the critical frequencies used in calculations were obtained from some sort of prediction scheme, it should be understood that the values have some measure of uncertainty which should be considered in interpreting the results. Put another way, it is the height of innocence to think that any measured physical quantity, from the ionosphere or whatever, is without uncertainty and to treat it as though it's without any probable error.

In the present discussion that idea, of uncertainty, really comes to the fore for the first time with noise, particularly that of man-made origin. Since noise power is a quantity that we'd have difficulty measuring ourselves, we use the results from various scientific studies. And in doing so, the first question deals with the noise power in a receiver, its average value, and then its variability.

To begin the discussion, we note noise is always present in the output of a receiver, the noise reaching an antenna being amplified along with the incoming signal. Of the three types of radio noise — galactic, atmospheric and man-made — consideration will be given only to the last two as galactic noise is negligible in all but the most remote sites. That results in the HF range as the ionospheric iris over a receiving antenna closes as the frequency drops below 30 MHz. But that is not to say that solar noise outbursts cannot be heard near the top of the HF spectrum during periods of solar activity but being sporadic, they don't fit in the discussion of HF prediction methods.

Of the other two types, atmospheric and man-made noise, the second one is probably more familiar, as most DX operators have been troubled at one time or another by impulsive bursts of noise from power tools, spiky ignition noise or the steady buzz of neon signs wreaking havoc on the bands. And noise, being broadband by nature, varies at one's receiver output according to the receiver bandwidth in use, say 500 Hz for CW to 2,400 Hz for SSB in amateur situations and 6,000 Hz for AM.

While man-made noise may be quite site- or time-specific, studies show that average noise powers may be categorized by population levels or locations — industrial, residential, rural and remote unpopulous. In that regard, the IONCAP program uses the following for the noise power relative to one Watt at 3 MHz and with 1 Hz bandwidth: –140 dBW for industrial, –145 dBW for residential, –150 dBW for rural and finally –164 dBW for rural unpopulous sites. Those values are from a 1974 report by the U.S. Department of Commerce.

In order to find the noise power to compare with the signal strength calculated earlier, the type of site must be identified and the bandwidth (b) specified so it may be used to multiply by (or added logarithmically to) the noise power at 1 Hz bandwidth. In addition, a correction must be applied to find the noise power for the 14-MHz operating frequency since the studies showed noise power falls with increasing frequency, as shown in Figure 9.1.

If we assume the receiving site in St. Louis is in a residential setting and SSB signals are being received, the –145 dBW value at 3 MHz

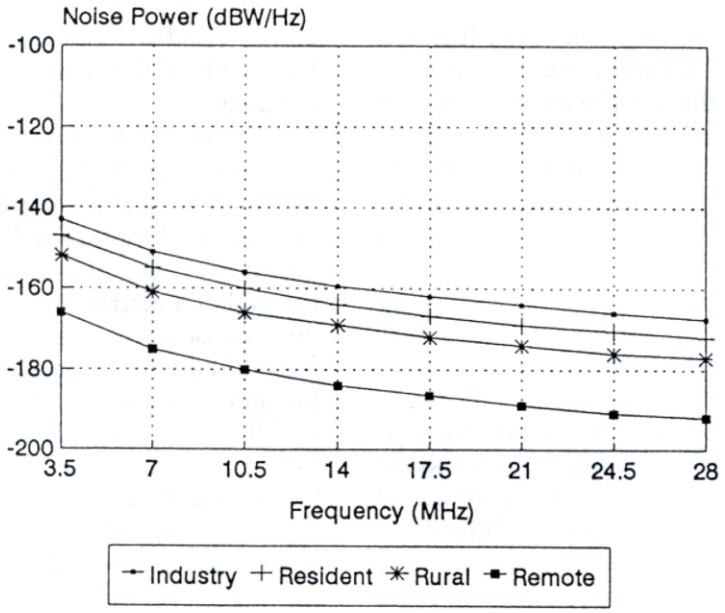

Figure 9.1 Average man-made noise power as a function of frequency for different environments.

must be reduced by about 18 dBW because of the lower noise power at 14 MHz. However, a bandwidth of 2,400 Hz means another adjustment upward by 34 dB to cover the greater amount of noise received, giving a final value for the average noise power of –129 dB above 1 Watt or –129 dBW. When compared to the –85 dBW signal from the LP's antenna, it means the LP's signal-to-noise (S/N) ratio could be as high as 44 dB in a residential area of St. Louis. And using the above method, one can see that the S/N ratio would be lower by 5 dB in an industrial setting and higher by 5 dB in a rural area.

While surveys provide data on the average level of noise power across the spectrum in the various settings, they also give information on noise variability. As one might expect, the man-made noise level in populated regions also shows daily variation, being greatest during waking hours of local time. That variation runs around +/–10 dBW when averaged over populated regions and the hours in the day.

Since all the noise calculations so far have used quantities which came from given or average values, results should be made more realistic by including their statistical fluctuations. In that regard, the +/–10 dBW variation in average noise power would cause S/N ratios to vary or fluctuate, even fall 10 dB below the values given, making reception difficult since 6 dB of signal or noise amounts to 1 S-unit.

Beyond variations in noise power, there are other statistical aspects of the S/N ratio to be considered, the various forms of fading affecting signal strength; every DXer knows those problems well. How does that happen and how much can it affect the S/N ratio during a contact? Those are good questions and will be treated later as they'd take the discussion too far afield at this point. Right now, we have to conclude the discussion of noise by turning to atmospheric noise.

As the term implies, atmospheric noise has its origin in the meteorological processes, from lightning strokes near and afar. Those discharges give rise to a broad emission of radio noise which is propagated just like any other signal, the higher frequencies largely confined below the F-region peak and the lower frequencies absorbed by the D-region during the day.

The geographic distribution of lightning strikes varies with the season, particularly strong sources being located in South America, South Africa and Indonesia during December, January and February and more "equator-

ward" during the months of June, July and August. In the USA, thunderstorm activity is concentrated in the southeastern and midwestern states during the summer months. Those features are reflected in the distribution of noise with seasons, atmospheric noise being most intense in those regions during the months indicated.

As for magnitudes, global noise maps have been produced by the CCIR for each three-month period of the year and in four-hour blocks of local time (LT). In that representation, map contours show atmospheric noise power available (in dB) from a lossless antenna relative to a thermal noise source at 288 degrees Kelvin. Those values differ from the ones for man-made noise in that a 1 Hz bandwidth is used at a frequency of 1 MHz instead of 3 MHz. The information on atmospheric noise from CCIR also includes how the noise varies with frequency.

Going to Little Pistol's contact with St. Louis, around sunrise in January, that's in the season when atmospheric noise is the lowest and the same is essentially true for the time of day. When one works out the details, the atmospheric noise power in St. Louis would be about –125 dBW, something like 1 S-Unit lower than the level for man-made noise in a residential area.

While it should be borne in mind that atmospheric noise, like man-made noise, has a statistical fluctuation to it, in this particular case the man-made noise would seem to be the most important factor, at least at the St. Louis end of the path. Of course, the Little Pistol will have noise of some sort at his QTH too so that would have to be taken into account in considering the other side of any QSO.

To summarize the discussion in the last three chapters, for any successful communication to take place, three conditions must be met: signals must get through on the operating frequency, signal strength must be adequate and the noise level must be well below the signal strength. Noise power, especially of man-made origin, can be important at any time and on any frequency while signal absorption dominates at the low end of the HF spectrum. Of course, solar activity is important for the choice of operating frequency, especially for the high end of the HF spectrum. But all three considerations are important at any time: MUF, signal strength and noise power.

10: NOW THE DETAILS

In discussing the propagation of Little Pistol's signals from Boulder to St. Louis, the methods used were straightforward and to the point, dealing with the questions of critical frequency, signal strength and the presence of noise. Now, in preparation for going on to more complicated paths and with more than one hop to them, it's necessary to consider some details which were either omitted or will come up shortly. The first matter deals with wave polarization.

As everyone knows from the experiments of Heinrich Hertz more than a century ago, electromagnetic waves are characterized as having some form of polarization. The usual approach is to consider the case of propagation where the electric and magnetic fields of the wave are in the plane of the wavefront and perpendicular to the direction of advance of the wave. For wave propagation through vacuum or an isotropic, homogeneous dielectric, the two fields, E and H, take their simplest form, perpendicular to each other and linearly polarized.

That last term, linear polarization, means the electric field E, for example, is parallel to a line or axis, changing its magnitude and direction at the operating frequency and the same is true for the magnetic field H. Graphically, in wave propagation, the fields for an advancing wave may be represented by arrows whose length and direction vary with time and space as shown in Figure 10.1. In that figure, an instantaneous view is given of how the electric field, Ey, varies in the y-direction and the magnetic field, Hz, in the z-direction for a wave advancing in the x-direction, to the right in the figure.

In the case of radio waves, their polarization depends on the transmitting antenna, at least at the outset. For a dipole, the electric field is parallel to the direction of the wire for waves radiated perpendicular to the wire's orientation. If the wire is parallel to the ground, the waves are termed horizontally polarized. By the same token, vertically polarized waves are radiated if the axis of the antenna, say a quarter-wave vertical, is perpendicular to the earth's surface. That's as simple as it gets but it doesn't last long.

The reason for that statement goes back to ionospheric sounding, the technique used in the late '20s to explore the structure of the ionosphere and the critical frequencies of the various regions. While not mentioned earlier, those studies showed there is not one but two wave echoes coming back from each RF pulse sent upward. One, called the ordinary wave O, is just what would be expected for an ionosphere that contains only free electrons and the other, the extraordinary wave X, results from the fact the ionosphere is immersed in the earth's magnetic field.

Those observations were obtained from displays which plotted the instantaneous frequency of RF pulses, as the ionosonde swept from 1-20 MHz, and the times of arrival of the echoes from overhead, using the X- and Y-axes

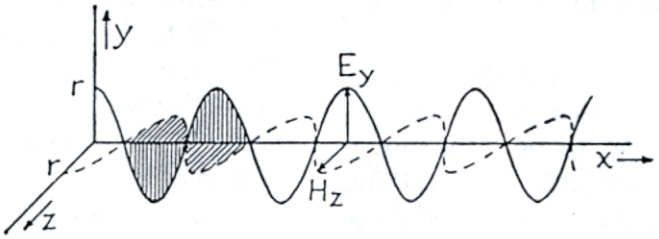

Figure 10.1 Electric and magnetic field vectors for a plane-polarized, sinusoidal electromagnetic wave.

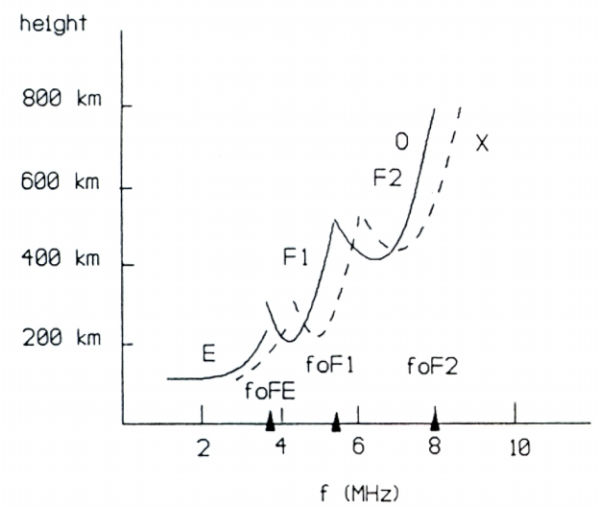

Figure 10.2 An idealized ionogram for daytime conditions showing echo heights as a function of frequency for O- and X-waves.

of an oscilloscope tube. The two echo traces, O and X, from a sweep in frequency are illustrated in Figure 10.2, an idealized representation of an ionogram. Of interest is the fact that the two traces are separated in frequency by about one-half the local electron gyro-frequency. In terms of the propagation of the Little Pistol's signals, that means the X-wave is returned from a region of the F-layer where the critical frequency fxF2 is about 0.5 MHz higher than foF2 for the O-wave.

Those results indicate the ionosphere is doubly refracting, just like a piece of mica or a calcite crystal, and with two different wave polarizations propagating through it. When electromagnetic theory was applied to the problem, it was found that the O- and X-waves are elliptically polarized and with opposite senses of rotation. If that's not complicated enough, features of their propagation depend on the direction of wave travel relative to the geomagnetic field!

A full discussion of those matters is very complicated and has to be left to the experts. For the present discussion, we need the fundamental points and how the Little Pistol's DXing would be affected. To that end, we should think of the signals leaving the LP's antenna as being horizontally polarized since that's how the LP's Yagi is set up. But knowing that the LP's signals will be propagated as both O- and X-waves, the next step is to represent the wave's original linearly polarized E-field as the sum of two elliptical waves.

But let's make life easy for ourselves, using the special case of circular polarization instead of the more general elliptical polarization that theory would suggest. We can do that if the signals are propagated along or close to the direction of the geomagnetic field. That'll be good enough for our present purposes and leads to less confusion. So, going to Figure 10.3, the electric field E of the wave which leaves the LP's antenna oscillating in a direction parallel to the earth's surface is now represented as the sum of two electric fields which rotate in opposite directions, i.e., circularly polarized waves.

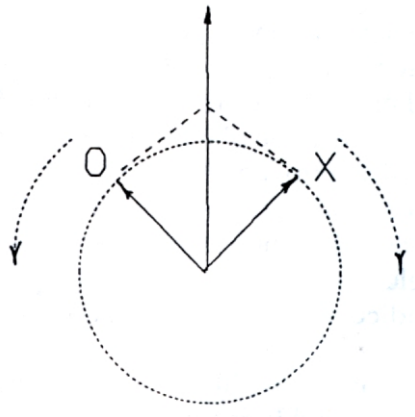

Figure 10.3 The representation of a linearly polarized wave as the sum of two circularly polarized waves, rotating in opposite directions at the same frequency.

If you stop and think about it, those two rotating field vectors add up to the original horizontal E-field from the LP's antenna, the perpendicular components always being in opposition and cancel while the components parallel to the original direction always add. Thus, the oscillating horizontal E-field is replaced by two circularly polarized waves, rotating in opposite directions around their direction of travel.

As with any doubly refracting material, we can expect the two circularly polarized waves to travel at speeds which are slightly different. The simplest illustration of the point

would be for S-to-N propagation at the magnetic equator. In that case, theory indicates the circularly polarized X-wave rotates in the counterclockwise (c.c.w.) direction, when looking northward along the magnetic field direction, while the O-wave has a clockwise (c.w.) rotation.

Beyond the two different senses of rotation for the O- and X-waves, theory indicates that the O-wave travels slower than the X-wave so in the time required for waves to reach a given location, the c.w. O-wave will have rotated more about the geomagnetic field direction than the c.c.w. X-wave. If the two instantaneous rotating fields are combined to obtain the equivalent linear polarization at that location, as in Figure 10.4, it's seen the plane of polarization has rotated a finite amount about the direction of propagation in the course of wave travel.

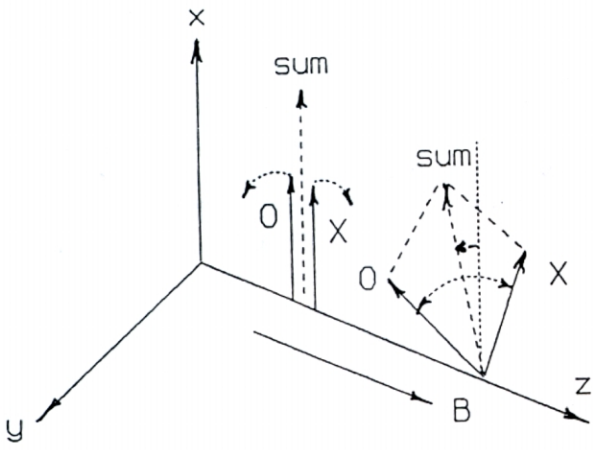

Figure 10.4 Rotation of the plane of polarization from two circularly polarized components traveling at slightly different speeds through the ionosphere.

When the problem is worked out in detail, it turns out that the plane of polarization rotates in proportion to the average magnetic field and columnar electron content along the wave path and inversely with the square of the operating frequency. That effect is called "Faraday rotation" and results in the Faraday fading of satellite signals as their plane of polarization rotates relative to simple linearly polarized antennas.

Obviously, there are other cases of ionospheric propagation which could be examined, say propagation perpendicular to the geomagnetic field. But in Amateur Radio there are no fixed paths, and directions of propagation relative to the geomagnetic field vary constantly, even on ascent and descent along a path. So the idea of rotation of the plane of polarization of RF is appropriate for discussions of HF propagation; but the case cited above, termed longitudinal propagation, is more for general illustration than any specific application.

With all the different directions of propagation as well as path lengths in use during amateur operations, it's quite unlikely that the original polarization of a wave would remain by the time propagation carries it to the receiving end of a path. And with large-scale changes in the height of the upper regions of the ionosphere taking place in the course of a day, reaching minimum heights at local noon in the winter hemisphere and maximum heights in the summer hemisphere, it would seem that just about any kind of wave polarization might be incident on a receiving antenna.

That being the case, for calculation purposes, it's assumed that incoming signals at a receiver are essentially unpolarized at any time, power divided equally between horizontal and vertical polarizations, and a receiving antenna does not respond to components of the incoming radiation which are perpendicular to its own polarization. Thus, a vertical antenna would not respond to the horizontal components of incoming unpolarized radiation and a horizontal antenna would not respond to vertical components. All that amounts to a polarization coupling loss of 3 dB, to be added to the other losses along a path and bring the LP's signal to –88 dBW in residential St. Louis and a S/N ratio that is corresponding lower at 32 dB.

At this point, we have to consider extending these methods to longer paths, now including surface reflections between hops. However, one thing is lacking, the effects of ground reflections. For that, it's assumed that reflecting surfaces are smooth and characterized by electrical conductivities and dielectric constants.

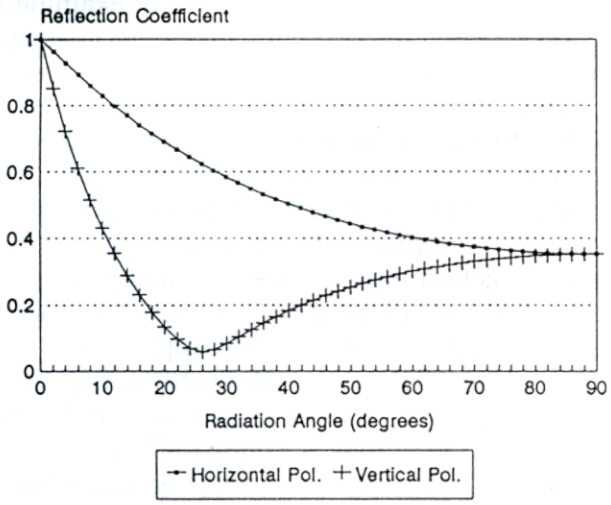

Figure 10.5 Reflection coefficients on 14 MHz for typical ground as a function of angle with the horizon for both horizontal and vertical polarization.

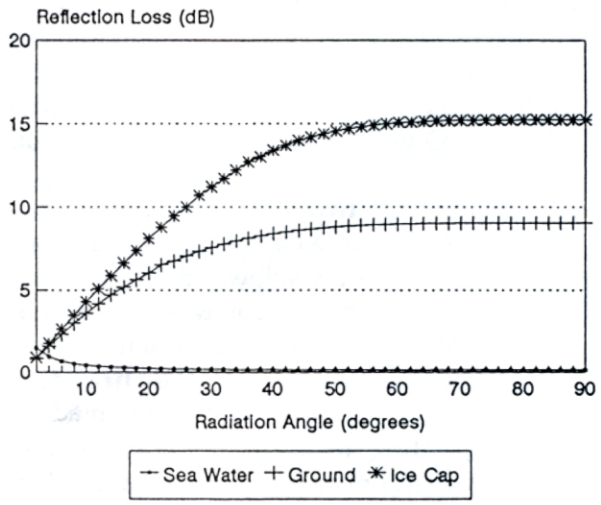

Figure 10.6 Reflection loss on 14 MHz as a function of angle with the horizon for three different surfaces.

Next, Fresnel's equations from electromagnetic theory are used to find the reflection coefficient, the ratio of the reflected E-field to that incident on the surface, for different operating frequencies, polarizations and angles of incidence. In that regard, Figure 10.5 shows how the reflection coefficient on 14 MHz varies with radiation angle for typical ground material and the two polarizations.

The striking feature of that figure is the behavior for vertical polarization where the reflection coefficient goes through a minimum around 26 degrees. That angle is called the pseudo Brewster angle after Brewster's angle for reflections from a pure dielectric in the optical case where the reflection coefficient for vertical polarization actually goes to zero. Under those circumstances, unpolarized light becomes horizontally polarized on reflection at the Brewster's angle for the material.

If radio waves are considered as unpolarized, as suggested above, one can calculate the intensity loss on ground reflection by averaging the reflection losses in intensity for horizontally and vertically polarized waves. Since the earth has vast oceans and ice caps as well as continents, one needs to consider where reflections might take place along a path and include the ground losses which result. For the three types of surface — ice cap, ground, sea water — the intensity losses on 14 MHz are shown in Figure 10.6. There, it is seen how low losses result from ocean reflections and high losses from reflections on polar ice caps. Beyond those results, calculation shows a weak variation of ground losses with frequency, being slightly lower on 7 MHz and higher on 21 MHz for the various materials.

While on the subject of reflections, it should be noted that reflection surfaces are not always smooth or parallel to the local horizon. While the angles of reflection from a surface will always equal the angles of incidence of waves on it, the radiation angle of the outgoing waves will depend on the inclination of the surface. That will be important if the size or extent of a reflecting surface is many wavelengths across. If the scale of variations of surface regularity is smaller, then the reflection process becomes more diffuse in nature, not the mirror reflection usually considered. That results in more of a scattering of incoming radiation, an additional loss to be considered every time a ray path reenters the ionosphere after a reflection.

Earlier, it was pointed out that some focusing gain might be expected from iono-

spheric refraction because of ray convergence resulting from the concave nature of the F-region. By the same token, some de-focusing loss would be expected because of ray divergence from the convex nature of the earth's surface. Those effects would produce a slight gain, say a dB or so, over a path with several hops as the number of ionospheric refractions along a path of N hops exceeds the number of surface reflections, N-1, by one.

The last point to consider, no matter how many hops on a path, is fading and its sources. That question comes up when one wonders if a contact can be maintained once it's made, in short a question of reliability. In that regard, there are fades and FADES, the latter taking a signal down to the noise level. One can cope with the former but a path starts to break down when a signal disappears, dropping by more than 3 S-units. So whether a path is reliable or not depends on the most optimistic estimate of the S/N ratio and whether it could suffer a drop of 18 dB or so and still be in the range where a signal would be readable.

Fading really has its origins within the higher portions of the ionosphere, movements of the refraction region affecting propagation along a path. Thus, a rise of the F-region might shift ray paths so that the skip region around a transmitter has suddenly increased, placing the receiver in the skip zone. That is more of a matter of propagation failing, the path no longer being open for that operating frequency, and amounts to what is termed "MUF fading," the maximum useable frequency for the path falling below the transmitter frequency in use and then perhaps rising again.

Of course, there is the other side to that coin, the shift in ray paths placing the receiver closer to or farther away from where it would benefit from skip focusing. That would still be fading in the sense that the signal strength would rise and fall but is far less catastrophic than skip fading.

Another form of fading results from changes in wave polarization. Thus, if the electron content along a path changes for any reason, there will be a rotation in the plane of polarization at the receiving antenna with a corresponding change in signal strength. Such fading may be observed even on single-hop paths. Of course, having antennas with both horizontal and vertical polarizations and the ability to switch the receiver rapidly between them would minimize fading of that kind. But it should be noted that technique is generally limited to simple antennas, say dipoles and quarter-wave or half-wave verticals.

At this point, the essentials have been covered and it's time to stop and take the first of several overviews of HF propagation. The next one will illustrate points that'll become important as the hop structure and propagation circumstances become more complicated.

11: MOVING ON

Now that a one-hop path has been examined, from its main features to some of the finer details, the next step is to move on to longer hops and the more general aspects of propagation. While one-hop paths could be part of the DX scene for the Little Pistol, they're usually not much longer than 3,500 km because of the range of F-layer heights. That being the case, any longer path will involve two or more hops, span more than one time zone and go off in all sorts of interesting directions. No wonder Little Pistol finds them exciting.

Just to show what possibilities are out there, look at Figure 11.1, which shows an azimuthal equidistant projection map centered on Boulder, CO. In that map projection, great circle paths are straight lines and the beam headings for DX are evident, as the map is centered on a line passing through the north and south poles. In addition, that map projection gives distances from its center on a linear scale, grid lines corresponding to locations which are multiples of 5,000 km from Boulder and all the way out to Boulder's antipodal point at 40° S, 75° E, 20,000 km distant and not far from Amsterdam Island (FT8Z).

Figure 11.1 Azimuthal equidistant projection map centered on Boulder, CO.

On the subject of map projections, distortions are important to note, the Mercator projection representing the two geographic poles as straight lines instead of points; in addition, the distortions in that projection become progressively greater for regions farther away from the equator. In contrast to the Mercator projection, distortions in the equidistant azimuthal projection become greater in going away from the center of the map and, as noted above, the extreme is when the antipodal point, 20,000 km distant, is represented by a circle. In any event, with the Mercator projection, great circle paths at low latitudes look like segments of sine curves but paths which go through high latitudes may look like segments of the terminator at the equinoxes.

While those maps present a wealth of information, they convey nothing about the nature or topography of the terrain along any great circle path. That being the case, those maps must be supplemented by other information about reflection surfaces as signal losses will vary along a path, differing by as much as 3-6 dB between sea water and ground reflections. While the earlier discussion involved a chosen path, Boulder to St. Louis, other possibilities present themselves and it is important to know where the great circle paths fall on a map, and for more than just concerns about poor reflection surfaces. But those questions are easily settled by a distance-heading calculation which starts with the coordinates of the transmitter and receiver and brings forth the great circle beam heading and distance. Knowing that F-region hops are in the 3,500 km range, it's a simple task to decide how many hops will be involved, the heading for the path and the significant features which would be encountered by RF going along the route in question.

The simple one-hop path treated earlier had critical frequencies, foFE and foF2, given at the outset, for daybreak on the path between Boulder, CO and St. Louis, MO in mid-Janu-

ary. The next question has to do with how one finds similar ionospheric features for another path, say one requiring two hops in going from point A to point B, and another time. That brings up the $64 question — how to predict critical frequencies of the ionosphere.

Of course, if one had maps like those in Figures 4.2 and 4.3, it would be a simple task — just work out the geometry of the path using an azimuthal equidistant projection map, locate the midpoints of its hops and then use the contours on an ionospheric map to find the critical frequencies involved. Sound simple? It is, but not quite as indicated.

For one thing, the height of the F-layer would not be the same at the local times of the two midpoints of the path. That means that if RF were launched at some angle, the hop lengths of the two sections of the path would differ in length, the result being that the RF might undershoot or overshoot the receiver at the end of the path. So how is the launch angle arrived at? There are two choices, the hard way and the elegant way.

The hard way involves using the idea of mirror reflections at the virtual heights along the path. By working out the geometry along the curved earth, mirrors and all, it is possible to find the launch angle which connects the transmitter and the receiver. But how much do virtual heights differ from true heights of refraction on a path and how close do path lengths agree for the two cases?

In regard to the first question, Figure 11.2 shows virtual heights for mirror reflection and their variations with local time using a typical ionosphere, in this case during the month of December. For a curved ionosphere, it turns out hop lengths at radiation angles between 3 and 15 degrees differ by about 1% or so when mirror reflection and ray tracing are compared. That should be quite satisfactory for the problem at hand so given the local times at the midpoints, a launch angle can be found by using virtual heights at midpoints of the hops.

The next step in finding whether the path from point A to point B is open or not for that launch angle is to find the values for foF2 at the midpoints of the hops and the time in question. That means using an ionospheric map. When those are in hand, the problem then becomes one of finding the effective vertical frequencies, mentioned earlier, for the launch angle that takes the path from point A to point B.

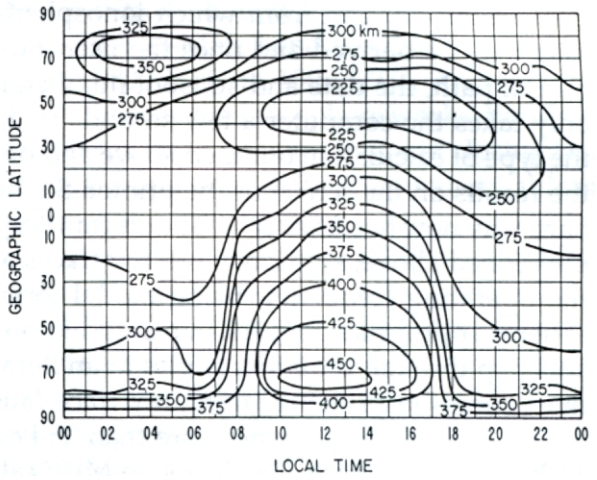

Figure 11.2 F2-layer heights for December.

While the radiation angles will be the same along the path, even after ground reflection, the differences in critical frequency and virtual height between hops will give different frequencies, f1 and f2, which may be returned to earth at oblique incidence. Clearly, the lower of the two is the one that ensures that RF will proceed from the transmitter to the receiver and is the maximum useable frequency or MUF for the path. Any higher choice of frequency will result in RF being lost to infinity on the hop with the lower value of foF2.

If that procedure were carried out for every hour of the day, the daily variation of the MUF would be obtained and indicate times when one amateur band or another might be tried in making contacts from point A to point B. All that's needed is ionospheric maps for the F-region critical frequency foF2- and F2-layer heights for the month in question; the rest is just arithmetic. And that's the tedious method that DXers used before PC programs came on the market, the National Bureau of Standards of the U.S. Department of Commerce providing all the ionospheric maps, nomographs and graphical aids needed.

Nowadays, HF propagation programs

contain information from which ionospheric data may be derived and once the user indicates a path, the date and sunspot number, it only takes the computer a few seconds to do the type of calculation outlined above and put the results on the screen or the printer. So the hard way now becomes easy. The elegant way, mentioned above, is to carry out ray traces at the operating frequency, using model ionospheres appropriate for each hop or local time, and step through radiation angles in an iterative process until the resulting ray trace falls within a target size, say no more than 25 km, at the end of the path. That's not an MUF calculation but does indicate whether a band is open or not at the time in question. Higher bands may be tried and limits set on the frequencies which may be used in the course of a day.

That sort of ray tracing can be carried out in the new Canadian computer program, SKYCOM, and used in many different ways to illustrate how HF propagation varies on a path, say with time, launch angle or frequency. And the program is quite flexible in the sense that any number of hops can be dealt with. While computing time is a factor, the limiting one is usually the curiosity and patience of the user.

But ray tracing brings up an important point about using computers in ionospheric calculations. In particular, ray tracing and MUF calculations require some sort of experimental database for critical frequencies, how they vary over the globe with seasons and sunspot numbers. In that regard, a user working with SKYCOM may employ either the URSI model ionosphere in calculations or the model ionosphere proposed by CCIR but most other MUF programs use just the CCIR database. In addition, SKYCOM gives critical frequency data from either model for any geographical location, date and sunspot number.

An important question is how the CCIR data is actually used in making MUF calculations. For example, the German program MINIFTZ4 carries out what seems to be a coarse interpolation of CCIR data in finding critical frequencies for its calculations. On the other hand, the methods of Raymond Fricker, formerly of BBC External Services, are based on the CCIR data but give the spatial and temporal variations of foF2 data by fitting them with a number of mathematical functions. Two of Fricker's better known F-layer algorithms, MICROMUF 2+ and MAXIMUF, give rather comparable results but they differ in complexity as the former algorithm uses 13 functions and the latter 26 functions. The last algorithm, MAXIMUF, with some modifications, has been used in HF prediction programs such as MINIPROP and IONSOUND.

While MINIFTZ4 and MAXIMUF are based on CCIR data, the amount actually used was limited to that from times around the equinoxes and solstices. MINIFTZ4 carries out interpolations in latitude, longitude and time using the CCIR data itself while MAXIMUF uses the data from the equinoxes and solstices but MAXIMUF's functions were optimized to give the best fit of the variations of foF2 with latitude, time of day and year.

The American HF prediction program, IONCAP, is well known and, after its development by the Central Radio Propagation Laboratory of the U.S. Department of Commerce, it was first distributed in 1978. The method by which IONCAP represents the spatial and temporal properties of the ionosphere is termed "numerical mapping" and uses a series of mathematical functions with coefficients adjusted for each month and time of day. In that regard, the IONCAP program includes data files to generate coefficients for each month of the year. While IONCAP may be used to find MUF information, it's much more flexible, having a total of 29 different methods to predict the performance of HF radio systems.

In its original form, IONCAP operated with computing systems which used IBM-punched cards for its data input. That format was carried over to the version of IONCAP developed for personal computers and is quite slow, tedious, even exasperating to use. Nowadays, one can enjoy all the benefits of IONCAP without those troubles as the CAPMAN program, based on IONCAP, employs a driver to allow data input without the problems that go with the punched-card format.

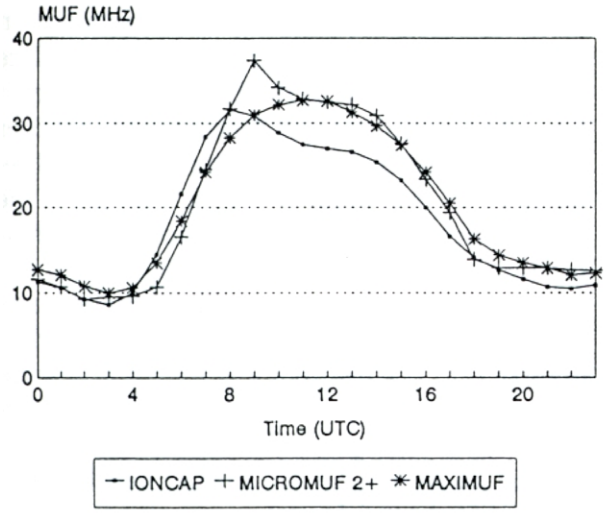

Figure 11.3 MUF curves from three propagation programs for the path from Frankfurt, Germany to Riyadh, Saudi Arabia.

Because of the large number of coefficients used in its numerical mapping, IONCAP is felt to give the best representation of ionospheric situations and has become the standard against which the results of other programs are compared. As an example, Figure 11.3 shows MUF curves for IONCAP and two of Fricker's algorithms, MICROMUF 2+ and MAXIMUF, for a 4,330-km path in the month of January, heading 117 degrees east of north from Frankfurt, Germany to Riyadh, Saudi Arabia. While there is general agreement in shape, one can see that significant departures, as much as +/-5 MHz, may exist between the results for MUF values from those two algorithms and those from IONCAP.

There are other prediction programs less sophisticated than those noted above, say Fricker's MINI-F2 and MINIMUF. Their predictions are far less satisfactory as they're both based on single-function algorithms, unable to deal effectively with the wide range of paths, seasons and solar conditions and still give results which are comparable to IONCAP and the other programs.

Returning to the MUF curves in Figure 11.3, one might conclude from their shape that the 14-MHz band would be open from about 0600 UTC to 1800 UTC. Then, depending on which curve is chosen, the 21-MHz band would be open from around 0700 UTC to 1600 UTC while the 28-MHz band would be open from about 0800 UTC to 1500 UTC. As a pattern, that's the way the ionosphere works, the lower frequency band opening first and closing last. It's just a matter of solar illumination, at least when it comes to opening.

And if one took those MUF curves at face value, it would seem that the 7-MHz band would be open 24 hours a day! And the same is true for the 3.5-MHz band. In that regard, I can only say it's just amazing what MUF data will suggest by itself, especially when used incorrectly. The problem, as you well know from the earlier discussion of the Little Pistol's path, is MUF curves do not contain any sort of information about the factors that go into signal strength, such as absorption and reflection loss as well as transmitter power and antenna gains, and noise, mostly from man-made sources. In short, MUF curves involve wave refraction at high altitudes and are only one-third of the story, not covering any of the ionospheric effects at low altitude or the noise factors that go into HF propagation.

One can use the present case, the path from Frankfurt to Riyadh, to show how propagation works, going beyond the MUF curves in some detail. Thus, there are actually two things which defeat full 24-hour usage of the 7-MHz and 3.5-MHz bands, ionospheric absorption and the E-region cutoff frequency. Absorption was discussed earlier, the situation where signal strength is reduced because of wave energy transfer to the atmosphere by the electron-molecule collisions in the D-region when the RF goes by.

And since ionization in the D-region results from illumination by the sun, absorption processes begin with sunrise and end with sunset. While not mentioned earlier, during daylight on a path, absorption varies inversely with the square of the frequency for ordinary or O-waves at the upper end of the HF range. At the lower end of the HF spectrum, extraordinary or X-waves suffer even greater absorption with frequency because magneto-ionic effects become more important when the radio frequencies are comparable to electron gyro-frequen-

cies. For frequencies like 3.5 MHz and 7-MHz, paths are more vulnerable to absorption than higher frequencies such as 21 and 28 MHz.

Returning to the present case, D-region absorption is so great from 0400 UTC to 1500 UTC as to make the path unworkable on 3.5 MHz. In the same fashion, the path drops out on 7 MHz from around 0500 UTC until 1400 UTC. But only part of that is due to signal absorption; the remainder is due to signals being cut off from the F-layer by the rise in critical frequency foFE of the E-region with solar illumination. In that regard, the screening of low frequency signals from the F-region by E-region ionization was illustrated earlier in Figure 7.5.

So the simple propagation mode that involves two F-hops during darkness changes to one with mixed modes, an F-hop on the dark end of the path and an E-hop in sunlight or just E-hops when the path is fully illuminated. The latter suffer from heavy D-region absorption and bring signal levels down to the point where the path is closed for all intents and purposes. Those changes in propagation mode are shown symbolically in the four parts of Figure 11.4: going from a 2F mode in (a) to a mixed mode, 1F1E, in (b), then the 2E mode suffers a blackout because of great absorption, so then to a mixed mode, 1E1F, in (c) and finally the 2F mode again in (d).

In analytical terms, the changes in the E-cutoff frequency and ionospheric absorption along the path are shown in Figures 11.5 and 11.6, respectively. The first of those two figures shows the E-cutoff frequency at each end of the path. Since the E-cutoff frequency does not exceed 10 MHz, signals on the 10-MHz band and all higher bands are not affected by the E-layer, at least as far as being cut off.

However, the 7-MHz and 3.5-MHz bands are seriously affected, as noted above. From Figure 11.5, one sees that the sunrise on the low latitude part of the path is earliest and thus the E-cutoff condition sets in there first. And since the higher latitude end of the path is about 40 degrees farther west in longitude, sunset on the path is later there and the E-cutoff condition ends there last. Those results are the basis for the mode changes in Figure 11.4.

The other effect of solar illumination on the path is signal absorption. That takes place when signals traverse the D-region, on ascent from the transmitter and descent to the receiver as well as just before and after the ground reflection. In that regard, Figure 11.6 gives the total absorption along the path for the five harmonically-related amateur bands. It should be noted that the absorption values were calculated without regard to whether the band was open or not. The results show that total absorption along the path rose with solar illumination and reached peaks of 12 dB (2 S-Units) or less on 14 MHz and the higher bands but it reached 50 dB (8 S-Units) or more on the lower bands, essentially shutting them down for communication purposes.

To those losses the signal loss on ground reflection must be added. The 2F mode is the most durable one, either at night on the lower frequencies or daytime on 14 MHz and above. Ground loss is independent of solar illumination and for the radiation angle (13°) which connects the end points of the path, reflection takes place on the ground in western Turkey where the loss would be about 4 dB of 14 MHz. The ground reflection points for the mixed modes would be different than the one given above for the 2F mode but those modes are only of brief duration and will not be considered

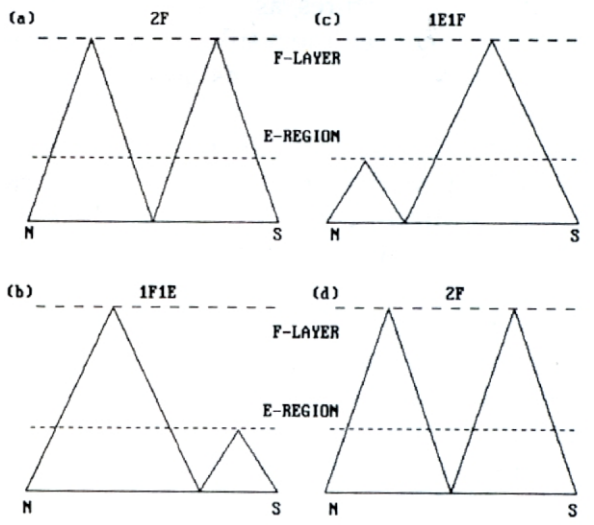

Figure 11.4 Symbolic representation of the propagation modes for the Frankfurt/Riyadh path.

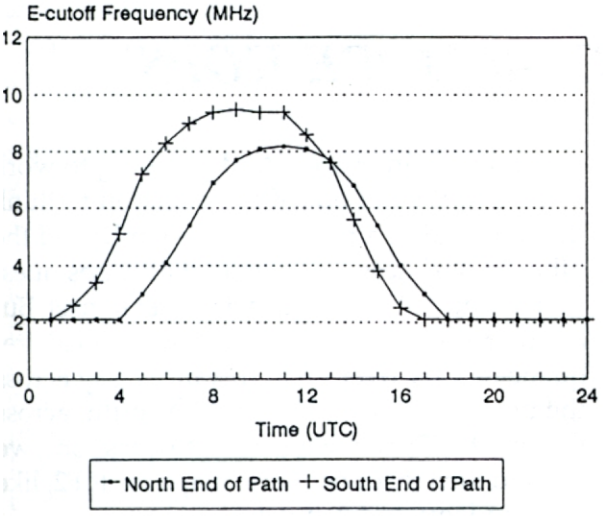

Figure 11.5 E-region cutoff frequencies at the two ends of the Frankfurt/Riyadh path.

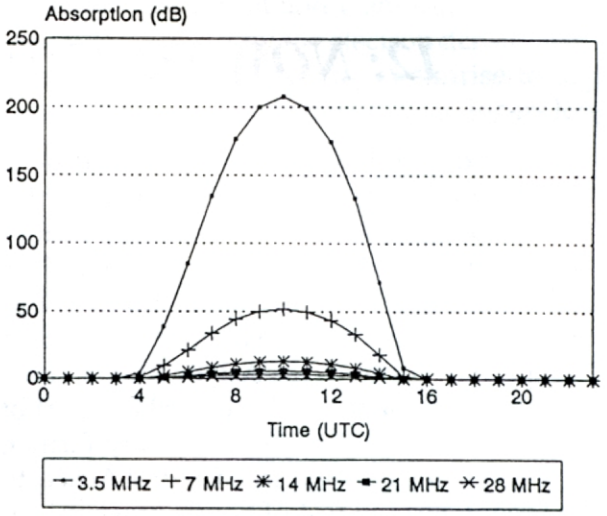

Figure 11.6 Ionospheric absorption for the Frankfurt/Riyad path as a function of frequency.

further.

The last aspect to consider for the present path is noise, either atmospheric or man-made in origin. With regard to atmospheric noise, the level at the northern end of the Frankfurt/Riyadh path in January would be comparable to that found at the same time in the eastern states in the USA while at the southern end of the path, the noise would be comparable to that in the Caribbean, but certainly nothing intense like the levels of noise in South America or South Africa. Man-made noise levels at the two ends of the path would probably be higher than atmospheric values, at a residential level as a minimum and more likely industrial since both locations are major cities.

In any event, propagation for other two hop paths could be worked out as done earlier but now using the ideas and details outlined above: MUF values, E-cutoff frequencies, D-region absorption, ground loss and man-made noise. The only details still to be settled are operating frequency, transmitter power levels and antenna gains at both ends of the path. But lest anyone has missed the point, let me stress again that whether propagation on a path is workable or not depends on whether three conditions are met, all at the same time: an open band (MUF), good signal strength and low noise levels. As we say in the trade, "MUF is not ENUF!"

12: NOW TO THREE OR MORE HOPS

The discussion up to this point has dealt with nothing more than two hops, paths which go out about 7,000 km from the Little Pistol's QTH. Thus, looking at the map centered on Boulder in Figure 11.1, one sees with two hops the LP's signals could reach out to Western Europe and North Africa, Asiatic Russia, some islands in the Pacific and the northern part of South America. But to reach out any farther, say beyond the Balkans, into Central Africa, to the Orient and the rest of South America, another hop would be needed. But what would that mean in terms of the ideas developed so far?

Let's take a round number, 10,500 km, for a path length; for that distance, 50% greater than the length of the two-hop path, the Little Pistol's signal strength would fall by about 3.5 dB due to additional signal spreading. That's not even a full S-Unit; not to worry. But another surface reflection would be involved, maybe off of sea water for a change. In any event, that would be another 1-4 dB loss, whether day or night. And then there's D-region absorption, maybe something like another 6 dB loss on 14 MHz if the path were sunlit or essentially nothing with darkness of the path.

Putting the losses all together, the sum would range from about 5 dB to 14 dB or about 1 to more than 2 S-Units lower signal at the DX end of the longer path. The good news is that the noise would probably be about the same unless the Little Pistol was trying to make a DX contact with Indonesia, South America or South Africa in their summer thunderstorm season. Those directions would cover about 270 degrees of the field of view from Boulder, assuming the Little Pistol's QTH is not too close to the Flatiron Range on the outskirts of Boulder. The rest of the compass directions would extend from Siberia to Central Europe, good DX paths all.

With DXing out to those distances, the range of longitude or number of time zones along a path increases. And in trying to work some DX, it's not out of the question to think that one end of a path could be sunlit and the other in darkness. Of course, that raises questions about critical frequencies after sunset. But another question would be how critical frequencies vary over great distances, say across the northern polar cap or to the south, across the equator. For answers to those questions, we need to turn to ionospheric maps for foF2, like those in Figures 4.2 and 4.3.

Take Figure 4.3 to start with; that's from a time of high solar activity and makes for a more optimistic and cheerful discussion. The left half of that figure is the part of the earth in sunlight and the right half is in darkness. Of course, full illumination of the part of the earth facing the sun continues as it rotates on its axis; the only thing that changes is the part in daylight, the sun moving across the sky, east to west.

Now the point has been made that the ionosphere is created by solar UV so one has to think that the creation of an ionosphere is a continuing process, centered at the subsolar point and thus extending over half the earth's atmosphere. Unlike the oceans which have tremendous inertia, the part of the atmosphere close to the earth co-rotates with it. Thus, while solar illumination of the earth is steady in time, fresh atmosphere rotates into solar view around dawn, then it's carried past the noon meridian and finally out of solar view at the dusk. Relative to us fixed on the ground, the ionosphere, represented by the foF2 contours in Figure 4.4, advances as a whole across the sky, just like the sun. But there are interesting features of the contours in Figure 4.3, first crowded around the Greenwich Meridian where the sun is rising at 0600 UTC and still going off into darkness, beyond the sunset line at 180° E longitude.

The rapid rise in foF2 values at sunrise is due to the buildup of electron density at F-region heights with the onset of photoionization.

But the slow decay of ionization in foF2 values after sunset is quite different from the rapid disappearance of ionization in the E-region, shown by foFE contours in Figure 4.4. Those changes, taking place at two different altitudes, should be discussed at this point so we will digress to indicate their differences and their similarities.

In its ionized state, a small volume of the ionosphere contains a number of negative electrons, important to propagation, and an equal number of positive ions, keeping the volume electrically neutral. Normally, the ionization is produced by the effects of solar photons in the UV and X-ray range. At low altitudes, the positive ions will come from nitrogen and oxygen molecules and at high altitudes there will also be positive ions from oxygen atoms.

In that volume, the electrons, ions and neutral constituents will all be colliding and interacting. Electrons can recombine with the positive ions and produce neutral structures again. With molecular ions, the recombination may result in the molecule being dissociated into atoms; for example, an oxygen molecular ion can recombine with an electron and result in the formation of two oxygen atoms. That process is called dissociative recombination. Another possibility is an atomic oxygen ion can recombine with an electron and result in a neutral oxygen atom and the emission of a light photon. That process is called radiative recombination.

If that wasn't complicated enough, a positive oxygen atomic ion (O+) can exchange places with a nitrogen atomic ion (N+) in a nitrogen molecular ion (N2+) and create a nitric oxide ion (NO+). That, in turn, can recombine with an electron and produce a nitrogen atom and an oxygen atom. In short, it's a big chemistry lab up there and anything that can happen between ions and molecules will happen.

Now it turns out that recombination goes slowly when an electron encounters an oxygen atomic ion (O+) and much faster when it encounters any of the molecular ions. But the oxygen atomic ion is found mainly up in the F-region and the molecular ions are found down in the D- and E-regions. From the latter, one can see why the D- and E-regions disappear so rapidly with sunset and from the former, one can understand why the electron density in the F-region builds up rapidly at sunrise to high concentrations and, in part, why it lingers long after sunset.

In those few paragraphs, some of the main ideas behind ionospheric chemistry have been pointed out. Obviously, the reactions between electrons and positive ions can affect propagation by shifting the electron density one way or the other. As a matter of fact, the "winter anomaly" for the F-region, higher foF2 values in the winter when the sun is lower in the sky, find its explanation when those simple reactions are combined with atmospheric chemistry. Actually that is great for DXing as with the sun lower in the sky, the MUFs are higher yet there is less D-region absorption. But we'll get to that shortly.

Other interesting features of the foF2 map in Figure 4.3 are the low values of foF2 in the polar regions and high values found at equatorial latitudes, particularly in the afternoon and early evening hours of local time. The low values of foF2 in the polar regions will be seen to have a solar origin, involving the interaction of the geomagnetic field and solar plasma streaming by, while the high values at low latitudes result from the redistribution of ionization by tidal effects in the atmosphere.

At this point in the discussion, features of the ionospheric maps across greater distances are of interest in that the Little Pistol can explore more of them with longer paths which reach beyond the middle range of latitudes. Thus, there is propagation on transpolar and transequatorial paths to consider. And there are the effects of solar activity to add to the discussion, how changes in sunspot numbers may affect the reliability and reach of propagation paths. As a matter of fact, once we get into paths of three or more hops, the discussion soon becomes wide open, almost to the limit of round-the-world (RTW) signals. So let's turn to it, starting with the discussion of MUF predictions.

On two-hop paths, the maximum useable frequency (MUF) at a given time is obtained

by finding the limiting frequency for each hop and then taking the lower of the two values. The same idea is used for longer paths but consideration is limited to hops at the two ends of the path, not in the middle. That approach goes back to WWII when Newbern Smith in the USA and K. W. Tremellen in the U.K. developed the idea of "control points" for a path.

Their argument was that propagation on a path failed most often at one end or the other. Thus, the approach was to find the MUF values at two control points on the great circle path, at 2,000 km from each end of the path, and use the lower of the two to represent the MUF for the path as a whole. An additional pair of points at 1,000 km from the ends of the path may be used to examine whether the E-region plays any role in controlling propagation, as discussed earlier.

That technique is used extensively in MUF programs for computers and gives reliable results for two hops when the role of the E-region is included. Going to three or more hops, results vary in reliability, depending on the path under consideration. For example, for three or more hops that stay within the mid-latitude range or go south toward or across the equator, the method proves to be quite reliable. That is the case as critical frequencies foF2 at the control points near each end are lower than that of the middle hop at a lower latitude, as may be seen from Figure 4.3.

But looking at that figure, one sees that foF2 values at high latitudes are lower than at mid-latitudes. As a result, the MUF on a middle hop of a longer, poleward path could be lower than the operating frequency and the full path fails to support propagation even though data from the control points at the ends would suggest otherwise. An illustration of those features may be seen in MUF calculations for a path from San Francisco to London for the same month, March. That path involves a great circle distance of 8,732 km, up across Hudson Bay in Canada and the southern tip of Greenland. The path can be broken down into three equal parts and when the IONCAP prediction program is used to find MUF values for each, the results shown in Figure 12.1 are obtained. There, the

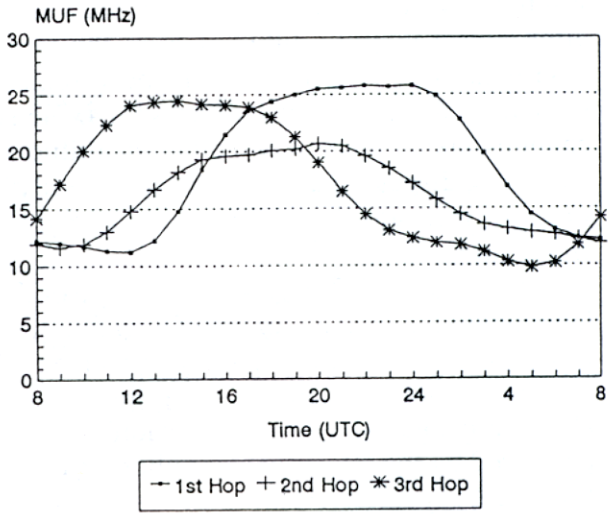

Figure 12.1 MUF variations as a function of time for three hops on a path from San Francisco to London, England.

first hop in Western Canada and the third hop in the North Atlantic show strong daily variations in their MUF values but the second hop is somewhat more poleward than the hop over the North Atlantic. As a result, its MUF variation in not as great and controls propagation for part of the day, as seen in Figure 12.2 which gives the MUF for the entire path but calculated using three control points as well as the usual pair of points.

In the case of three hops on a path which

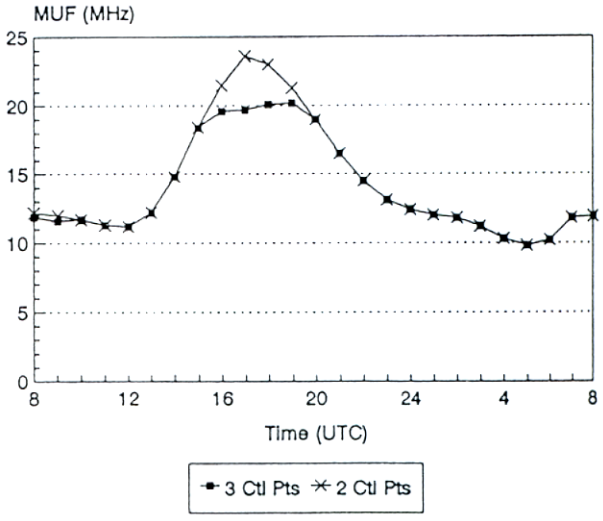

Figure 12.2 MUF variations as a function of time for the entire path from San Francisco to London.

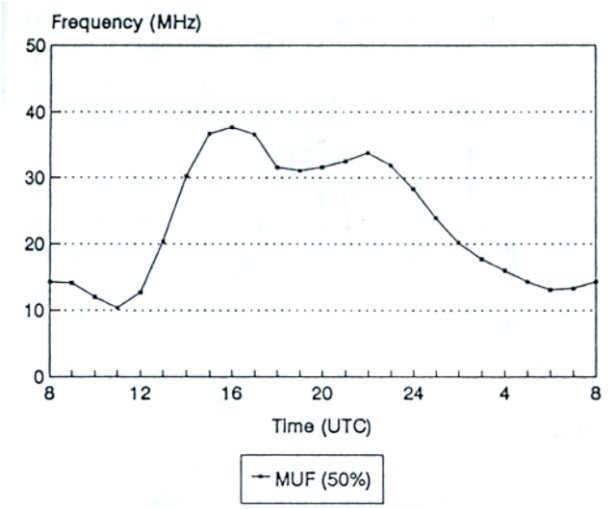

Figure 12.3 MUF variations as a function of time for the path from Boulder to Asunçion, Paraguay.

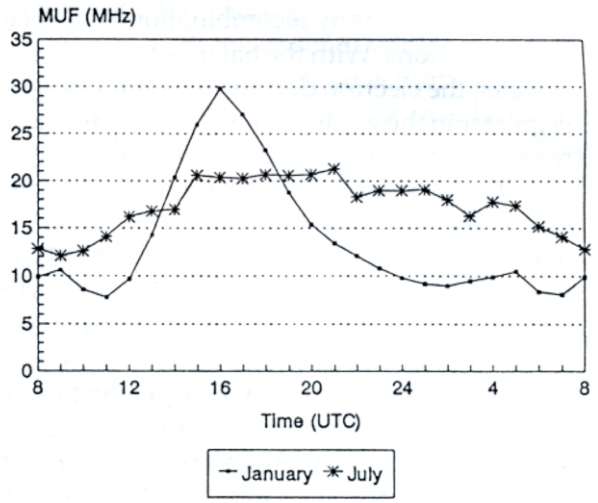

Figure 12.4 MUF variations as a function of time for the path from Boulder, CO to Madrid, Spain in January and July.

crosses the geographic equator, the critical frequencies at the ends of the path are the controlling factors. But for that type of path, the value of the MUF may be significantly larger than for another path of comparable length which stays within one hemisphere.

That is the case because of the higher critical frequencies at low latitudes and is illustrated by MUF curves derived using IONCAP, shown in Figures 12.3 and 12.4. There, two paths are used, both from Boulder in the month of January but one path (8,798 km) going across the equator to Asunçion, Paraguay (Figure 12.3) and the other path (8,061 km) to Madrid, Spain at almost the same latitude as Boulder (Figure 12.4).

The striking feature of Figure 12.3 is the magnitude of the peak MUF value at 1600 UTC, almost twice that shown for the northerly path in Figure 12.2. However, since the calculations were for the month of January, it is not clear from the MUF curve for the path as a whole if the difference is due to winter conditions north of the equator or summer conditions to the south. The foF2 map in Figure 4.3 is of no help either, being appropriate for an equinox instead of close to a solstice, as in Figure 12.3.

But that's where the results for the second path in Figure 12.4 come in. The great circle path goes from Boulder to Madrid, Spain, starting and ending at 40 degrees north latitude and never going above 47 degrees north latitude. The two MUF curves are for July and January; the first shows only a broad, featureless variation during summer while the second shows a large, striking peak in MUF during winter.

The winter increase in the foF2 frequency, as shown by MUF values in Figure 12.4, is termed the "winter anomaly" as it is just opposite to the behavior of other critical frequencies like foFE which decrease with lower solar elevation in winter. By way of explanation, the winter peak in MUF means more ionization exists in the F-region or less ionization is lost by recombination in the winter. Thus, the winter anomaly has to do with the ratio of the production and loss of electrons. Production is directly related to the presence of atomic oxygen in the region and losses are due to recombination of molecular ions, or equivalently, the number of molecules.

Now the study of atmospheric chemistry has shown that the ratio of the number of oxygen atoms per unit volume to that for nitrogen and oxygen molecules varies during the year at F-region altitudes. In fact, that ratio is greater in winter than in summer, thus favoring the production of electrons from O-atoms over

losses of electrons by recombination in molecular interactions. With the balance tipped in that manner, the electron density at F-region heights is greater in the winter months and, by the same token, so are MUFs for propagation.

Those variations in critical frequencies take place on a long time scale — months. The question then is whether there are other large variations of critical frequencies on a shorter time scale, say from one day to the next at a given hour of the day. The answer there is in the affirmative and the effect is greatest in the winter months. That brings up the larger question of statistical fluctuations of critical frequencies, a very important subject for Amateur Radio.

But first, to anchor the discussion in the reality of experimental observations, look at Figure 12.5 which shows foF2 values recorded from ionospheric sounding at Slough, England in January 1969. For the month of January, there are 31 measured values of foF2 for each hour of the day and the data points in the figure tell the story, the ionosphere showing considerable variation in its characteristic features. As is the custom in dealing with such situations, the first quantity that's derived for an hour of data is the monthly median value. That value divides the data set, half of the data points for that hour lie at higher values of foF2 and half at lower values and the line in the figure traces the median values through the hours of a day. But that only settles the middle of the range of foF2 values for a particular hour of the day in the month; the spread of values above and below that median value remain to be determined. Again, use is made of statistical definitions and terminology, the upper and lower decile values; they are the dividing lines for the upper 10% of the 31 data points for the hour in question, say the three highest values of foF2, and the lower 10%, the three lowest values of foF2.

A close examination of the data in Figure 12.5 shows the monthly median value at 1600 UTC is 7.6 MHz, the upper decile value is 9.2 MHz and the lower decile value is 6.8 MHz. Another way of expressing the meaning of the upper and lower decile points is to say that 90% of the observations at that hour were above the

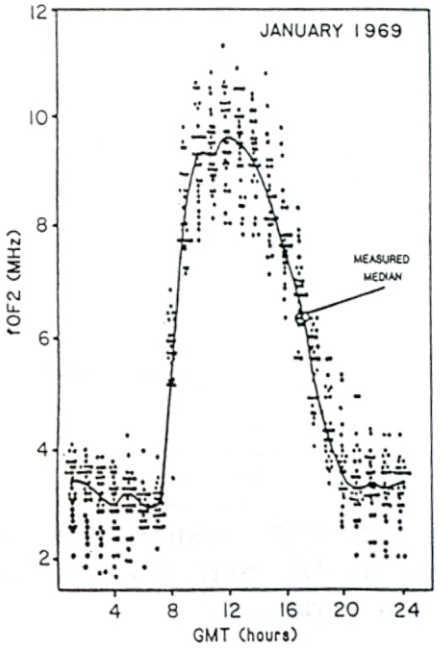

Figure 12.5 Ionospheric variability shown by foF2 soundings from Slough, England. From Piggott and Rawer [1972]

lower decile value, 10% above the upper decile value and 80% of the observations between the two decile values. If the ionosphere over Slough, England were the control point for a one-hop path, at 1600 UTC, the observed maximum useable frequencies on the path would have exceeded those derived from the lower decile, median and upper decile values of foF2 on 90%, 50% and 10% of the days, respectively.

Clearly, the daily variation of foF2 values shown in Figure 12.5 means that predictions based on them would show the same variability. So, noting the large change in foF2 between day and night as well as the near constant spread in daily foF2 values, it follows that the percentage variation in predictions would be particularly large during a winter night. But experience shows that the percentage variation at night decreases as the seasons change, being smallest during summer. In regard to variations in predictions, the IONCAP program gives three different values for the maximum useable frequency at a given hour on a path: the highest possible frequency (HPF) from the upper decile value mentioned above, the MUF for the median (50%) value of foF2 and the FOT

(an abbreviation of optimum working frequency from French) which is taken as 0.85 of the median MUF.

In practical terms, that means if an operating frequency falls on the HPF of a path, the chances are one-in-ten that the band will be open at the time in question. The chances are 50-50 if the band frequency falls on the median MUF and close to nine-in-ten if it falls around the FOT. But it should be borne in mind that "open" has nothing to do with signal strength or noise, the other two quantities which determine the reliability of propagation at a given hour.

In that regard, an interesting exercise in propagation is to compare how long a path is available just in terms of operating frequency and how long signals are strong enough for real communication. The latter is usually a small fraction of the former, meaning that a lot of time could be wasted pursuing a DX contact just on the basis of MUF data alone when signal strength information would be more to the point, achieving success on a path.

Of course, the remarks in that last paragraph imply that the propagation program in use is one that includes signal strength, perhaps even noise, in its predictions. In the early days of computer predictions, the amateur community relied heavily on programs which only had a MUF capability. That was adequate on the higher bands, say 10 and 15 Meters, during times of high solar activity but fails miserably at low levels of activity, toward solar minimum. Now, with computers having greater memory and MUF programs coming closer to IONCAP's predictions, full-service propagation programs are the norm, not the exception.

But progress in that direction has come at a price in another, the loss of awareness of the ionosphere as a whole. Earlier, when more tedious, manual methods were used in making HF predictions, the user had access to ionospheric maps and could see how the ionosphere changed with time, say shifting northward, largely within the bounds of the terminator, with the coming of summer and then southward with the onset of winter. And then there are the changes in solar activity, the ionosphere puffing up with the rise in activity toward solar maximum and then the deflation on going toward solar minimum.

The idea of puffing up may be seen by comparing Figures 4.2 and 4.3, in that order, and that of deflation may be sensed by thinking that an ionosphere at solar maximum, as in Figure 4.3, is then followed 6-8 years later by one at solar minimum, as in Figure 4.2, when the cycle ends. But the exciting thing for Amateur Radio is that the whole process will start all over again, a renewal with the next cycle, with everything that goes with solar activity to be repeated again, DX in all its glory!

Beyond those ideas, the decline in the use of ionospheric maps resulted in the ionosphere being taken for granted, thought of more as a large, distended mass of ionization, not something with detail or structure to it like the valley of foF2 contours around sunrise or the mountain of ionization around the equator (actually the geomagnetic equator). That meant a shift away from understanding the details of ionospheric refraction, as shown by ray tracing, to a reliance more on symbolic methods, using mirror reflections.

By not using the variation of refraction with frequency, the symbolic methods only show how gross deviations in paths result from tilts or changes in electron density of the ionosphere, either from variations in layer height or differences in critical frequency along a path. But the role that frequency plays is important to the magnitude of simple effects like hop length, and it separates other refractive effects, chordal hops and ducting in propagation over great distances. So without a good map and the methods to make use of it, it's impossible to develop a good feeling for the lay of the land in ionospheric terms and the quantitative sides of important features of propagation for great distances. That being the case, we turn to ionospheric maps to see what they can tell us.

13: GOING FURTHER AND IN MORE DETAIL

When one travels, whether on foot, by automobile or boat, even by radio, it pays to have a map or chart to go by. As discussed earlier, radio propagation involves two types of maps, one for the E-region and the other for the F-region, and they may be thought of as stacked, with one above the other, at about 115 km and around 300 km altitude. But just which region controls propagation at a given time depends on the frequency involved and where the region in question is encountered.

In some circumstances, say frequencies above 14 MHz, the E-region is of minor importance, only deviating RF rays slightly on penetration and not screening them off from the F-region. Thus, one could consider only the effects from ionization in the F-region and use a foF2 map to set the level of ionization at the F-layer peak; how the ionization is distributed with altitude below the F-peak is another matter and depends on the time of day.

That brings up another aspect of ionospheric maps: half of the E-region map is essentially blank or empty, solar UV not reaching the dark side of the earth and E-region ionization on the day side being lost rapidly at sunset. That being the case, if one thinks of the maps as being stacked, HF propagation by the part of the F-region above an empty or blank part of the E-region map is pretty much the same at low frequencies in the HF spectrum as when the higher part of the spectrum freely penetrates the illuminated portion of the E-region. Thus, while operations of the 3.5-4.0-MHz band typically involve short hops during the day, longer paths are possible across the ionosphere at night. Beyond that, any further details would depend on how foF2 contours are organized and the distribution of ionization with altitude.

The ionospheric maps considered so far involved symmetrical illumination of the earth at the spring equinox. But the latitude of the subsolar point shifts during a year, reaching 23.5° N and 23.5° S at the summer and winter solstices, respectively. Since differences in solar illumination at the two solstices go according to which hemisphere contains the subsolar point, consider the summer solstice around June 21; any results for that time would essentially apply also around December 21 in the Southern Hemisphere.

Let's start with the ionospheric map for the E-region and take the time as 0000 UTC, when the sun is on the International Date Line out in the Pacific Ocean. Now, instead of dealing with the ionosphere in abstract terms, the land masses below it will be included. So consider Figure 13.1 which shows the Mercator map of foFE contours, centered over the West Coast and with contours in 0.5-MHz steps, from 1.0 MHz to 3.5 MHz. Solar illumination is centered on 23.5° north latitude and 180° longitude and the 1.0-MHz contour falls close to the Mercator projection of the terminator, the line dividing sunlit regions from those in darkness.

Now consider the foF2 contours for the same circumstances, shown in Figure 13.2. On comparing the two maps, one sees the influence of sunlight on the F-region, sharp and strong around the sunrise portion of the terminator but declining beyond the line of darkness. By way of interpretation of the experimental data, it's clear that all F-region ionization is not lost with sunset, as in the E-region. Instead, it lingers for quite a while, as shown by the lower critical frequencies foF2 in the region of darkness.

Beyond the shape of the foF2 map and its relationship to the terminator, there are interesting features within the contours, the high values of foF2 on contours at low latitudes and, curiously, in the late afternoon region of local time. Those prove to be geomagnetic in origin but for the moment, the higher foF2 values at low latitudes go to explain the MUF curves for the Boulder-Asunçion path in Figure 12.3. That

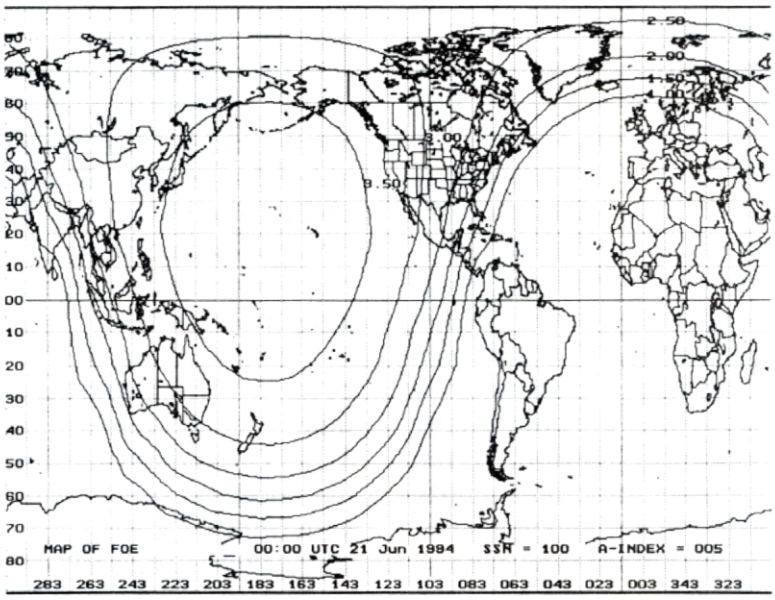

Figure 13.1 Global foFE map for 21 June (SSN=100).

figure was for the month of January but if one thinks of swapping hemispheres in Figure 13.2 to get a foF2 map for December, the results are fairly obvious.

Next, looking at mid-latitude contours in the summer and winter regions of the ionosphere in Figure 13.2, one can understand the results obtained earlier on the path from Boulder to Madrid, shown in Figure 12.4. In particular, one notes that foF2 values vary only slowly with longitude in the Northern Hemisphere, explaining the weak variation in MUF on the path around at 40° N latitude and with termini separated by about 100 degrees of longitude. During winter months in the Northern Hemisphere, the situation would be similar to that in the lower portion of Figure 13.2. Thus, the strong peak in the MUF on the Boulder/Madrid path finds its explanation the closely spaced foF2 contours around the dusk meridian.

Now this section was touted as "Going

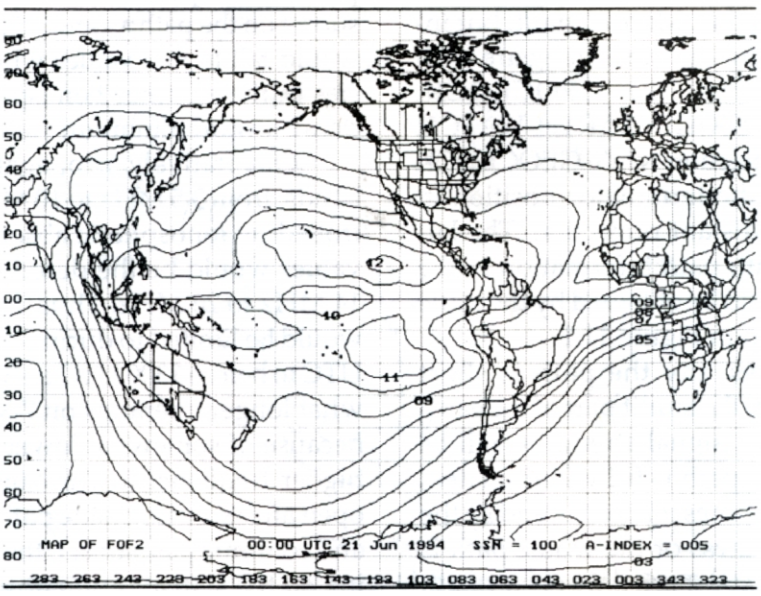

Figure 13.2 Global foF2 map for 21 June (SSN=100).

Further and in More Detail" but we've come to the point where the going gets tough. That is the case as the paths discussed so far essentially all fell within the main parts of an foF2 map, contained within the bounds of the terminator and something which is fairly easy to keep clear in one's mind. But going to paths which reach beyond 10,000 km distance, one-quarter the way around the world, and keeping appropriate ionospheric features straight in one's memory becomes quite a challenge. Beyond that, operating frequencies and their relation to critical frequencies are not the only parts of the propagation equation; signal strength and noise are other important quantities too. And the statistical variations in critical frequencies and in the propagation of noise are important as well.

While knowledge of MUF values requires calculations with a propagation program, either on a computer in the shack or from the curves published monthly in *QST,* qualitative aspects of signal strength can be obtained by looking at the amount of illumination on a path and how it varies in the course of a day. That is done by looking at how the path lies relative to the terminator. A quick and easy way of doing that is with the DX EDGE, a series of plastic slides with the shape of the average terminator in every month, which can be slid along a Mercator map of the world to simulate the earth's rotation in a day. More elegant, but involved ways of doing the same thing are with computer programs like GEOCLOCK, EARTHWATCH or DXAID. EARTH-WATCH uses a Mercator projection while GEOCLOCK and DXAID show the terminator position in the azimuthal equidistant projection. The latter fit quite well with path information in the same format, as would be obtained by the Little Pistol using the map in Figure 11.1.

In simple cases, say the path is short enough to fall within the sunlit part of the earth sometime in the day, signal strengths will be the lowest when the path is fully illuminated, and will improve at times when one end or the other goes into darkness or the whole path is in the dark. But that approach only gives qualitative information on signal strength and the operating frequency must be taken into consideration, as suggested in the earlier discussion that went with Figure 8.1. And those times would have to be compared with MUF data for the times when the path would be available for operation. Finally, the matter of reliability would be settled by considering the presence of noise, greatest during waking hours from man-made sources or seasonal from atmospheric origin.

A good example of how those matters can be handled from both the qualitative and quantitative standpoints is found by considering the 3Y0PI DXpedition in February '94. At the time, the smoothed sunspot number was 35 and the path from the Little Pistol's QTH to Peter I Island (68.8° S, 90.5° W) relative to the terminator is shown in Figures 13.3 and 13.4. In those projections the sun's position is shown about 12.6 degrees south of the equator and the termini are at the ends of the path. Local noon on the path is about 1845 UTC, as indicated in Figure 13.3.

From the earlier discussion, some tentative conclusions may be drawn just from the terminator in Figure 13.3. For example, sunrise on the path would be around 1300 UTC and with that, critical frequencies foF2 would show a rapid increase along the sunrise portion of the terminator. The ionospheric absorption on the path would peak around 1845 UTC and with sunset on the path around 0100 UTC, absorption would fall to low values while critical frequencies in the summer hemisphere would slowly decay toward minimum values around dawn.

Qualitatively, propagation on the lower bands, from 3.5 MHz to 10 MHz, would be controlled by ionospheric absorption while MUF values would be the determining factor from 14 MHz to 28 MHz. Thus, low-band openings would be limited to during darkness, after 0100 UTC to before 1300 UTC on 3.5 MHz and somewhat longer openings on 7 MHz and 10 MHz, because of somewhat lower absorption at the higher frequencies. The higher bands would open after sunrise on the path, about 1300 UTC, and continue past sunset, the duration depending on the statistics of ionospheric critical frequencies for a sunspot number of 35.

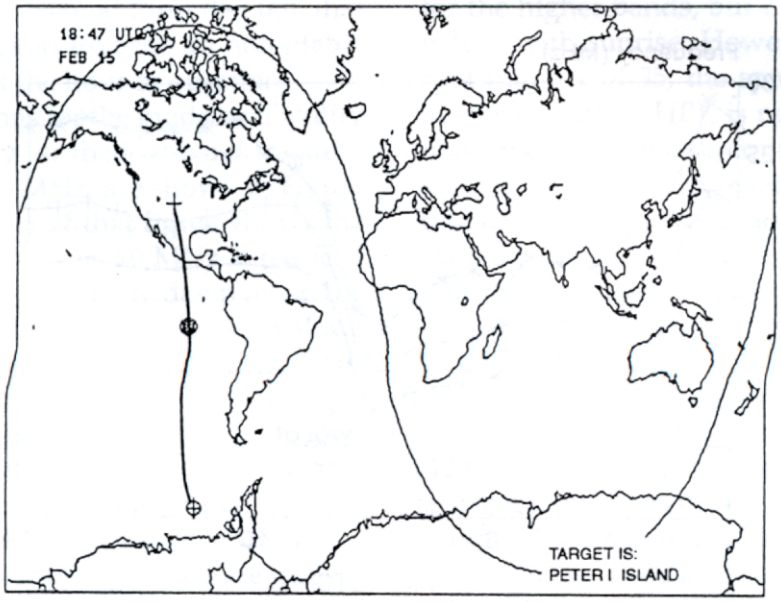

Figure 13.3 Mercator map showing the path from Boulder, CO to Peter I Island.

Of those qualitative considerations, the low-band features would be fairly firm and could serve as a guide in trying to make a contact with Peter I Island . But the high-band features suffer from quantitative uncertainty and could only be firmed up with data on the spread in frequencies between the FOT and HPF for the path. Clearly, though, with a low level of solar activity, the highest bands, 24 MHz and 28 MHz, would be more uncertain and spotty. So it would seem that operations would be most likely limited to transition bands, between 10 MHz where absorption is a large factor and 21 MHz where high values of foF2 are necessary.

From the quantitative standpoint, the predictions of Methods 9 and 22 from IONCAP can be used to give the necessary details to fill

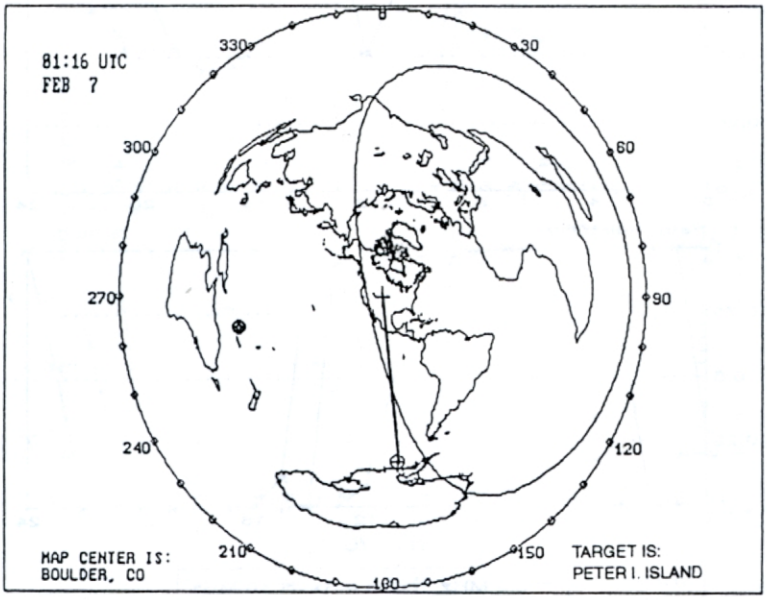

Figure 13.4 Azimuthal equidistant map showing the path from Boulder, CO to Peter I Island.

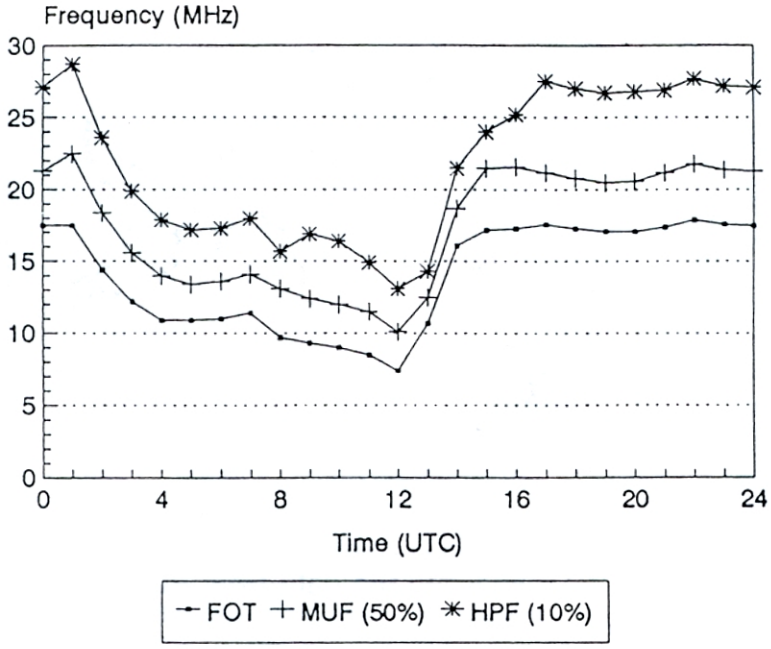

Figure 13.5 Critical frequencies for the path from Boulder, CO to Peter I Island.

out what was outlined above. Method 9 calculates the MUF and two other critical frequencies for the path and are shown in Figure 13.5. Method 22 takes those features over to provide a measure of the mode availability and which is expressed as a probability, in decimal form (0-1.00), that the operating frequency is below the maximum useable frequency at the hour in question. Similarly, Method 22 gives a measure of the path reliability and it is expressed

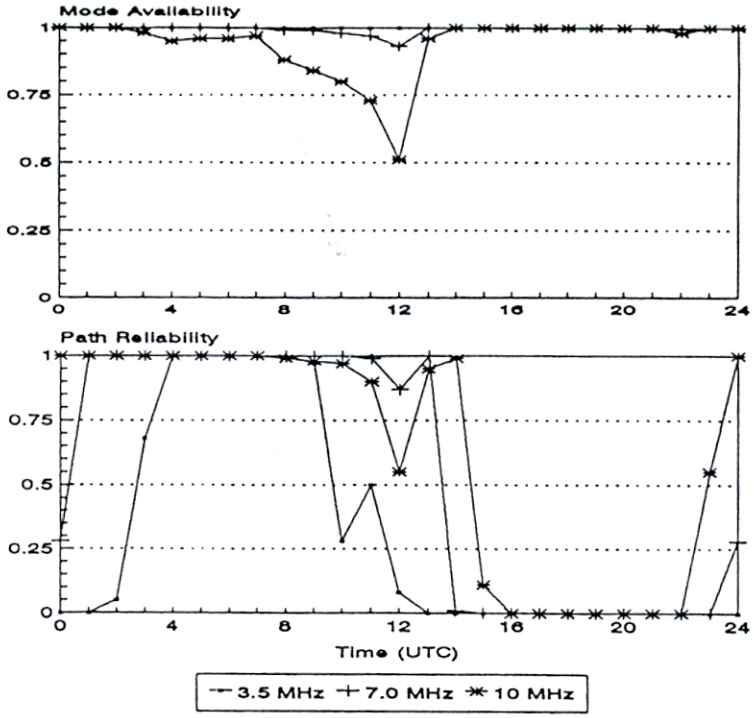

Figure 13.6 Mode availability and path reliability on 3.5 MHz, 7 MHz and 10 MHz for the path from Boulder, CO to Peter I Island in February 1994 (SSN=35).

as a probability, in decimal form (0-1.00), that the signal/noise ratio exceeds an acceptable minimum value at the hour in question.

The predictions for the mode availability and path reliability for the low-band frequencies, 3.5 MHz to 10 MHz, are shown in Figure 13.6. The upper part of that figure shows the availability of the path on 10 MHz is reduced somewhat in the hours before dawn when the critical frequencies reach their lowest values. After sunrise, the availability goes back to 1.00. The path reliability, on the other hand, is high during hours of darkness and then drops to low values as absorption increases with the approach on sunrise and remains low during hours of daylight on the path. Since the operating frequencies on the low bands are generally below the critical frequencies throughout the entire day, the qualitative suggestions given earlier were on a sound basis and confirmed by the more detailed calculations.

The same type of mode availability and path reliability curves for the higher bands, 14 MHz to 28 MHz, are shown in Figure 13.7. There it is seen that mode availability falls with sunset on the path around 0100 UTC, especially for the higher bands, but then rises to higher values with sunrise. However, with the sunspot number of 35, the spread in critical frequencies, FOT to HPF, is not large enough to make the higher bands equally available after sunrise. And the path reliability curves show the effects of ionospheric absorption being lowest, according to increasing frequency, during the hours around noon on the path.

With operations on the low bands hampered by absorption and limited on the high bands by critical frequencies of the ionosphere, it is of interest to examine the mid-bands, say 14 MHz and 18 MHz, where the two effects are each in transition, as it were. To that end, a new quantity, "DX feasibility," is defined here, the product of the mode availability and path reliability. That is done in the interest of finding times of operation which offer the greatest combined promise of success. Since both the separate quantities range from zero to unity, that will be the same range for DX feasibility and the results for the 14-MHz and 18-MHz bands are shown in Figure 13.8.

While the DX feasibility factor for the 14-MHz band falls to below 0.2 around local noon

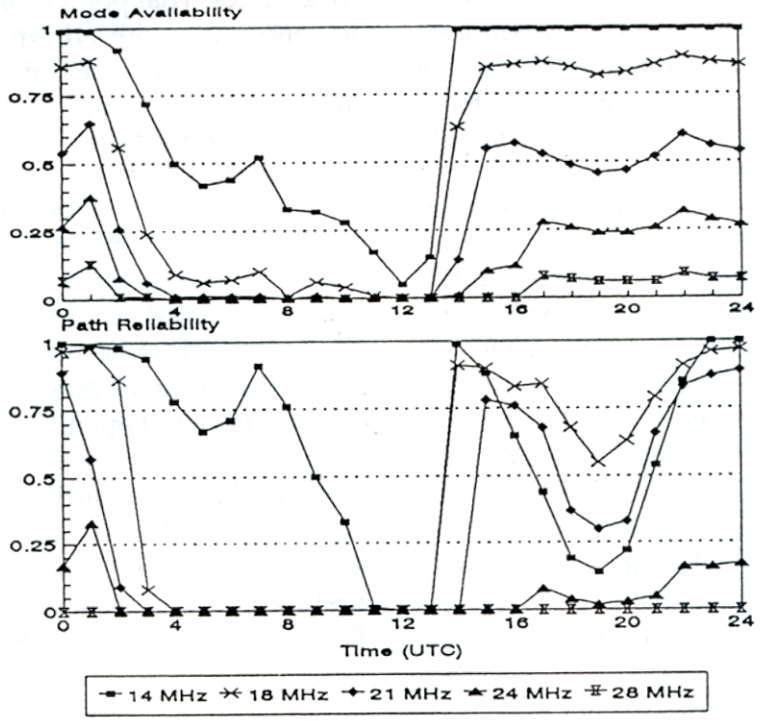

Figure 13.7 Mode availability and path reliability on 14 MHz, 21 MHz and 28 MHz for the path from Boulder, CO to Peter I Island in February 1994 (SSN=35).

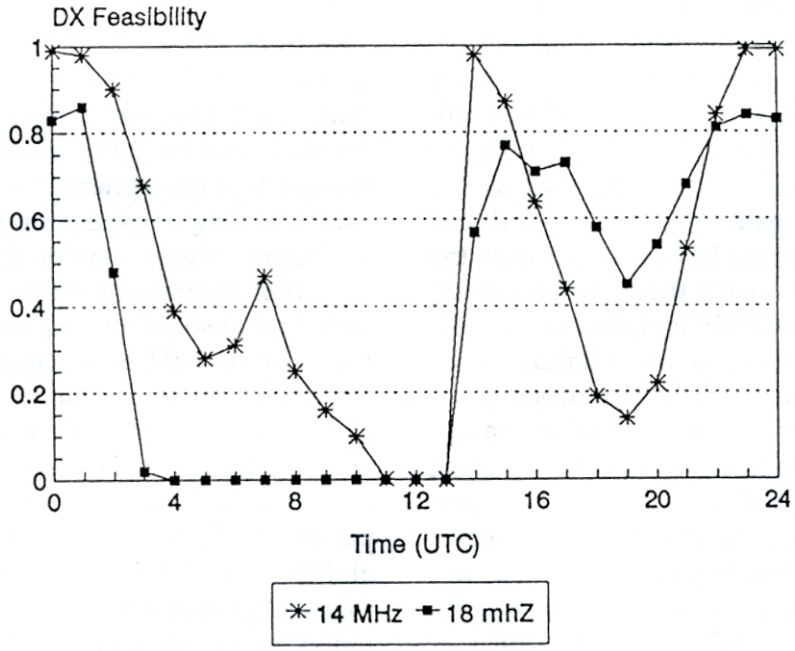

Figure 13.8 DX feasibility for the 14-MHz and 18-MHz bands for the path from Boulder, CO to Peter I Island in February 1994 (SSN=35).

on the path, when the ionospheric absorption is the greatest, the average feasibility (0.49) for the day as a whole exceeds the corresponding value (0.39) for the 18-MHz band. Looking at Figure 13.8, one sees that the greatest chances of making a contact on the 14-MHz band are in the morning when the band opens rapidly and then in the afternoon hours as the band slowly closes. But the 18-MHz band is largely open during daytime hours on the path.

To continue the discussion, other qualitative aspects of HF propagation may be inferred from the example in hand. Of particular interest are the consequences of the near N-S nature of the path from Boulder to Peter I Island . One effect is the rapid rise in MUF with sunrise as the terminator sweeps across the path. The effect would be even more pronounced with a northern terminus in the Midwest, say in Chicago, where the longitude is about 90° W, and at an equinox when the terminator is also in the N-S direction.

In that regard, it should be noted that sunrise occurs earlier at F-region altitudes than at ground level or in the D-region. As a result, the increase in D-region absorption on a path that goes with sunrise would lag behind the rise in foF2 values. That point is of particular interest in connection with HF propagation covering very great distances, more than halfway around the earth. But that will have to wait until some aspects of foF2 maps have been examined in more detail.

In closing the discussion of the ideas behind mode availability and path reliability, it would seem fair to say statistical features in amateur operations are encountered when a band seems closed even though the MUF was predicted above the operating frequency or an unexpected band opening when the MUF was predicted to be below the frequency in question. While one would think that statistics would be evenhanded and balance out in the long run, the disappointment in cases like the first are more than balanced out by the joys from the second. That's what keeps DXers going.

14: PATHS BEYOND 10,000 KM

Looking at Figure 11.1, the azimuthal equidistant map centered on the Little Pistol's QTH in Boulder, one sees that some of the rarer DX stations are beyond 10,000 km distance, those beyond the north coast of Africa and the countries of Southeast Asia. That means DX paths of at least four hops on short path and a good fraction of them across the northern polar region. The paths over the pole are uncertain because of their susceptibility to magnetic disturbance and paths toward Africa are difficult because of the "aluminum curtain" along the East Coast. That brings up the other possibility, sneaking signals into Africa and Southeast Asia by the back door, via long-path propagation. That last idea proves to be quite practical so let's turn to a discussion, from simple to complex, of long-distance propagation.

To begin, it was pointed out earlier that it's often convenient to show how HF propagation proceeds along a path by using a symbolic method, using reflections of rays from curved mirrors at ionospheric heights. Mirrors, of course, do not have any refractive properties so the technique is limited to geometry and does not cover how propagation along paths behaves at different frequencies.

The simple case of a mirror reflection for a single hop can be extended to two or more hops. And as discussed earlier, mirror heights may be different from one hop to the next, making hop lengths different along a path. Of course, critical frequencies may also vary along a path so the MUF for each hop could be different. That last idea was used to introduce the idea of a maximum useable frequency (MUF) for a path as a whole.

No mention has been made of mirrors being tilted within an individual hop; that change in geometry would make the ascent and descent portions of a hop unequal in length. Since mirrors are more symbolic than physical, the question then turns to the physical meaning of ionospheric tilts, as they are called. The answer, of course, is quite simple; the refraction or bending of a ray is different on one leg of a hop from the other or, equivalently, the critical frequency foF2 and electron density profile varies, positively or negatively, along the hop.

Consider the case of one hop in the flat earth representation, rays going from left to right. If the far right end of the ionospheric mirror is higher than the nearby left end, the downleg for the one-hop path will be longer than the upleg, etc., and the electron density should be less in the second half of the hop than in the first half. But electron density in the ionosphere translates into critical frequencies so the foF2 value would have to decrease along that hop.

Considering that ionospheric hops can cover up to 3,500 km or so in horizontal range, increases or decreases of foF2 along a path are not unreasonable. Indeed, all the ionospheric maps shown so far have variations like that in many regions. And the maps also have regions where changes in foF2 are rather small. For example, Figure 4.3 shows large increases and decreases in foF2 for paths in the N-S direction, especially in the early evening hours of local time (around 210° E longitude). And there are slow variations in the E-W direction at polar latitudes and increases or decreases, depending on the direction of a ray path, for paths in N-S and E-W directions. In short, critical frequencies and ionization vary widely over the entire ionosphere. Of course, HF propagation programs carry that sort of information in their databases and make use of it in making MUF predictions. But the user does not really come into close contact with that reality and its consequences, especially if thinking only in terms of simple hops from mirrors which are parallel to the earth's surface. That being the case, it's worthwhile to illustrate what's buried deep in propagation programs and note some of the interesting features that come to the fore, first

qualitatively by using mirror reflections and then quantitatively by going to ray tracing.

For discussion, consider a path from Los Angeles (34.0° N, 118.3° W) to Kiev (50.5° N, 30.5° E) at 0600 UTC in June, during a period of high solar activity (SSN= 150). The path length is about 10,080 km and would involve three hops. One can break the path into any number of small segments but for discussion purposes, consider breaking each hop into 8 segments. Using the F-layer algorithm from the MAXIMUF program, one can calculate foF2 values every 420 km along the path.

By taking differences in foF2 between adjacent segments and dividing the result by the distance, one obtains a rough measure of how the ionosphere varies along the path. Thus, if foF2 decreases between adjacent steps along a path, the ratio is negative; that corresponds to an upward tilt of the ionospheric mirror along the path or less downward refraction of the far end of the hop than when it's parallel to the earth's surface. In a similar way, positive ratios mean the mirror is tilted downward and more downward refraction would result.

Ultimately in this sort of discussion, the matter will come down to ray tracing, so the discussion should be put in appropriate terms at the outset. Now differences in critical frequency foF2 are really related to differences in electron density at the F-layer peak and when that conversion is made, the ratio can be expressed in more physical terms. In order to do that one needs the fundamental equation which related peak electron density and foF2 values. From that it is seen that differences in electron density are proportional to differences in the squares of foF2 values.

So the ratio which shows whether the mirror is tilted one way or another has the physical dimensions of MHz^2/km. That number gives a measure of what is termed the electron density gradient and looking at the differences in foF2 values across an ionosphere, one finds electron density gradients from 0.005 or 5E-3 (MHz•MHz)/km up to about 0.1 or 100E-3 (MHz•MHz)/km.

With that discussion concluded, let's go back to the LA/Kiev path and look at how foF2 values and the electron density gradient varied step by step along the path, as in Figure 14.1. There it is seen that foF2 went through a minimum around the midpoint of the path, from about 7.5 MHz at the start to 5 MHz at the middle and back up again, while the electron density gradient began weakly negative, with a numerical value around 1E-3 (MHz•MHz)/km and slowly increased to about the same positive value at the end of the path. All in all, there was little variation along the path and that is quite reasonable considering the path was mainly mid- and high lati-

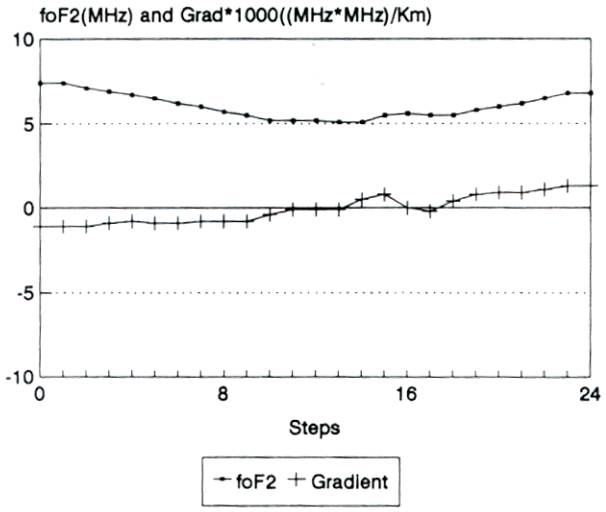

Figure 14.1 foF2 values and gradients in 420-km steps along a path from Los Angeles to Kiev, Ukraine.

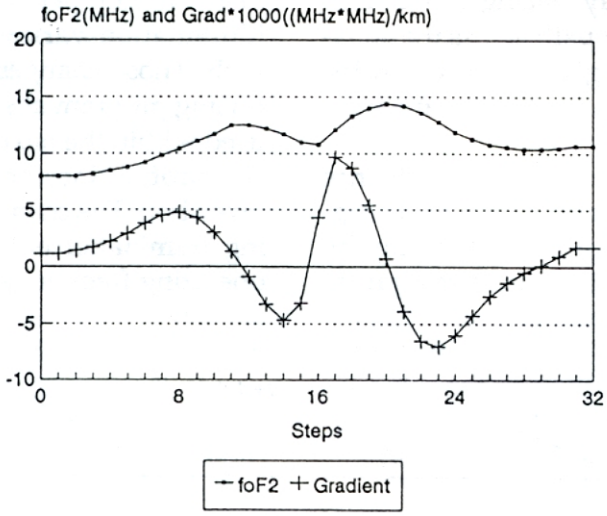

Figure 14.2 foF2 values and gradients in 375-km steps on a path from Los Angeles to Sydney, Australia.

tudes in a summer month.

Now consider a path going in the opposite direction at the same date and time, from Los Angeles to Sydney, Australia (33.9° S, 151.3° E). That path is about 12,000 km in length and would involve 4 hops. By breaking the hops into 8 segments, each 375 km long, and working out the foF2 values and the electron density gradient along the path, the results shown in Figure 14.2 are obtained. In contrast to the LA/Kiev path across higher latitudes, the path from LA to Sydney goes across low latitudes, the equator and into low latitudes in the Southern Hemisphere.

As noted earlier, much higher critical frequencies are encountered in those regions, reaching values almost twice that found along the other path. And the electron density gradient shows much greater variations too, both positive and negative and reaching values 7-10 times larger. And the high, double peak in foF2 values along the path as it crosses low latitudes is termed the "equatorial anomaly." It originates around the geomagnetic equator and is the result of a redistribution of photoionization by the action of an electric field of atmospheric origin. That electric field moves equatorial ionization across magnetic field lines and a fountain effect lifts and carries it to the north and south, giving foF2 peaks as seen in Figure 14.2.

Where the gradient is positive, one can expect greater downward refraction or shorter hops and just the opposite when the gradient is negative. From Figures 14.1 and 14.2, it's clear that ionospheric tilts differ greatly along the two paths, being much more significant on the path crossing the geomagnetic equator. In that connection, ionospheric tilts in the equatorial region have been suggested as the origin of high MUFs and strong signals on transequatorial paths.

To continue with the discussion, Figure 14.3 gives symbolic representation of a chordal hop, one which involves two ionospheric refractions without an intervening ground reflection. On that path, the first ionospheric tilt (upward) gives less refraction on the downleg than on the upleg, resulting in the ray missing the earth and going on to another region with an ionospheric tilt (downward) which refracts the ray back to earth. Without a surface reflection at the midpoint of the path, signal strength would be higher by 1-6 dB and if the chordal segment of the path went above the D-region, an additional gain in signal strength would result.

Going now to ray tracing, the variation of foF2 along a path, as in Figure 14.2, can be converted to a variation of peak electron density.

That, in turn, can be put into mathematical form and used in the ray-tracing program to work out details of a ray path across the equatorial anomaly. Before giving those results, however, a few words on ray tracing are in order.

First, the technique follows the advance of a ray, the height and orientation of its segments being plotted, step by step, along the path. The change in ray direction in going from one step to the next depends on the frequency and the rate at which the electron density changes with position. As ray segments are located, their orientation determines whether the ray is ascending or descending.

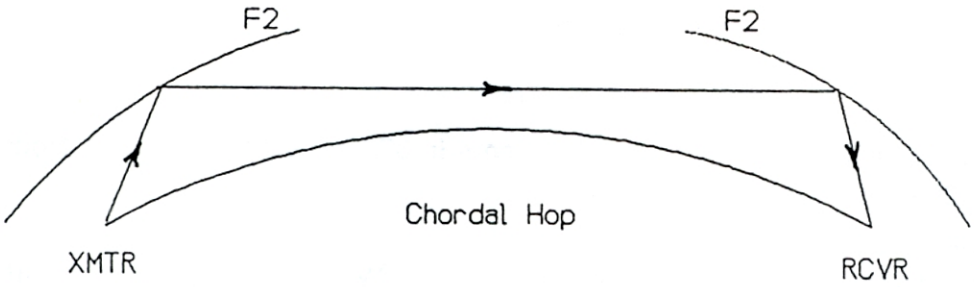

Figure 14.3 Symbolic representation of a chordal hop between two tilted regions in the F-layer.

In its simplest form, ray tracing assumes that the electron density in a hop varies only with height above ground but not along the hop. The density rises from essentially zero at ground level to a small plateau or ledge at the E-region, around 110 km altitude. Above that level, the electron density rises and goes through another ledge in the F1-region at about 175 km during daytime and reaches the F-peak at about 300-400 km altitude. Numerical values for electron density at the critical heights are obtained from data based on ionosonde records and the shape of the electron density curve obtained from various model profiles. For ray-tracing calculations, the model profiles must join smoothly, in magnitude and slope, at every transition.

An improvement in ray tracing is when critical frequency data is changed from one hop to the next along a path. That usually means changing foF2 values and heights of F-peaks in a multihop path to reflect the fact that solar illumination varies with distance along the path. Those changes can be made in the ray-tracing program at each surface reflection and used within the next hop but the electron density profile does not change shape within a given hop. The changes in ray paths from varying illumination are generally small unless the operating frequency is such that the E-region is called into play, making the next part of the path an E-hop instead of another F-hop.

Ray tracing in that approximation uses one-dimensional methods within a given hop and discontinuous changes in critical frequency data in going from one hop to another. The calculations are done using Snell's Law for wave refraction but in a special form for spherical geometry in which the electron density varies only with height. The next step in ray tracing is to move up to a two-dimensional approach with continuous variations in critical frequency data, both with height and along the path.

Now leaving the mirror approach, as shown in Figure 14.3, consider a ray trace for a path across an equatorial distribution in ionization where the peak electron density varies along the path in a manner like that suggested by Figure 14.2. Thus, the highest foF2 value was taken as 15 MHz and a value of 10.6 MHz used at the minimum. The critical frequency data for the F1- and E-regions were taken as 2 MHz and 1 MHz, respectively, for late-afternoon or early-evening conditions at equatorial latitudes.

Using a rectangular format to display the results of calculations in spherical geometry, Figure 14.4 shows the ray trace for a 28-MHz signal going through that ionosphere and results in a chordal hop that covers almost 7,000 km distance. At 28 MHz, the signal goes through the E- and F1-regions with practically no deviation in direction and the major changes in direction in ray direction are seen to take place around 250 km altitude. On descent from the first peak, the ray is in a region of decreasing electron density and suffers less downward refraction than on ascent. As a result, the ray leaves the lower part of the E-region, misses hitting the earth, as in Figure 14.3, and then goes on for another F-region refraction where the increasing electron density refracts it back to ground level.

Earlier, ray traces were shown in which rays with increasing frequency were sent upward into the ionosphere. The result that comes from such displays is that higher frequency rays go deeper into the ionosphere, probing as far as the region just below the F-layer peak, while lower frequency rays get as far as the lower part of the F-region or are stopped by the E-region and refracted downward. In terms of ray-tracing calculations, those results are manifestations of the general features of ionospheric refraction, the refraction per step along a path varying as the inverse square of the frequency as well as directly with the rate of change of electron density with height. Thus, 28-MHz rays are refracted back to earth more slowly than 7-MHz rays and 7-MHz rays are refracted back to earth at lower altitudes than 28-MHz rays.

And one other simple result is that rays in the ionosphere below the F-peak are always refracted back toward the ground as long as the region is one where the electron density is increasing with altitude. Where the electron density might be constant over a short distance, say at the E-region or F1-region ledges, rays simply continue onward undeflected, whether ascending or descending, until the electron density increases again.

Those ideas are part of the basis of the chordal hop in Figure 14.4, less refraction taking place on the downside of the first part of the path because of a smaller variation of electron density with height. The other part of the matter has to do with the earth's curvature, making it fall away from under the ray as it advances. Actually, the direction of every step of an advancing ray results from a competition between the two factors, ionospheric refraction back toward earth and apparent refraction in the opposite direction because of the earth's curvature.

The competition between those two processes in the same ionosphere will be faster at lower frequencies as the rays are refracted more strongly. As a result, lowering the frequency

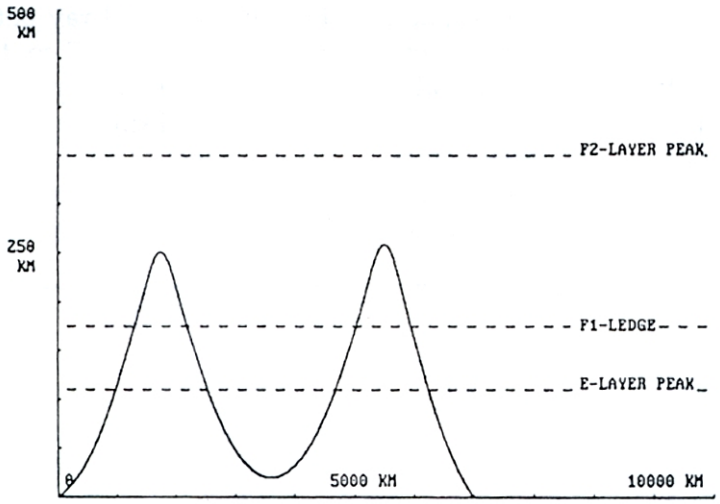

Figure 14.4 Ray trace for a chordal hop on 28 MHz.

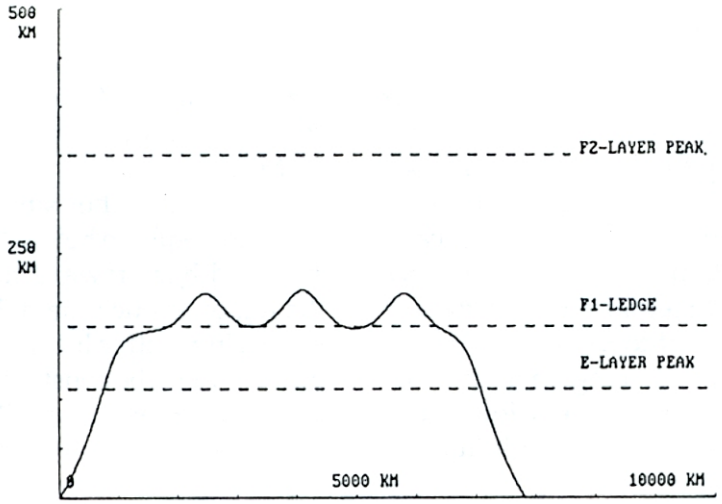

Figure 14.5 Ray trace of chordal ducting on 14 MHz.

from 28 MHz to 14 MHz replaces the slow, large-scale refraction which gave a chordal hop by fast, small-scale chordal ducting, as in Figure 14.5. There, because of the lower frequency, the ray barely penetrates past the F1-ledge and for the same reason, it is refracted more rapidly and oscillates up and down in a height range of about 30 km while advancing along almost parallel to the earth.

The robust ionosphere in Figure 14.2 was for late-afternoon and early-evening conditions across the geomagnetic equator. At later times, more toward the dawn hours, critical frequencies along the same path are lower and also admit long-distance propagation by chordal ducting at lower operating frequencies. Thus, for 7 MHz and lower in frequency, ray traces similar to Figure 14.5 will result, the difference being that with stronger refraction at a lower frequency, a somewhat greater number of oscillations take place along the path. Obviously, those circumstances go to explain, at least in part, long-distance propagation on the lower bands.

The discussion above deals with the effects of longitudinal gradients in the ionosphere, the circumstances when a ray path crosses foF2 contours perpendicular to their orientation. It takes no stretch of the imagination to think that ray paths could also go almost parallel to foF2 contours. The most obvious case would be a path parallel to the terminator around sunrise and the electron density gradient would be transverse to the ray path.

Earlier, the effects of longitudinal gradients were illustrated using ionospheric mirrors,

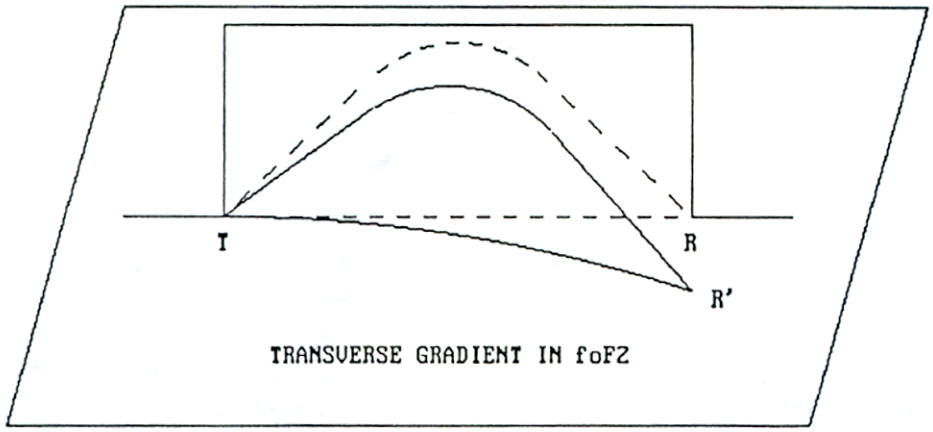

Figure 14.6 Schematic drawing for a non-great circle hop due to a transverse foF2 gradient.

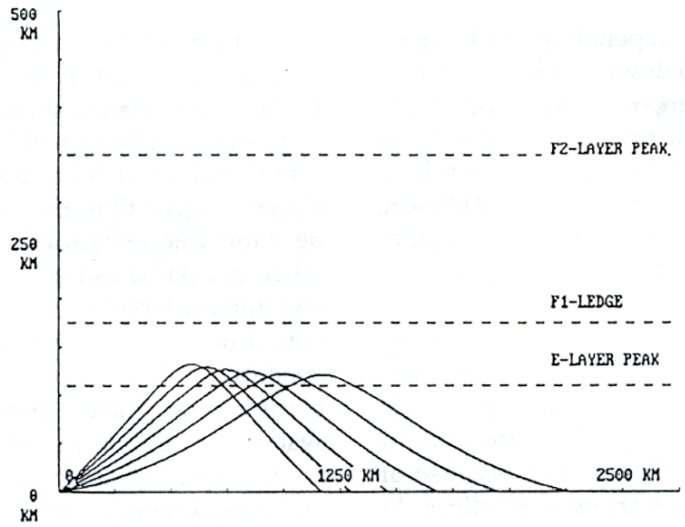

Figure 14.7 Projection of ray traces for non-great circle (NGC) hops on a vertical plane.

tilted one way or the other along a ray path. The same can be done for transverse gradients, the ionospheric mirror now being tilted across instead of along the path. As before, the higher side of the ionospheric mirror would be where the electron density is lower, toward darkness around the sunrise terminator.

By tilting the ionospheric mirror in that fashion, rays reflected off the mirror would be deviated toward the high side of the mirror, in the direction of decreasing electron density and foF2 values. As a result, where ray paths are normally expected to lie in the plane of a great circle path, they now are deviated out of the plane, resulting in non-great circle (NGC) propagation. That is illustrated in Figure 14.6 where a NGC hop and its projections in both the vertical and horizontal planes are given.

As might be expected, ray tracing can be applied to this type of situation but the problem is more complicated in that another dimension has to be added to the calculations, allowing now both longitudinal and transverse gradients along a path. To illustrate the quantitative side of the problem, traces are shown in Figures 14.7 and 14.8 for a sunrise situation where 7-MHz rays start along the terminator.

As seen in the first figure, under those cir-

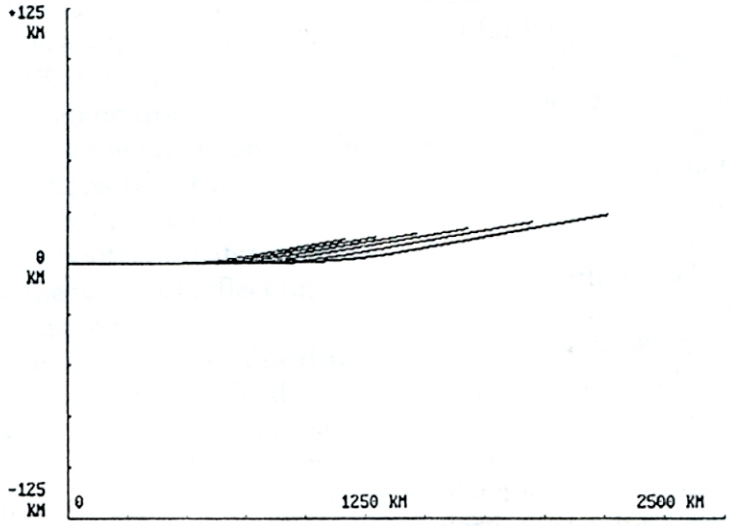

Figure 14.8 The projections on the earth's surface of sideways deviations of non-great circle (NGC) paths due to a transverse foF2 gradient.

cumstances the rays just penetrate the E-region before being refracted downward. The effect of the transverse gradient, operating above the E-region, is to deviate the ray path away from the region of higher ionization (in sunlight) by a modest amount. For the ray going out 2,000 km, the side deviation is about 25 km or an angular deviation in path direction of 1.5 degrees.

In the dawn situation, the sideward deviation remains about the same as long as the ray paths stay below the F1 ledge. At a higher frequency, say 14 MHz, ray paths may penetrate the F1-ledge and undergo deviations about twice those shown in Figure 14.8 because of greater exposure to the transverse gradient. At an even higher frequency, say 21 MHz, there would be greater penetration and exposure but the net deviation would remain small because the sideward refraction also goes as the inverse square of the frequency.

In any event, non-great circle (NGC) propagation results from transverse gradients in the ionosphere, as shown above for a single hop, and the effects will be cumulative along a multihop path. With the frequency dependence of refraction, the largest effects would be at low frequencies and at times of darkness when ray paths can go past E-region heights and into the F-region. While various types and magnitudes of gradients can be found by inspecting an ionospheric map, it should be borne in mind that the ionosphere is a dynamic system, more than just the average environment displayed in foF2 maps. Thus, while propagation effects from average gradients are to be expected, day in and day out, unusual gradients are not out of the question, especially in disturbed times, and propagation beyond the normal range may be encountered at those times.

15: LONG-PATH PROPAGATION

The varied features of the ionosphere, as represented by foF2 maps, become more important the longer the path. Thus, for the shortest, single-hop paths, all that's needed is the critical frequency nearby but with multihop paths, the spatial gradients of critical frequencies become important as well. In a sense, it's like rolling a ball down a hill. At the start, the ball's path depends on the slope of the hill but its ultimate destination will be determined by all the hills and valleys beyond the starting point.

Turning to long-path propagation, that begins when RF goes beyond the antipodal point of the transmitter, signals reaching more than halfway around the world. And long-path DXing has been a popular mode in spite of the distances involved and the potential losses in signal from adding more distance, surface reflections and D-region absorption in extending a path. At times of high solar activity, it is a regular mode of propagation, open every day except at times of magnetic disturbance. That is an important point and will be discussed at some length at the end of this chapter and in the chapters which follow.

But getting down to long-path propagation, the length of the path is the least concern, the inverse square law only lowering signal strength by 6-10 dB if a path length were doubled or tripled in going from short to long path. More ground losses would be significant for additional reflections off of dirt but the threat may not be all that great as considering the earth as a whole, about 80% of its surface is covered by oceans, the next best reflecting surface after a conducting metal foil.

That leaves D-region losses as a threat and in the last analysis, it will prove to be the controlling consideration in long-path propagation. So knowing that ionospheric absorption would be a factor, DXers try to limit its effect by sending signals off into an ionosphere in darkness or where the sun is low to the horizon, close to the terminator. Under those circumstances, long-path DXing has a possibility of being successful if the dawn/dusk ionosphere still supports propagation. The other losses and noise may still be factors, say ground instead of ocean reflections and noise propagated from thunderstorm activity.

Now to a first approximation, paths from point A to point B are great circles so the thing to do for long-path DXing is find the long-path direction to the DX location. That's simple; just add 180 degrees to the beam heading for a short-path connection. If the Little Pistol in Boulder wanted to make a contact on long path, the thing to do would be to look at a map like that in Figure 13.4. That figure was obtained by using the DXAID program and not only shows the azimuthal equidistant map centered on Boulder but also an oval to represent the shape of the terminator at the chosen time. In the context of the Peter I Island operation, the figure shows the sun is north of Australia and the path to 3Y0 is partially in darkness around 0100 UTC.

Now consider a different path, to Saudi Arabia. For a short-path connection to Saudi Arabia, the Little Pistol's tribander should be headed in a direction 29 degrees east of north but for long path, it would be changed to 209 degrees. That would still be along a straight line on the azimuthal equidistant map, going out at 209 degrees bearing to the antipodal point (now represented by a circle at 20,000 km from Boulder) and then continuing back in toward the center of the map at the 29 degree heading until it reaches HZ-land.

At that heading, the long-path distance to HZ-land is 27,880 km, a factor of 2.3 greater than the short-path distance, 12,150 km. Because of signal spreading, the mere thought of going long-path means the Little Pistol would take a loss of at least 7.2 dB. But it would be worth the try for a contact as it's a way to get signals into HZ-land via the back door, as it

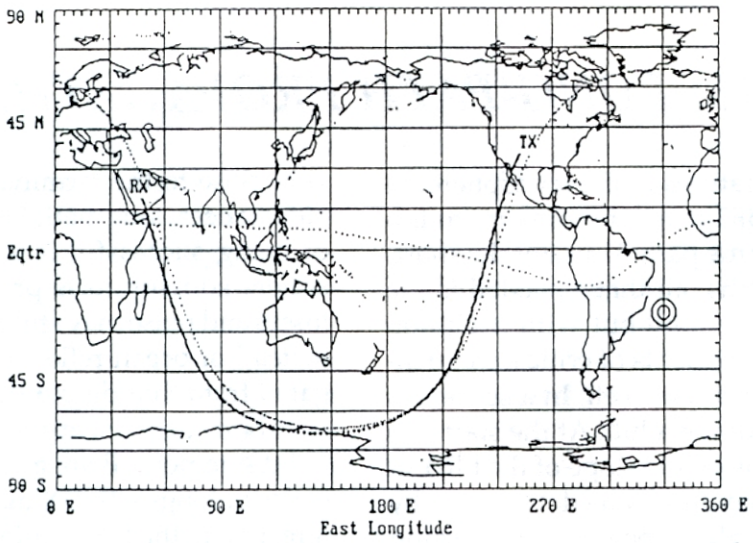

Figure 15.1 A Mercator map showing the path from Boulder, CO to Riyadh, Saudi Arabia and the terminator at 1400 UTC on 21 December.

were, and not in direct competition with the hordes of operators on the East Coast and in Europe. And looking at the map in Figure 13.4, it's clear that most of the path would be over sea water. That minimizes the effects of surface reflections and leaves D-region absorption and the effects of darkness on critical frequencies to worry about. So back to maps and the terminator.

The azimuthal equidistant projection is fine for showing great circle paths from one's QTH but all other great circles not centered at the same location come out as ovals, the terminator in Figure 13.4 being a case in point. And on a given day, the ovals rotate about the QTH at the center of the map. When it comes to judging how a path is illuminated, that map projection tends to be confusing so consider the problem again, now using the Mercator map in Figure 15.1.

That figure shows the path from Boulder to Riyadh as a heavy, sinusoidal-like trace. Unlike an RF path which is a great circle and fixed for all time, the terminator is a great circle but its shape and projection on a Mercator map changes with season, as seen earlier in the discussion of the foFE contours. For the present discussion, long path to HZ-land, the date and time have been chosen to illustrate how D-region absorption may be minimized. Thus, the date was taken as 21 December, the winter solstice, and the time as 1400 UTC when the subsolar point is off the east coast of Brazil at 23.5° S, 330° E.

Looking at Figure 15.1, it's clear the portion of the great circle for the path and the terminator are almost in spatial coincidence, with half of the path on the dawn side of the terminator and the other half along the dusk side, making for a situation with low D-region absorption. That situation gives a gray line path and is an important part of long-path DXing. But obviously, with the shape of the terminator changing markedly with seasons and the great-circles for paths being fixed, long-path DXing will have strong seasonal aspects.

The circumstances in Figure 15.1 show other possibilities for long-path DXing from Boulder in the winter months, into Europe and Africa. For those directions, Figure 13.4 shows that the Little Pistol's beam headings would be similar to that for Saudi Arabia, to the west of south. And Figure 15.1 shows that with the advance of time past 1400 UTC, the sun will rise on the first part of the long path off to the west and set on the other part to the east.

The long-path possibilities for other directions during winter, say toward India and Sri Lanka, would be less propitious, signals going off to the east of south and into the sunlit hemisphere. Beyond that, paths to India and Sri Lanka would go to high latitudes, both geo-

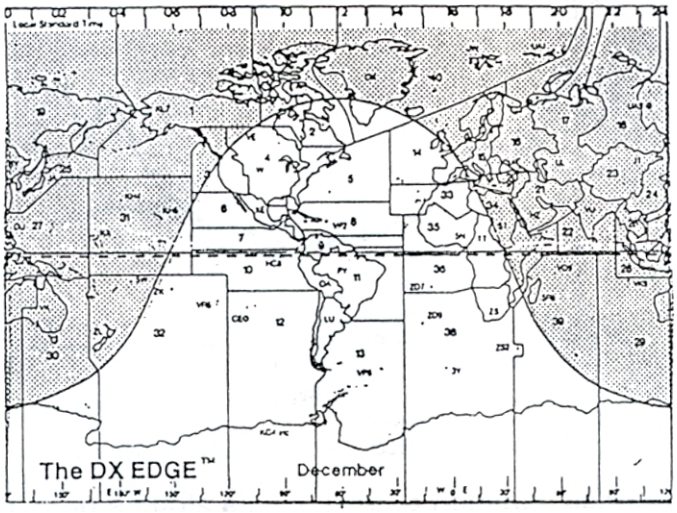

Figure 15.2 The DX Edge setting for 1530 UTC during December.

graphically and geomagnetically. The latter proves particularly important when it comes to the reliability of making long-path contacts to that part of the world as the paths from Boulder which go to high magnetic latitudes are more susceptible to disturbance, as will be seen shortly.

There is another time, in June at the summer solstice, when long-path openings are possible from Boulder to HZ-land by gray-line propagation. The path and terminator would be exactly the same as shown in Figure 15.1, the difference now being that the time is 0200 UTC and the subsolar point is southeast of Japan at 23.5° N, 150° E. The gray-line situation will be the same but since the time is changed by 12 hours, the path at summer solstice is dusk to dawn from Boulder whereas the path discussed earlier, at winter solstice, was dawn to dusk.

Physically, that means the winter anomaly of the F-region has exchanged hemispheres, the early morning long path from Boulder in December going into summer in the Southern Hemisphere, with lower foF2 values along the path, while the early evening long path in June goes into winter in the Southern Hemisphere, with higher foF2 values. But perhaps the largest difference in the two situations is in connection with sociological factors, there being more QRM from local operators on the bands in the USA than at the less populous DX end. That being the case, early morning hours prove more productive than evening hours for long-path DXing.

In an effort to show more of the details of long-path propagation, consider another set of paths, from here in the northwest corner of the USA. First, take the case of the winter solstice again and the time as 1430 UTC, now shown by the DX Edge in Figure 15.2. There, paths to Europe go off into the dark hemisphere and are not open while the first hops from the Northwest are still in darkness. That is the case as they're in the winter hemisphere and foF2 values for sites along the path fall to low values when in darkness for 14 hours or so. In that regard, the opening of a long path to HB-land results from the rise of foF2 values at sunrise, after 1530 UTC, on points along the great circle, as shown in Figure 15.3.

For that figure, the path was divided into 36 sections of 450 km length and foF2 values were calculated at each step along the path for every half hour, starting at 1430 UTC. In order to be successful in making a long-path contact with HB-land on 14 MHz, foF2 values in excess of 5 MHz are required along the path. From Figure 15.3, it is seen that foF2 values were more than enough along the major portion of the path, even displaying the high values in the equatorial anomaly.

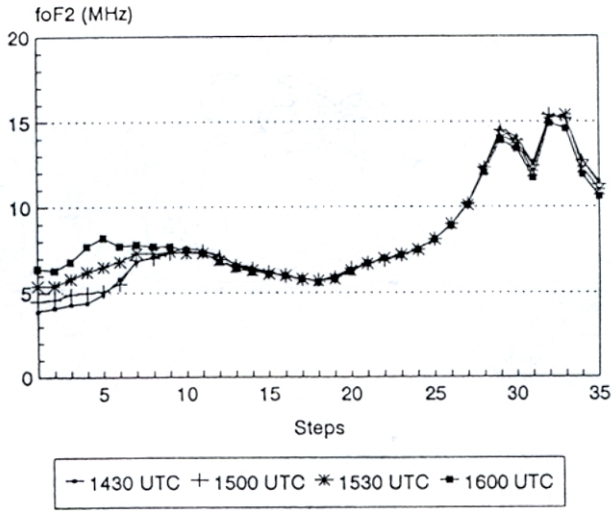

Figure 15.3 Sunrise variation of foF2 values along a great circle path from Washington to Switzerland in December.

But on the first hop from here in the Northwest, foF2 values are too low and won't support propagation along the entire path until the sun starts to rise on the first hop, around 1500 UTC and out about 1,400 km west of Los Angeles. After the sun rises at F-region heights, quickly raising the foF2 values and opening the path, it rises somewhat later on the D-region and ionospheric absorption sets in and starts closing the long-path circuit to HB-land.

The long path from the Northwest to India and Sri Lanka is closed in the winter months, just as for Boulder, because it goes off into the sunlit Southern Hemisphere. However, it is open in the morning hours of the summer months, as may be seen from Figure 15.4. That figure is for the summer solstice and 1230 UTC. In that case, the terminator which cuts across the Northwest also goes across the tip of South America and then the southern waters of the Indian Ocean, finally coming close to India and Sri Lanka.

The paths to those locations are close to the terminator and propagation to India and Sri Lanka opens and closes for the same reasons as before, sunrise bringing foF2 values up to where propagation is supported along the entire path and then closes somewhat later

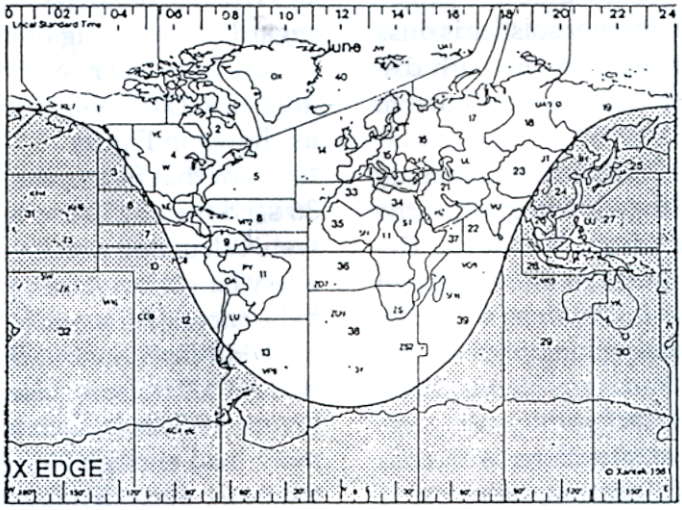

Figure 15.4 The DX Edge setting for 1230 UTC in June.

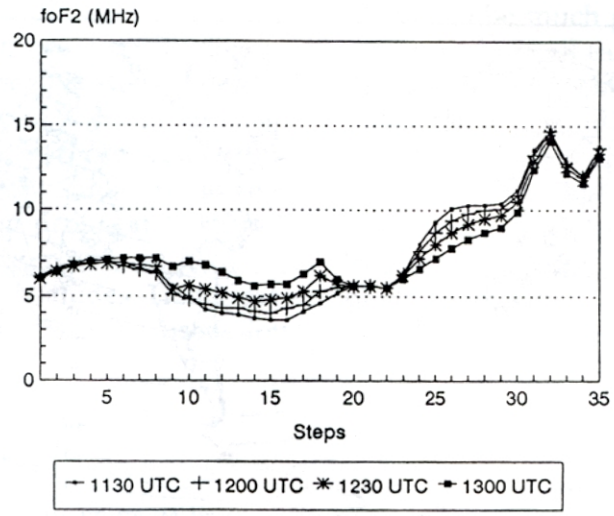

Figure 15.5 Sunrise variation of foF2 values along a great circle path from Washington to India and Sri Lanka in June.

when ionospheric absorption sets in as the sun rises on the D-region. Those processes still take place in the winter hemisphere, where foF2 values have fallen during the long night. The case for the path to India is shown in Figure 15.5 where the rise in foF2 values takes place between step 9 (13° S, 103° W) and step 19 (76° S, 37° W) after 1200 UTC.

From the above discussion, however, it would be a mistake to think that long-path DXing is only possible along the gray line where solar illumination is weak. For any type of successful propagation, three conditions must be met: a MUF value sufficient to support the frequency in use, good signal strength at the receiving station and a low level of noise. During times of high solar activity, say around solar maximum, critical frequencies do not fall to low levels in the long hours of darkness.

In that regard, experience here in the Northwest during the peak phase of Cycle 22 showed that long-path contacts with Africa were frequently possible in the morning hours during the northern summer, as in Figure 15.4, by sending signals on long-path directions almost at right angles to the terminator. With solar activity at that level, foF2 values in the dark hemisphere were still sufficient to support the propagation. But during the winter solstice when the gray line was more favorably positioned, as in Figure 15.2, it proved very difficult to contact South Africa because of all the atmospheric noise propagated from tropical thunderstorms during the southern summer season.

So far, the discussion has dealt with long-path propagation opening due to the growth in foF2 values with sunrise on the F-region and its closing due to the increase in absorption as the sun rises later on the D-region at lower altitudes. Beyond those ideas, it should be pointed out that some of the extreme long-path circuits profit from chordal hops across the equatorial anomaly, the resulting signals being greater for the lack of losses that would have occurred from an intervening surface reflection. That would be true of paths with a significant longitudinal ionospheric gradient; other long paths lacking that benefit would be weaker in signal strength, limited by the losses on typical earth-ionosphere hops.

At the higher part of the HF spectrum, say from 14 MHz and above, chordal hops may be simple, as in Figure 14.4, or show some ducting, as in Figure 14.5. At lower frequencies, signals do not penetrate as deeply into the F-region and chordal ducting would dominate when it comes to long hops on DX paths. That would be particularly true for frequencies of 10 MHz or lower as hops would be shorter and more numerous, quickly dissipating RF energy were it not for long, efficient ducted hops.

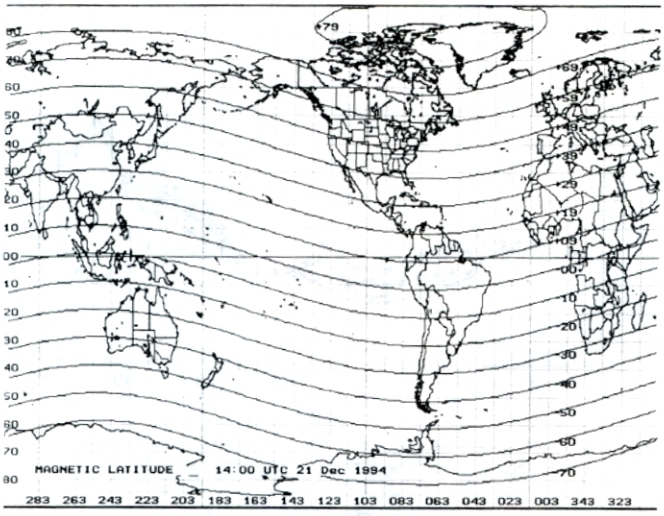

Figure 15.6 Parallels of magnetic latitude for a centered dipole.

Finally, as remarked earlier, great circle paths are fixed with respect to the earth but the terminator varies in position and shape, moving along with the hours of the day from East to West on a Mercator map or changing shape with the seasons. In connection with long-path propagation, the most poleward reach of a path is important for reasons other than simply their relationship to the terminator. In particular, it is important to know which region of geomagnetic field was involved in the poleward excursion of a path as propagation disturbances of magnetic origin vary in degree according to the highest latitude on a path.

In that regard, regions on the earth are classified according to a system of geomagnetic coordinates based on the dipole model discussed earlier in connection with geomagnetic data. That model resulted from a large-scale analysis of magnetic observations and has an axis of symmetry which passes through the center of the earth, tilted about 11.5 degrees with the geographic axis. With an equatorial plane perpendicular to the magnetic axis and passing through the center of the earth, the geomagnetic coordinate system has parallels of magnetic latitude as shown in Figure 15.6.

The auroral zones, where luminous displays are seen most often, generally fall between 60 and 70 degrees magnetic latitude while the polar plateau lies above 70 degrees and subauroral latitudes are just below 60 degrees magnetic latitude. With that system, the paths from here in the Northwest to southern Africa would be classified as auroral as their most southerly excursions in latitude range between 61 and 69 degrees south geomagnetic latitude for termini from Pt. Elizabeth to Swaziland. Only Cape Town, at the most southern tip of South Africa, is in the subauroral category. After that, paths to Zambia and Saudi Arabia fall in the polar category as their most southerly excursions in latitude range between 71 and 85 degrees south geomagnetic latitude.

The category of the path to a particular DX site depends on the location of the transmitter. Thus, from here in the Northwest, the path to India goes through the auroral zone while from Boulder, it goes across the polar plateau. Similarly, from here in the Northwest, the path to Spain crosses the polar plateau but from Boulder, it passes through the auroral zone. In terms of geographic distinctions, those path differences would be related to the solar illumination and all that follows from it, reflection surfaces, D-region absorption and foF2 values.

But more significant in categorizing paths are differences in the geomagnetic field lines they go across. With the ionosphere under geomagnetic control, low latitude field lines go out a few earth radii but the high latitude ionosphere has its electrons gyrating around the feet of magnetic field lines which go out to great

distances, many earth radii, above the lower ionosphere itself. Since geomagnetic disturbances are strongest at high latitudes, they are accompanied by ionospheric disturbances of signals propagating across those regions.

That last statement would seem to suggest that a discussion of propagation disturbances would be in order now, at least for paths going across high latitudes. That is certainly the case but the scope of the discussion proves to be much greater than would seem apparent from all that has been developed so far. The matter goes to a larger subject, the environment surrounding the earth, and it begins with a major revision in the model for the geomagnetic field. That result came from exploration in the Space Age and we turn now to that in the next section, continuing the discussion of HF propagation.

PART TWO

16: TOWARD A NEW ERA

The discussion up to this point has dealt largely with the effects of solar UV radiation incident on the atmosphere, the chemical changes resulting from photodissociation and the creation of the ionosphere by photoionization. That was the focus of the early work on propagation, an era before WWII when photochemistry dominated the scene. True, disturbances of propagation did occur, with shortwave fade-outs and ionospheric storms. The fade-outs (SWF) were associated with solar flares, and ionospheric storms were coincident with magnetic storms but there was no unifying understanding of the origin of the effects.

That had to wait until the end of WWII when the Space Age got under way. Then, high-altitude balloons, rockets and satellites began probing the upper reaches of the atmosphere and ionosphere, regions where only radio waves had been before. In less than two decades, a picture emerged which brought together the diverse aspects of radio propagation, the formation of the ionosphere and its disturbance.

The discussion which follows will deal with the new ideas that appeared on the scene as the "photochemical era" came to an end and was replaced by the "plasma and fields era" that we're in now. In considering the new understanding of HF propagation, it should be noted that we're moving away from a quasi steady state scene where the basic ionospheric properties change on a time scale characteristic of solar cycles. Now the discussion shifts to where changes occur on a more rapid scale, the time it takes UV and bursts of solar X-rays to reach the earth or the time for puffs of ionized matter to arrive at the earth's orbit.

The photochemical era really dealt with the physics and electromagnetic theory of the bottom side of the ionosphere. The new era started at the F-region peak in ionization and went outward through the topside ionosphere, finally reaching the sun. In that regard, we can begin the discussion where we left off, with long-path propagation, and look at how a new understanding of the geomagnetic field, particularly at high magnetic latitudes, emerged with space exploration.

The earlier view of the geomagnetism was that the earth was surrounded by a field like that of a dipole, as in Figure 6.1, and orbited the sun in a region containing little more than a handful of planets, meteors and interplanetary dust. That view has changed drastically and one of the first new ideas that impacted on propagation was the modern understanding of the shape and dynamics of the earth's magnetic field. It is best explained by examining the current view of the geomagnetic field, shown in Figure 16.1.

That figure shows the magnetic regime surrounding the earth, the magnetosphere, with the earth's field compressed by the solar wind on the dayside and drawn out on the nightside. In essence, the earth's field is confined to a cavity carved out of the stream of solar plasma flowing by, something like the wake behind an object fixed in a stream. In the

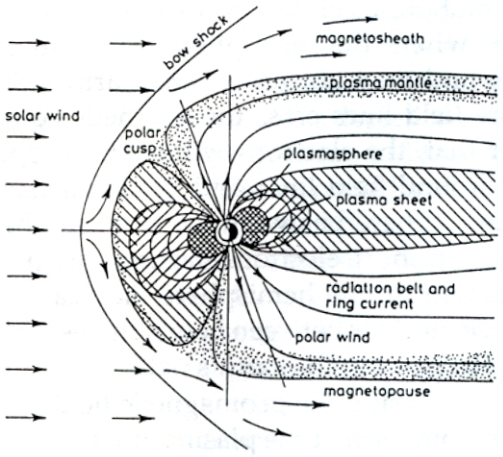

Figure 16.1 The magnetosphere formed by the interaction of the solar wind and the geomagnetic field. From Davies [1990]

figure, the magnetic axis is tilted forward and the geometry of field lines vary, depending on their magnetic latitude of origin

In that configuration, there is a low-latitude toroidal arrangement of dipole-like field lines, then an asymmetrical region of field lines which still go from one hemisphere to the other and finally field lines from polar regions which extend away from the direction of the solar wind, back into the magnetotail. Those distinctions emerged as the geomagnetic field was examined by magnetometers on spacecraft, the compressed field extending out 10-12 earth-radii on the sunward side and the magnetotail reaching back many tens of earth-radii in the opposite direction.

It's on those various types of field lines that ionospheric electrons find themselves when released by photoionization. While their origin is different than the electrons in the earth's radiation belt, the physics of their dynamical motions is the same, resulting in electrons gyrating around magnetic field lines. But if the ionospheric electrons have a component of motion along a field line, they may spiral either down or up the field line. With downward spiralling motion, electrons go to lower altitudes and may recombine with positive ions in the time they spend there or, failing that, they may be reflected upward by the converging magnetic field lines, just like electrons trapped in the radiation belt.

On the other hand, with upward spiralling motion, electrons move into higher altitudes where the ionosphere thins out even more and may go out several earth-radii to where field lines cross the magnetic equator. After that, the electrons will continue spiralling around field lines and go down toward the ionosphere below, in the opposite hemisphere. In short, electrons starting with photoionization in one hemisphere may carry out bounce motions between hemispheres and become trapped in the earth's field.

As a result, the geomagnetic field acts as a reservoir, termed the plasmasphere, holding electrons released initially in the sunlit atmosphere at the feet of field lines. The spiralling electrons will bounce between hemispheres as well as drift slowly in longitude because the geomagnetic field weakens with increasing latitude. And when the source of F-region electrons is turned off at sunset on the atmosphere below, the electron content in the reservoir starts to decrease as electrons recombine with positive ions at one end or the other of their bounce motion or are scattered out of trapped orbits and spiral down to the atmosphere below and become lost.

That description shows how the F-region is maintained at night, unlike the E-region which decays rapidly, and it holds as long as field lines are closed, going from one hemisphere to the other. Looking at Figure 16.1, it would not apply to field lines in the polar cap which go back into the tail of the magnetosphere. F-region electrons may be released on the feet of those field lines but their population would not build up nor be maintained by durable trapping as the polar field lines are not closed in the usual sense.

The distinctions between closed and open field lines are not sharp nor steady in time as it is found that the location of the outer boundary of the plasmasphere varies with geomagnetic activity. Indeed, it is on that basis that the association of ionospheric storms with geomagnetic storms is understood, high-latitude field lines which were closed on the front of the magnetosphere suddenly being swept back into the magnetotail with the onset of magnetic activity, taking their supply of electrons with them. When that happens, the field lines at a high-latitude site are no longer closed in the usual sense and unable to retain electrons spiralling up from ionospheric heights. As a result, F-region critical frequencies drop drastically and propagation is no longer supported at the same level as before. In addition, there is an effect on the electron density profile, not only lowering the peak value but also raising the height of the F2-maximum somewhat, as shown in Figure 16.2.

In order to complete the discussion, distance scales and time scales must be added. As for distances, the ionospheric electron population held on magnetic field lines extends out to about 4-5 earth-radii (Re). Beyond that, out

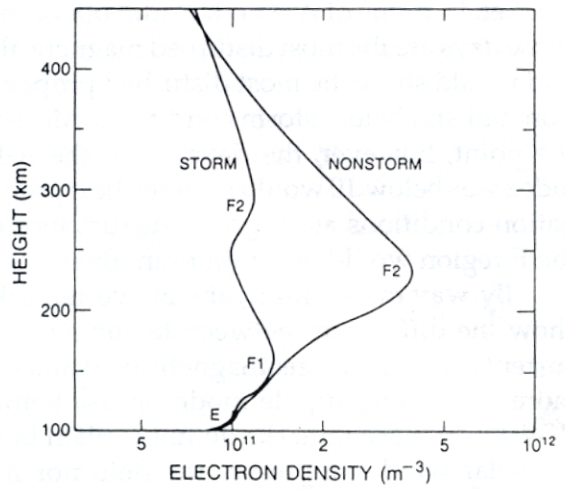

Figure 16.2 Electron density profiles during quiet and storm conditions. From Norton [1969]

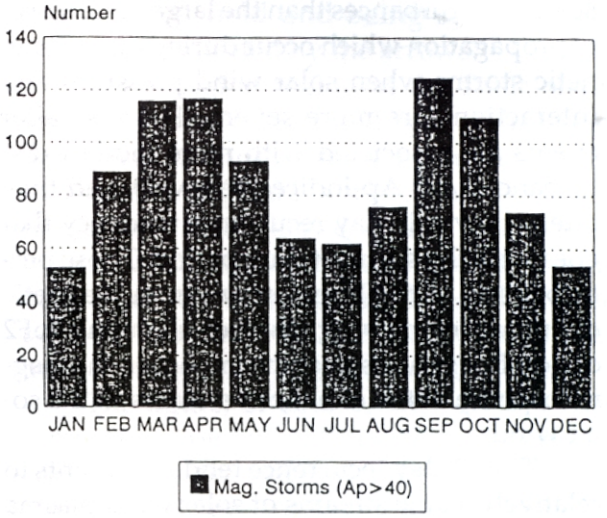

Figure 16.3 Distribution of magnetic storms (Ap>40) by month.

to 8-10 Re, the trapping or containment of electrons is not as durable, field lines being subject to disturbances that are propagated inward from the impact of solar wind on the boundary of the magnetosphere.

The trapping of ionospheric electrons is on the dipole-like field lines at lower latitudes and the outer limit of containment translates to an upper limit of 60-65 degrees magnetic latitude at the earth's surface. Poleward of that limit, critical frequencies foF2 show large variations and propagation across the polar caps is more uncertain than at lower latitudes and fails badly during magnetic storms.

As for time scales, several are involved in the discussion of ionospheric disturbances. For one, there's the time scale of the magnetic disturbance itself which brings on the ionospheric changes. The study of geomagnetism shows many types of disturbances, at different latitudes and with different time scales. Limiting the discussion to magnetic storminess, those times are listed in the Boulder Report or WWV broadcasts and are characterized by high A-and K-indices, major storms having values of A above 40 and K above 5.

The time scale for onset of magnetic storminess is measured in hours and storm durations may be in days. The frequency of storms is seen from data collected over the years by NOAA. Thus, in the previous 5 solar cycles, there were 1,033 major magnetic storms with Ap of 40 or higher. That works out to about 206 storms per solar cycle, 19 storms per year and corresponds to significant ionospheric disturbances for 10-15 percent of the time.

There is a seasonal dependence for magnetic storminess, as shown in Figure 16.3. Thus, it is seen that magnetic storms are most frequent at the equinoxes, a time when the geomagnetic field is facing more directly into the solar wind direction. There is also a solar cycle variation for magnetic storminess but that will be discussed later in connection with solar activity and its effect of HF propagation.

Returning to time scales, beyond those which would be associated with drastic changes in field lines and the depletion of ionospheric electrons, the question of ionospheric replenishment needs to be considered. In that regard, the source is solar UV and it creates ionospheric electrons at a steady rate, magnetic storm or not. Thus, the greater the magnetic disturbance and depletion of ionospheric electron content, the longer the time required for solar UV to restore the F-region electron population and return critical frequencies back to normal. That goes a long way in explaining why HF propagation is poor for so long after the onset of a large magnetic storm.

Of course, there are less drastic ionospheric disturbances than the large-scale losses of propagation which occur during major magnetic storms when solar wind pressures and interactions are more severe. Those smaller events are associated with more modest disturbances, say Ap-indices below 40, and they often show a 27-day recurrence tendency that goes with the solar rotation period. Those perturbations of the F-region are from magnetic disturbances moving inward, changing foF2 critical frequencies after the impact on the magnetosphere of the enhanced streams in the solar wind.

The 27-day recurrence tendency points to relatively stable streams of solar wind plasma with small angular widths, fixed relative to the sun and rotating with it. Thus, the model for the recurrent disturbances is one with streams of solar plasma rotating around every 27 days, sweeping past the slower moving earth and the streams perturbing the geomagnetic field lines as well as the F-region electrons bound to them. The stability of the streams is such that some of them persist for months on end, sometimes for almost a year.

A contemporary example of data on this type of phenomena is given in Figure 16.4 where the A-index from the Fred-ericksburg magnetometer is plotted against time for three solar rotations. Clearly, magnetic activity peaks about 3-4 days after the arbitrary 27-day marker. In terms of Amateur Radio operation, those days are the most disturbed magnetically and would show the most disturbed propagation, but still below storm conditions. More to the point, however, the days when the A-Fr index was below 10 would offer the best propagation conditions as magnetic disturbance of the F-region would be a minimum then.

By way of summary, the above remarks show the differences between features of the current model of the geomagnetic field and the more elementary dipole model in use before WWII. But those remarks do not explain how the solar wind compresses the field nor the mechanism that operates during magnetic storms, moving field lines on the front of the magnetosphere back into the tail region, carrying their supply of ionospheric electrons with them. That discussion will deal not just with the flow of ionized material leaving the sun but also its close relationship to the interplanetary field. The matter proves to be quite involved and only the essentials will be given here, leaving the details to those who want to pursue the full range of solar/terrestrial relationships.

To begin the discussion, ionized material coming from the sun, solar plasma, has an extremely high electrical conductivity. In fact, the conductivity is so high that any electric field or separation of charge that might be induced

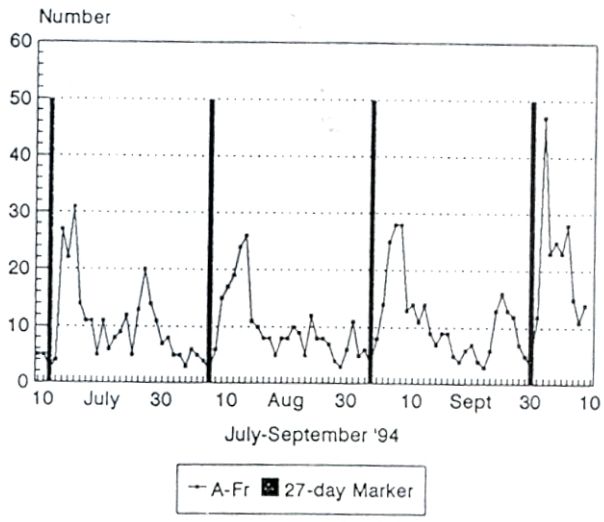

Figure 16.4 Recurrence of magnetic activity, as given by A-Fr. From NOAA/ SESC data.

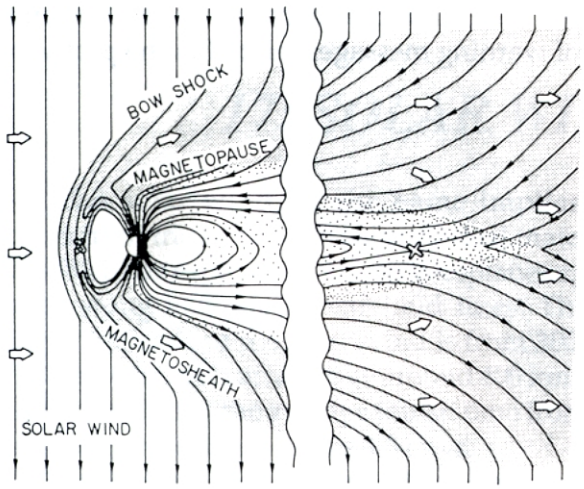

Figure 16.5 A schematic view of magnetospheric structure due to the interaction between the solar wind and the geomagnetic field. From Akasofu [1978]

by a change in magnetic field conditions in the plasma is immediately counteracted or neutralized by charge flow. So electric fields do not exist in the flowing plasma and the magnetic field is constant, frozen in the plasma.

It was suggested by J.W. Dungey in 1962 that the solar plasma, carrying the interplanetary field, interacts with the terrestrial magnetic field in an interesting way. Earlier, the classic geomagnetic model had field lines come out of the Southern Hemisphere, cross the geomagnetic equator and then go downward into the Northern Hemisphere. Dungey's proposal was that the interplanetary field could merge with the terrestrial field when it had a southward component relative to the earth. In that type of circumstance, interplanetary field lines being carried past the earth by plasma flow would join continuously with the terrestrial field lines. But with the plasma motion, terrestrial field lines would then be carried in the direction away from the sun by the solar wind plasma.

A snapshot of the process is shown in Figure 16.5, simplified to show field lines in the noon/midnight plane and with the magnetic axis perpendicular to the plasma flow. There it is seen that high-latitude field lines from the Southern Hemisphere that would have crossed the equatorial plane and closed with the Northern Hemisphere now are merged with the interplanetary field and being swept downstream, as indicated by the arrows.

The merging region at the front of the magnetosphere is indicated by an X-like symbol. There is another merging region in the magnetotail, marked in a similar fashion. In this model new field lines, on being swept back, exert inward pressure on other lines in the tail and oppositely directed field lines, above and below the equator in the magnetotail, may merge and become closed field lines again.

The figure, of course, only gives a two-dimensional picture of three-dimensional processes. Thus, the transport of field lines is really a convection process, field lines from the front of the magnetosphere being swept back into the tail and then, after reconnection, moving forward again. For a steady-state situation, the rate of field line removal on the front of the magnetosphere must be balanced by the transport of field lines forward after reconnection. But those processes require time and experience shows that field line erosion can occur to the extent that the front of the magnetosphere is inside the orbital location (6.6 Re) of the synchronous satellites. Those excursions are brief, measured in minutes, and then the magnetopause moves outward again.

Qualitatively this model can explain the new shape of the geomagnetic field as well as the erosion and transfer of field lines from the front of the magnetosphere to the rear. Quantitatively a number of other aspects have to be added: the flow speed of solar plasma and its variation, the strength and general orientation of the interplanetary field and how the location and rates of magnetospheric processes, for erosion of field lines at the front and reconnection in the tail, vary with them.

The above discussion, only a few paragraphs in length, deals with a topic which has kept magnetospheric physicists busy for two decades. Needless to say, there's much more to the story and some further mention will be made of the model, mainly in connection with the ionospheric aspects of auroral electron and solar proton bombardment. That will be done because it's important to have an appreciation

of the phenomena which have a negative impact on propagation, probably 15-20 percent of the time, and to understand the full meaning of warning messages related to the problems.

17: SOLAR WIND AND FLARES

The solar wind, as the name implies, comes from the sun and is solar coronal material which has expanded out into interplanetary space along extended solar field lines. The range of speeds of the solar wind is from 300-1,000 km/sec, with an average around 400 km/sec. On that basis, the average transit time from the sun to the earth is about 4.3 days.

The solar wind consists of protons and electrons in equal numbers, keeping it electrically neutral, and their energies are low, about 1/4 electron-Volt (eV) for the electrons and the proton energies are higher (about 500 eV) in proportion to the proton/electron mass ratio. Typical number densities in the solar wind are 5 protons per cubic centimeter. On that basis, if one thinks of the earth's magnetosphere as a target or collector whose aperture is about 10 Re in radius, the power input available from the solar wind would be about 2E+10 Watts for average conditions. That figure is small compared to the 1.8E+17 Watts that the earth receives as sunlight.

Solar flares take place in the vicinity of active regions on the sun and are described as sudden brightenings in radiation, as typically observed by solar astronomers in hydrogen emissions. Increases in radiation may take place in other parts of the spectrum, bursts of energetic X-rays giving rise to ionospheric effects, such as sudden shortwave fade-out (SWF) or sudden ionospheric disturbance (SID), from ionization released in the D-region of the sunlit portion of the atmosphere. An example of an X-ray burst is found in Figure 5.4, showing that flare X-ray fluxes may reach levels like 3E-5 Watts per square meter and continue on for hours after a rather sudden onset.

The relation of SWF events to solar flares was discovered by Dellinger in 1937. A classic example of the SWF effect on a radio link is shown in Figure 17.1 where 9.570-MHz signals on a 600-km path fade out for the better part of an hour. In terms of Amateur Radio operations, effects of that type are well known, especially at the lower frequencies where D-region absorption is the greatest. They occur most frequently around the maximum of a solar cycle and if the absorption is intense and of long duration, they serve as indicators of flare activity and possible magnetic storm effects on HF propagation, delayed by some 20-40 hours.

Flares are listed in the weekly Boulder Report according to location on the solar disk and the times in UT when the flare began, peaked in brightness and ended. Those times may be given in terms of hydrogen emissions from ground-based observations or X-ray bursts at satellite altitude. In addition, they are classified according to brightness in hydrogen emissions (faint, normal or bright) and X-ray flux in Watts per square meter in the 1-8 Angstrom range. Finally, flares are listed in importance according to the area in square degrees of solar surface at maximum brightness. All that information is summarized in the *Users Guide for the Boulder Report.*

Both optical and X-ray flares vary in number during a solar cycle, the optical flares being far more numerous and in phase or step with the sunspot number. The Space Environ-

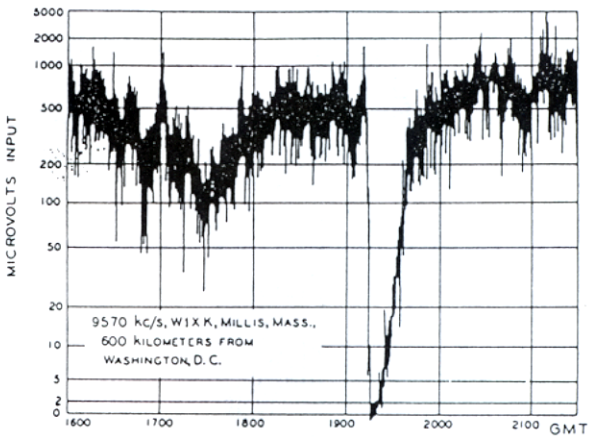

Figure 17.1 Shortwave fade-out on 9.57 MHz at 1915 UTC on 24 November 1937. From Snyder and Bragaw [1986]

ment Laboratory of NOAA has compiled flare statistics on the last three solar cycles and finds the number of optical flares varies between 15,000 and 19,000 per entire solar cycle and with flare rates around 1,000 per month at the peak of a cycle. But X-ray flares, those which are most likely to affect the ionosphere, are far less numerous, something like 50-80 per solar cycle and maximum flare rates the order of 15 per month. Obviously, with so few X-ray flares per cycle, it is impossible to chart any sort of solar cycle dependence.

There is another aspect to the flare process which affects the D-region of the ionosphere, the acceleration of solar protons to energies in the MeV (1E+6 eV) range, even to the BeV (1E+9 eV) range. Those flare events are not as numerous as X-ray flares, between 20 and 40 per solar cycle and with peak rates the order of 2-4 per month. Beside the difference in energy, keV for X-rays and MeV for protons, proton events are longer lasting in their effects, often measured in days as compared to an hour or so for X-ray events.

In reporting flare events, the Space Environment Laboratory distinguishes between "proton events" and "PCA events." The former are small events, where the solar proton flux is weak and only detected at satellite altitudes. In that regard, the proton detectors on the GOES satellites record proton fluxes above four thresholds: >1, >10, >30 and >100 MeV. An example of satellite recordings is shown in Figure 17.2, with three proton flare events within a single week. Considering the long duration of the proton fluxes at satellite altitude, the question comes up whether that is characteristic of the acceleration process at the source or protons are leaking out of a magnetic containment region. The latter is the favored interpretation, with acceleration taking place during the optical flare itself.

Solar protons with energies above 10 MeV may penetrate to D-region altitudes and create ionization there by collision processes. However, that is limited largely to high-latitude regions as the geomagnetic field acts as an energy filter, admitting particles mainly where the field lines are close to the vertical direction and deflecting away incoming protons from other regions where the field is more horizontal. Hence, the term PCA for polar cap absorption events as D-region absorption takes place all across the polar cap during solar proton bombardment.

The ionization of the D-region continues as long as solar protons penetrate to those depths but the resulting electron density depends on the degree of illumination. In particular, D-region electrons remain free during daylight hours and may give rise to huge absorption effects (measured tens of dB in the HF

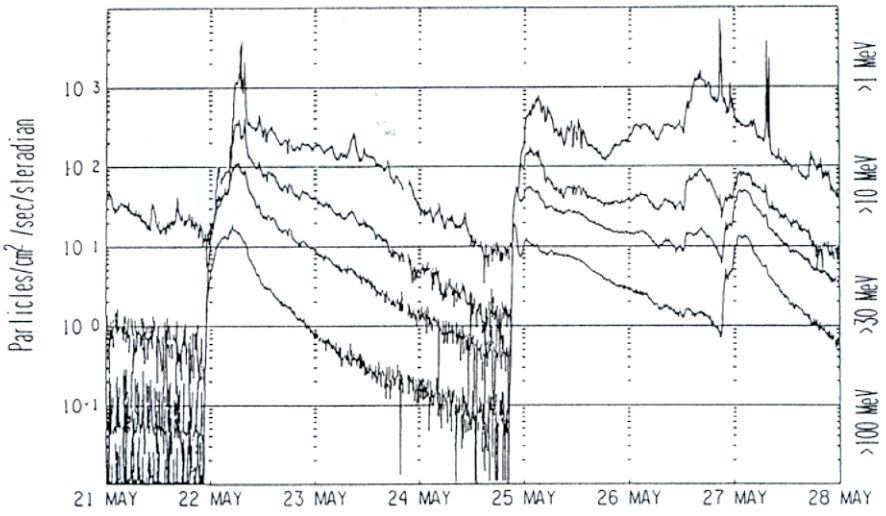

Figure 17.2 Examples of solar proton events recorded at satellite altitude. From NOAA/SESC Report 29 May 1990.

range) but at night, electrons attach themselves to oxygen molecules and the massive negative ions are far less effective than free electrons when it comes to signal absorption.

In Amateur Radio operations, the existence of a PCA event is revealed by a blackout of long duration of signals coming across the polar caps, say from northern Europe to the West Coast or from Asia to the northern parts of the East Coast. Around the equinoxes, there will be some nighttime recovery of signals when the polar caps go into darkness but during polar summer, signals recover slowly as the proton flux declines.

Beyond absorption effects in the HF range, radiation effects from energetic solar proton events pose a threat to high-altitude aircraft flight, disturb VLF navigation and communication systems that depend on the D-region. The additional ionization which results from an influx of solar protons looks like a sunrise to those systems, perhaps out of character for a site in darkness if the protons have been deflected into that region by the geomagnetic field.

Solar flares do generate noise in the radio spectrum, all the way from the HF range (10 MHz) to the microwave range (30 GHz). While emissions vary significantly from one flare to the next, there is a sweep aspect to frequencies in the solar radio spectrum, illustrated in Figure 17.3. In that diagram, the emissions which may be heard at a given time lie along a vertical line, say a broadband continuum of noise in the 10-300 MHz range about 40 minutes after the flare began. Similarly, along a horizontal line, one would note noise bursts which drift down in frequency, rapidly past 100 MHz very early in the noise storm and then more slowly about 10 minutes into the noise emissions. In present practice, discrete frequencies, 245 MHz and 2,695 MHz, are monitored and when the peak fluxes reach certain threshold levels above background, NOAA will issue an Alert message to interested parties.

As a result of solar noise emissions, amateur operators on the higher HF bands may also hear the sort of whooshing sound that goes with flares. Of course, being in the HF portion of the spectrum, solar radio noise bursts do not contribute to ionization processes like the accompanying X-rays do. Thus, except for being a warning signal for flare activity, solar noise bursts are more of a nuisance than anything else.

Earlier in this section, it was mentioned that flares may be followed by magnetic storms, some 20-40 hours later. That was the classical approach to magnetic storms, dating back to the 19th century when it was found that a mag-

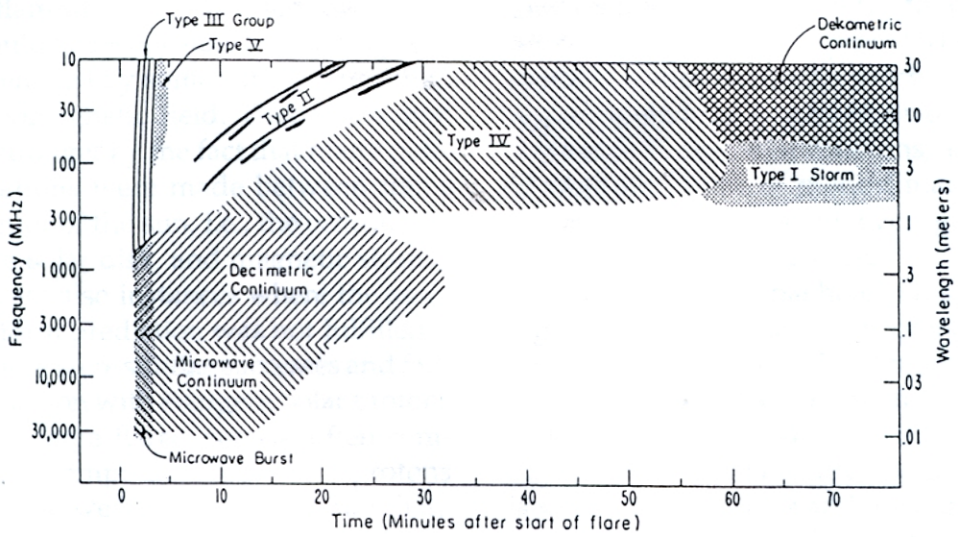

Figure 17.3 Dynamic spectrum of solar radio noise emissions. From NOAA Preliminary Report and Forecast User Guide.

netic storm occurred about a day after a large, bright flare. So, up to the 1960s, the idea was put forward that a blast wave was generated in the flare process, ionized material moving at 1,000-2,000 km/sec then arrives at earth's orbit and somehow triggers a magnetic storm. That was in addition to the electromagnetic emissions (radio, light and X-rays) which came promptly. The idea of a blast wave had some support from the fact that many disturbances start with a sudden storm commencement (SSC), suggesting the arrival of a puff of solar material. On the other hand, a good number of magnetic disturbances of storm proportions began with gradual commencements (GC) so there was still some room for new ideas and we turn to them next.

18: MAGNETIC STORMS AND AURORAE

As noted earlier, the earth's magnetic field is monitored with the aid of magnetometers, devices which follow changes in the magnitude and direction of the field. Under quiet conditions, the components of the field vary by only a few tenths of a percent in the course of a day. But during magnetic storms, departures from quiet day levels may reach several percent and last for times ranging from hours to days. And storms can be either sudden (SSC) or gradual (GC) in commencement.

But the association between magnetic storms and solar flares has not always been one-to-one as some large flares are not followed by magnetic storms. Then, too, magnetic storminess occurs in the absence of significant flare activity. The one idea that now seems beyond dispute is that the sun evaporates ionized matter, solar plasma, part of the solar corona becoming so hot that even the sun's gravity is unable to retain it. That steady sort of emission is the source of the solar wind, streaming outward at about 400 km/sec.

The earlier idea that associated flare activity with magnetic storms suggested that denser, faster-moving solar plasma left the vicinity of a flare site and if directed toward the earth, it would be responsible for the magnetic storm that ensued by some sort of interaction with the geomagnetic field. That association was made stronger by the fact that many positive associations were made between flares near the center of the sun, i.e., the central meridian of the solar disk, and magnetic storms. But there were also instances where the association or storm prediction was not fulfilled.

And there were similar successes and failures in connection with energetic solar protons coming from large flares, success often coming with the prompt arrival of solar protons from a flare site west of the central meridian. But then there were exceptions, large flares west of the central meridian and no protons or else protons but quite delayed in their arrival at the earth's orbit. And some proton events had no association with flare activity on the disk at all, perhaps coming from an active region that had rotated past the western limb.

All of the above discussion was in connection with ground-based observations. But it was based on older techniques, before recent advances in the technology of solar astronomy. There the solar coronagraph was perfected after WWII to the point that the solar corona could be examined without the aid of eclipses, even with instruments flown on satellites. And there were advances in the technology of spectroheliographs as well, giving solar images in selected wavelengths. Those new techniques provided opportunities to look for associations between magnetic storms and other solar phenomena, especially what are termed "coronal holes" and "coronal mass ejections" (CME).

Now a few words about coronal holes. Coronal holes are regions where solar field lines go off into space and from which solar wind material may readily escape. The speed of streams from those regions is high by solar standards, around 600 km/sec, and it is thought that the flow of material from the regions extracts so much energy that the regions are cooled down and appear darker, like sunspots, in comparison with nearby regions. The regions seem to be long lived, on occasions lasting many 27-day solar rotations, and give rise to recurrent forms of modest magnetic activity, as in Figure 16.4, or even geomagnetic storms of some significance.

A series of coronal hole maps is shown in Figure 18.1; those maps are coronal hole contours from 1,083 nm (10,830 Angstrom) images of the sun taken by the spectroheliograph at Kitt Peak, NM. The rotation of the coronal hole, day by day, toward a central meridian position is seen from the figure and the high-speed solar wind stream from the region contributed, in part, to the change from quiet conditions for 26-28 October to major storm levels on 29-30

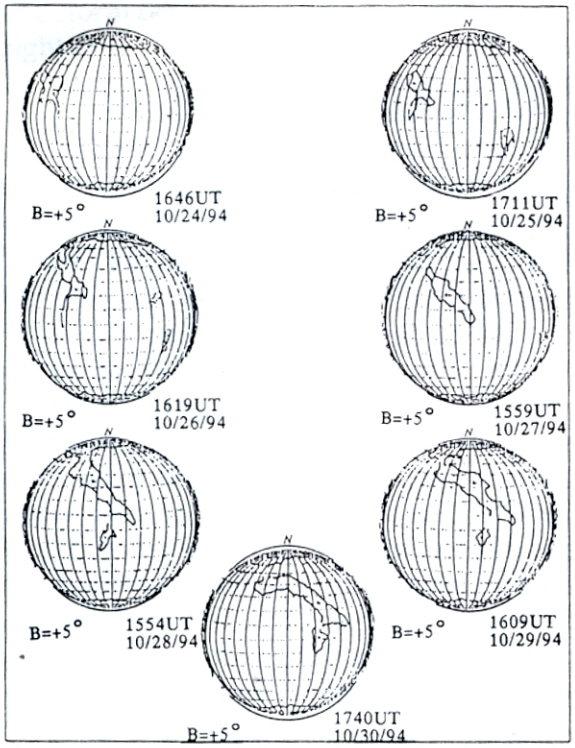

Figure 18.1 Coronal hole maps for 24-30 October 1994. From NOAA/SESC Report

October 1994. In that latter period, a magnetopause crossing was observed briefly by the GOES spacecraft, at 1430-1433 UTC on 29 October.

In contrast with the long-lived solar streams associated with coronal holes, there are other emissions of coronal material, sporadic or noncurrent in nature and not flare related. From coronagraph observations at satellite altitudes, it appears that large quantities of solar material are ejected sometimes into interplanetary space, thus amounting to coronal mass ejections (CME) when they occur. And currently, studies in relation to other forms of solar activity suggest that CMEs have a close association with eruptive prominences or disappearing filaments, having comparable widths at the sun but generally removed from active regions.

And observations indicate that CMEs originate in regions where solar field lines are closed, away from regions around coronal holes where solar wind plasma is expanding outward. What associations in time there are with flare activity show that CME's usually lift off before the flare activity begins. But the leading edges of CMEs have speeds from around that of the ambient solar wind, 400 km/sec, up to 1,200 km/sec. The higher range of speeds suggests that when a CME moves outward, into normal solar wind from the sun, it may drive a shock wave ahead of itself in the surrounding solar plasma.

In substance those are the circumstances now suggested to lead up to sudden commencement magnetic storms; all that's needed is solar wind in the vicinity of the earth with the interplanetary field it carries pointing southward. When a CME-driven shock wave reaches the earth's orbit, geomagnetic field lines merge with the field lines in the shocked plasma and a magnetic storm gets under way, complete with strong ionospheric effects. The scheme has no need to be associated with flare activity although it may be present after a CME has started. Of course, the time delay and magnitude of the effects which result from a CME depend on its speed, with delays ranging from 1-4 days.

During the recent '94 CQ WW DX SSB Contest all those factors came into play, as may seen by reading the sections of the Solar Report issued at 2200Z on 29 October on the NOAA/SESC BBS. The Report is quite long so only the Geophysical Activity Summary for the period 28/2100Z to 29/2100Z is given and the Geophysical Activity Forecast for the next day is quoted:

"The geomagnetic field began the period quietly. However, a sudden impulse of 24 gamma (24 NT) was observed at 29/0025Z. This is attributed to a long duration (CME) event that occurred on 25/1000Z for a lengthy 86-hour delay. The field became active shortly after the impulse and minor to severe storm conditions followed in the 0900-1500Z interval. Some high-latitude sites experienced K-indices of 9 in the 1200-1500Z interval. A brief magnetopause crossing was observed at GEOS-7 between 29/1430-1433Z. At the end of the period, the field calmed to unsettled levels. Energetic electron fluxes (capable of disabling controls on some spacecraft) began the period at high

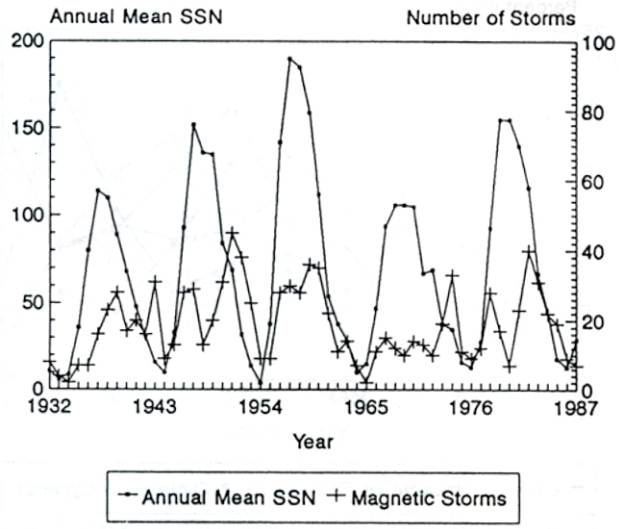

Figure 18.2 Annual mean sunspot number and magnetic storms per year, 1932-1987.

levels but dropped to normal background levels by 29/0300Z.

"The geomagnetic field should be active to major storm levels for 30 Oct. As the current disturbance ebbs, it will be replaced by a coronal hole related one. Unsettled to minor storm conditions would be experienced through 03 Nov as a result of that high speed stream. Energetic electron fluxes should return to high levels around 01 Nov."

Those remarks pretty well summarize where matters stand now as far as the initiation of magnetic storms is concerned. Of course, storms have been known for more than a century and the same is true of the importance of sunspot counts when it comes to taking a measure of solar activity. As noted earlier, solar flares occur in numbers proportional to the rise and fall of sunspot numbers. That is not true of magnetic storms, as may be seen in Figure 18.2 where both the distribution of magnetic storms and sunspot count are shown for 5 solar cycles. Except for Cycle 19, an exceptional cycle in many ways and shown in the middle of the figure, it's seen that magnetic storm activity is delayed relative to the peak in sunspot numbers.

A more detailed view of the relationship of storm activity and the phase of a solar cycle may be seen in Figure 18.3 where storm data for the 5 cycles are superimposed and plotted year by year in terms of the percent of storms in the entire cycle. While there is no unique relationship evident, the delay of storm activity relative to solar maximum is clear and the statistics show that for those 5 cycles, the magnetic storms after each solar maximum outnumbered those before by a 3-to-1 ratio. By way of interpretation, the post-maximum peak in magnetic storm activity is related, in part, to the fact that high-speed streams from coronal holes are more frequent after solar maximum.

With the initiation of a magnetic storm, large-scale changes take place within the magnetosphere — high-latitude field lines are drawn back into the magnetotail, solar protons bombard more of the polar cap if a PCA event is in progress, energetic electrons rain down at auroral latitudes and result in auroral luminosity and ionization at altitudes above 100 km. All that signifies the dissipation of energy but then the question becomes one of the energy input from the solar wind and its transfer, especially to the far side of the magnetosphere where the aurora occurs.

Those are some of the questions which keep magnetospheric physicists busy and even after three decades, there is no universal agreement on any detailed theory. But that shouldn't be surprising considering the great magnitude

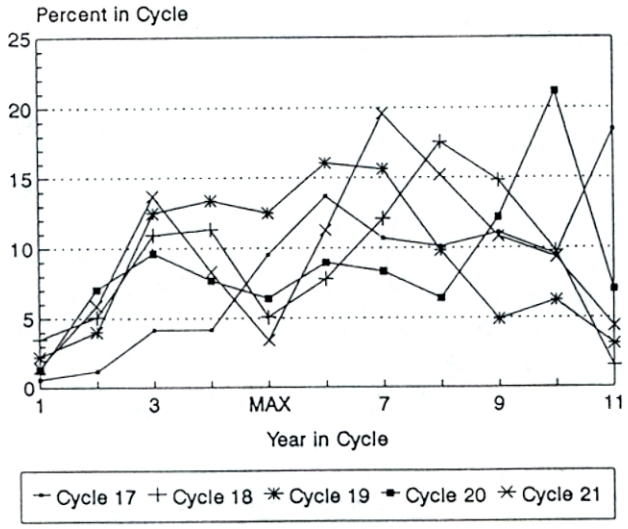

Figure 18.3 Percent of magnetic storms per year during Solar Cycles 17-21.

and scope of the problems and the fact that the vast expanses involved make data samples seem meager, even with a vigorous space research program. But progress has been made, stemming from the revision of the model for the geomagnetic field and the realization that a transfer of energy takes place from the solar wind to the magnetosphere whenever the interplanetary field has a southward component. The rest is in the details which remain to be settled: whether the energy input from the solar wind is dissipated continuously or possibly stored, to be released at a later time, and how low-energy electrons in the magnetosphere are accelerated from about 1 eV to the 10 keV or so required to produce auroral displays.

Those are good questions but may be of less interest to those concerned primarily about HF propagation. For them, the ionospheric aspects of the various phenomena are more relevant so let's turn first to auroral ionization. In that, the electron influx during auroral displays not only excites atoms and molecules to emit their characteristic radiations but also gives rise to intense ionization by collisions at the end of the electron's range and X-ray fluxes which can penetrate deep into the atmosphere.

Just as with the quiet ionosphere under solar illumination, the electron density that builds up with auroral bombardment depends on a competition between ionizing and loss processes. First, the rate of electron production in a region depends on the velocity and flux of the electrons as well as its atmospheric composition and density. At auroral heights, atomic oxygen is an important constituent, as shown by the green color in auroral displays. The other parts of the auroral spectrum depend on the presence of molecules of nitrogen and oxygen.

Next, loss processes take place because of electron recombination with positive ions and are fairly rapid around 100 km altitude, in contrast to the higher F-region where the rate of recombination is much slower. But with high incoming fluxes, significant electron densities build up and strong ionospheric absorption of signals may occur during auroral displays, even showing rapid changes in absorption much like changes in auroral luminosity. An example of such variations is shown in Figure 18.4 where the intensity of green auroral emissions during an auroral event after local midnight is compared with the ionospheric absorption of 27.6 MHz cosmic radio noise, both along the same field of view from the vertical direction.

Even though ionospheric absorption events show large, rapid variations during auroral displays around local midnight, auroral absorption is evident at other times of day throughout the year. The former events are as-

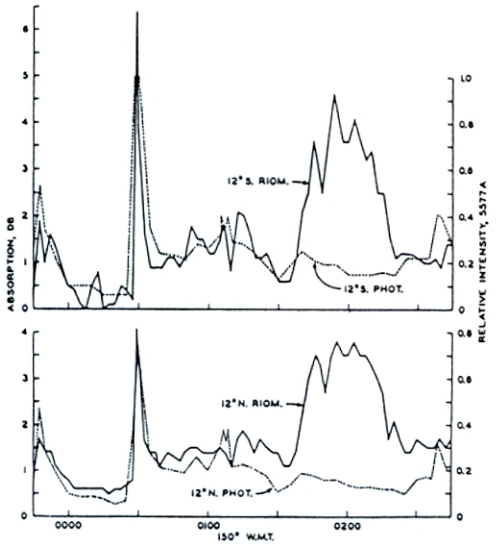

Figure 18.4 Variations in ionospheric absorption and auroral intensity for directions 12 degrees north and south of College, AK. From Ansari [1964]

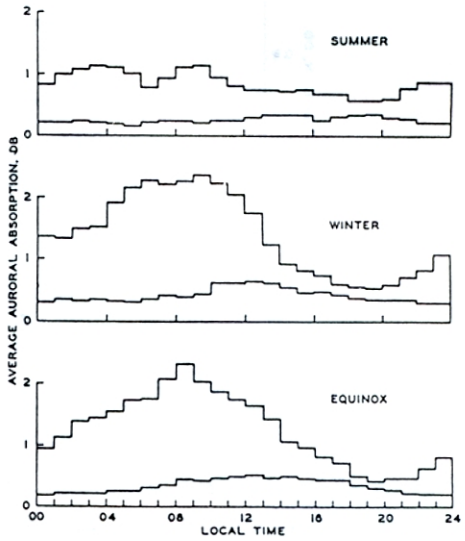

Figure 18.5 Daily variation of auroral absorption at College, AK for 5 magnetically disturbed (upper curve) and 5 quiet (lower curve) days from September 1957 to August 1962. From Basler [1963]

sociated with the breakup phase of auroral displays while the other, more enduring absorption events are associated with well-defined decreases in the local magnetic field on magnetometer records or extend into morning hours and beyond.

In that regard, Figure 18.5 shows the daily variation of auroral absorption at College, Alaska during the 5-year period centered on the peak of activity in Cycle 19. The variations are divided between the five most magnetically disturbed (upper curves) and five most quiet (lower curves) days for summer, winter and equinoctial periods and show how the absorption of 27.6 MHz varied with local time. Clearly, absorption is not limited to just when auroral displays might be visible and would have to be reckoned with when it comes to HF propagations as results indicate that absorption effects extend over a considerable range of local time or longitude.

But the region of ionization giving rise to the absorption of signals during auroral activity is more limited in latitude, just as is the case for auroral displays, and may be seen in Figure 18.6 where the auroral absorption zone in Alaska is compared with the visual auroral zones (incidence and occurrence) from all-sky camera data. From those data, it is seen that auroral absorption (AA) events are restricted to a fairly narrow range of geomagnetic latitudes, in contrast to PCA events which cover the entire polar cap. Another difference between the two types of absorption events is that PCA events are slowly varying and of long duration, measured in days, while AA events show rapid changes, as in Figure 18.4, and last only for hours at a time.

It should be noted that the magnitude of auroral absorption events around 30 MHz may reach several dB, but not tens of dB. But at auroral heights just above the 100-km level, the relative absorption efficiency of electrons is quite low, as shown in Figure 8.1, and that implies high electron densities, around 1E+6 per cubic centimeter, over a small range of altitude. That is the origin of auroral E-layers that the VHF enthusiasts enjoy so much.

For most HF operators, however, auroral E-layers amount to another absorbing region that's below the F-layer, extends E-W along auroral displays and is narrow in the N-S direction. And there's no day/night effect for absorption events at auroral heights like that found in the D-region during PCA events. That

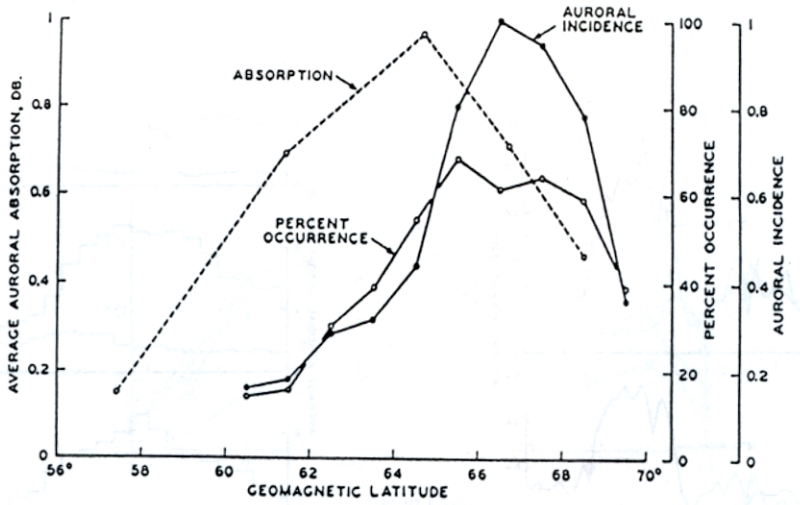

Figure 18.6 A comparison of the auroral absorption zone in Alaska with visual auroral zones from all-sky camera data. From Basler [1963]

is seen in Figure 18.7 where auroral events observed during various levels of local magnetic disturbance showed no day / night variation in absorption, when plotted according to the solar elevation angle at the time of observation.

Another aspect of auroral events that would be of interest to the HF operator, particularly one engaged in making long-path contacts across high latitudes, is that auroral phenomena show similar effects in conjugate regions, i.e., regions on the earth connected by magnetic field lines. Thus, auroral electrons may spiral down field lines from the magnetotail and produce similar effects at sites in the two hemispheres which are separated by as much as 14,000 km. An example of a conjugate auroral absorption event is shown in Figure 18.8 where the absorption of 27.6 MHz cosmic radio noise during a magnetic storm is seen to be comparable at conjugate auroral sites, Kotzebue, Alaska (KL7) and Macquarie Island (VK0), Australia.

Finally, it should be pointed out that the above discussion, while not all that complicated, goes beyond what is experienced in typical Amateur Radio situations, dealing with results of observations obtained by looking up at a small region of the sky instead of obliquely, off to the horizon, as in Amateur Radio operations. And, when you get right down to it, that difference is what makes propagation a challenge, not only for what is attempted but for the range of circumstances, even conditions that may exist along a path.

To see what I mean, think of a path for a distant contact you might attempt to make: it starts in sunlight, goes across the magnetic equator, through mid-latitudes and the auroral zone in the opposite hemisphere and back toward a station in darkness in the original hemisphere. That has the all the makings of a dusk-to-dawn long-path contact. But what about all the ionospheric phenomena that would be in-

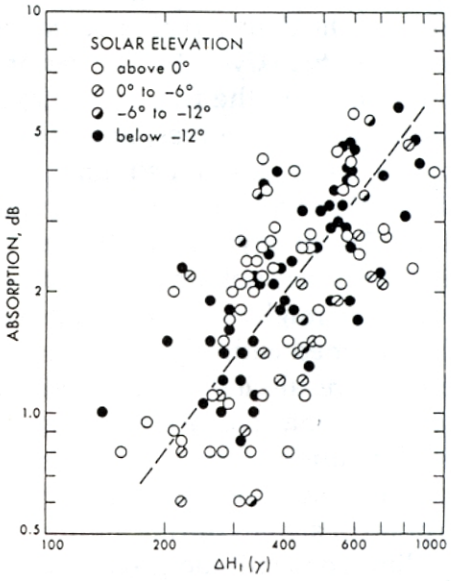

Figure 18.7 Auroral absorption for different solar elevation angles as a function of horizontal magnetic disturbance. From Brown and Barcus [1963]

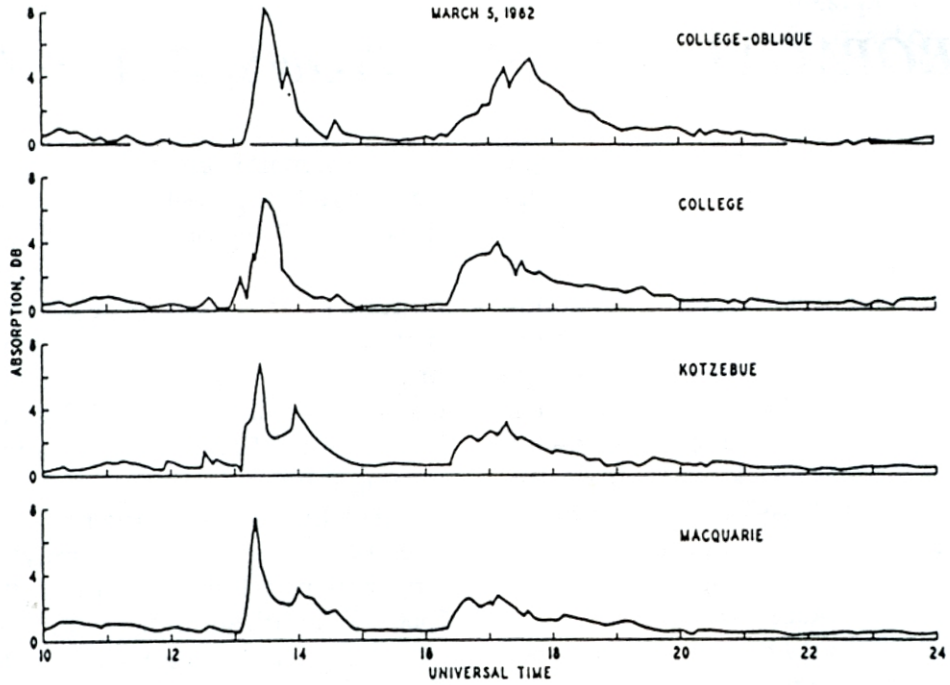

Figure 18.8 Time variations of auroral absorption during an event recorded at three riometer sites in Alaska and one in the Southern Hemisphere. From Leinbach and Basler [1963]

volved along the way — first, transequatorial propagation, then from mid-latitude to auroral zone conditions and finally ionospheric gradients, to name a few.

That sounds like an ionospheric smorgasbord or something that's been put together by a committee. But it's no miracle when that sort of contact is made; it happens all the time. More to the point, it'd be satisfying to understand how it all works and then be able to make it a reality, on the right frequency and at the right time. That would make any Little Pistol happy, no doubt about it.

19: PROPAGATION CONDITIONS, BAD & GOOD

Whether the Little Pistol thinks propagation is good or bad depends on his knowledge of what propagation should be like under the best of circumstances and what it happens to be, given the state of solar/terrestrial conditions. As for "should be," that goes to the properties of an undisturbed ionosphere for the smoothed sunspot number (SSN) which characterizes the phase of the solar cycle. Knowing the SSN, the LP could check out the rosy scenario for various DX possibilities by running his HF propagation program to see what predictions it comes up with for openings, at least MUF values and workable S/N ratios.

Better yet, LP could have done his homework in advance and knowing the season, already have a prediction in hand for the earliest DX opening of the day on 14 MHz. That would be off to the East of his QTH (Boulder, CO), say, when the West Europeans might start coming in. For example, with an SSN of 50, West Europeans start to come through after sunrise, around 1500 UTC in the winter. Listening then, it would be a question of what is heard and what it means.

Suppose the LP points his beam toward northern Scandinavia and listens for signals, say from LAs, SMs or OHs; from Boulder, those paths go across the northern auroral zone, close to the polar cap, and the presence or absence of those signals means something for the state of the magnetosphere. If the Scandinavians were heard, that would suggest a quiet magnetosphere with nothing in the way of auroral activity. But if they were not heard within a reasonable time, the next thing to do is check on signals from northern Europe, say Fs and DAs; those paths go across the southern tip of Greenland and are at the lower edge of the auroral zone. If nothing is heard from them, that raises the spectre of a magnetic storm, minor or major.

To check that out, the LP would have to look for signals from southern Europe, say EAs; paths like that go below the auroral zone and depend on F-region ionization that's held on field lines deeper in the magnetosphere. If nothing's heard from those paths, it's either a matter of a major magnetic storm in progress or something's wrong with LP's antenna. To check on the latter point, LP would turn the beam toward South America and see what's coming through.

For LUs and PYs, the path from Boulder goes off to the southeast, maybe 1,000 km longer than to Europe and in full sunlight at 1500 UTC. With sunlight on the path, LP could expect signals on the weaker side but there should be no problem with the MUF for the path as only the robust equatorial ionosphere is involved. So the LP would have an answer, one way or the other.

Now I have to confess to dragging out that discussion, perhaps unduly, for pedagogical purposes, taking you through the steps in the analysis of band conditions, something like the qualitative analysis scheme you used in your high school chemistry course to identify an unknown compound. It's a valid approach but there are shortcuts in almost anything we attempt and so it is with propagation, the LP just pointing the beam toward Europe and listening for calls on the band. On 14 MHz, a triband Yagi has a forward pattern which is broad enough, typically 70 degrees between –3 dB points, to include directions from Finland to Spain. So with one beam setting and some serious listening, the LP may come up with an answer as to how propagation shapes up or whether storm conditions have already taken over.

But there are other shortcuts for the LP to use; the simplest is just to tune in the WWV broadcast at 18 minutes after every hour and listen to the statements about solar and geomagnetic activity. If there was a magnetic storm

in progress, the LP would hear about it. But what do the statements about solar activity and magnetic activity mean?

On WWV broadcasts, solar activity is described as being between very low and very high, with low, moderate and high bounded by those extremes. Magnetic activity uses an A-index derived from the magnetometer at Boulder and estimates are given for the average of the A-index for the current day and also the K-index in the last three-hour interval.

Solar activity is expressed in terms related to the number and type of X-ray flares observed at satellite altitude. The type or class of flare is given with alphabetic designations — A, B, C, M and X — the X-ray flux increasing in that order. For example, "moderate activity" would be solar conditions where the satellite X-ray detector recorded 1-4 M-Class flares while "very high activity" would mean five or more 5M-Class flares. No mention is given for optical flare activity, coronal holes or coronal mass ejections.

The description of magnetic activity begins with conditions which are "quiet" or "unsettled"; that means the estimated A-index for the day is less than 16 and the most recent three-hour K-index was probably less than three. That's a very good omen! But when the geomagnetic field is said to be "active," the A-index is then between 16 and 30 and the K-index is up to 4.

It's at that point when the warning light should go on in LP's head, especially if the A-index is in the high end of the range. That's close to some form of serious disturbance, the first being "minor storm" when the A-index is between 30 and 50 and the K-index is up to 5. At those times, one can clearly notice problems with HF propagation and they only get worse if followed by "major-storm" conditions when the A-index is between 50 and 100 and with the K-index 6 or above, or "severe storm," then the A-index is greater than 100 and K-indices are 7 or greater, the highest possible being 9.

The information broadcast on WWV at 18 minutes past each hour, and on WWVH at 45 minutes past each hour, is a 45-second "Geophysical Alert Message" and can also be obtained by telephone, calling (303) 497-3235 at any time. The message on that line is a tape recording giving solar and geophysical activity and indices for the most recent 24 hours and for the next 24 hours, updated every three hours.

If a computer and modem are available, the price of a phone call to Boulder is better spent by calling the Public Bulletin Board System (PBBS) at (303) 497-5000 and getting more complete information and forecasts. In calling the PBBS, use a protocol with a conventional 8-bit word, one stop bit and no parity. The PBBS will operate at 300, 1200 and 2400 baud. A wide selection of options is offered on the menu that is presented but for LP's purposes, the Solar and Propagation Reports would be the ones to copy and can be downloaded in less than a minute with a 1200-baud modem.

The long-distance charge for a call to the NOAA PBBS will be minimal, especially if the call is made at night or in the morning, before working hours. For here in the Northwest, the current Solar and Propagation Report is in the shack every morning for a cost less than $5 a month. Your charges may be different so check with your phone company for the best times to call and toll charges.

In order to see what is included in those Reports, consider first the Solar Report for 3 October 1994. It consists of six (6) sections which will be quoted as received from the PBBS. On reading through it note the contrast between geomagnetic and solar conditions — severe storm levels, surely with major disruption of HF propagation, and very low solar activity, no problem. So read on; the report follows:

IA. Analysis of Solar Active Regions and Activity from 02/2100Z to 03/2100Z: Solar activity was very low.

IB. Solar Activity Forecast: Solar activity is expected to be at very low levels.

IIA. Geomagnetic Activity Summary from 02/2100Z to 03/2100Z:
The geomagnetic field has been at quiet to unsettled levels until 02/2230Z when activity increased to minor to severe storm levels. This activity is believed due to a favorably positioned recurrent coronal hole feature. The greater than 2 MeV energetic electron flux has been mostly normal to moderate. At about 03/1400Z the flux exhibited a rapid rise to peak in the high range at about 03/1600Z.

IIB. Geophysical Activity Forecast: The geomagnetic field is expected to be at major storm conditions on day one and then becoming minor storm levels the second day of the forecast. Active conditions are expected on day three.

III. Event Probabilities 04 Oct 06 Oct

Class M	01/01/01
Class X	01/01/01
Proton	01/01/01
PCA	Green

IV. Penticton 10.7 Cm Flux

Observed	03 Oct	074
Predicted	04 Oct-06 Oct	074/074/074
90-Day Mean	03 Oct	078

V. Geomagnetic A Indices

Observed	AFr/Ap	02 Oct	012/009
Estimated	AFr/Ap	03 Oct	070/065
Predicted	AFr/Ap	04 Oct-06 Oct	050/060-035/040-020/030

VI. Geomagnetic Activity Probabilities 04 Oct-06 Oct

A. Middle Latitudes		
	Active	20/30/30
	Minor Storm	30/30/30
	Major-Severe Storm	30/20/20
B. High Latitudes		
	Active	20/20/30
	Minor Storm	30/40/30
	Major-Severe Storm	40/30/20

So that was the bad news and forecasts of things to come, from the solar and geophysical standpoint. Now what about propagation? That's covered in a separate report. However, Propagation Reports are given every six (6) hours and include a forecast for the next six (6) hours. That being the case, consider the following:

Primary HF Radio Propagation Report issued at 03/0520Z Oct 94.

Part I. Summary 03/0000Z to 03/0600Z Oct 94
Forecast 03/0600Z to 03/1200Z Oct 94

		Quadrant I	II	III	IV
		0 to 90W	90W to 180W	180 to 90E	90E to 0
Region	Polar	U2/-25	U2/-25	U3/-20	U3/-20
	Auroral	U2/-30	U2/-30	N4/-20	N4/-20
	Middle	N4/-20	N4/-20	N5	N5
	Low	N5	N5	N6	N6
	Equatorial	N6	N6	N7	N7

Part II. General Description of Propagation Conditions Observed during the 24-hour period ending 02/2400Z, and Forecast of Conditions for the next 24 hours.

Conditions were normal until the last 6 hours of the day when geomagnetic storming in the polar and auroral areas caused degradation, mostly in the night sectors, multipathing and absorption caused very poor to fair conditions in those areas.

Forecast: Conditions should get worse, especially in the night sectors, and may cause some transauroral/polar paths to be unuseable. Multipathing, absorption, sporadic-E and fading may occur, and MUFs should be depressed significantly. The storming may persist for several days.

Part III. Summary of solar-flare induced ionospheric disturbances which may have caused shortwave fades in the sunlit hemisphere during the 24-hour period ending 02/2400Z Oct 94. . .
Start End Confirmed Freqs Affected . . . None
Probability for the next 24 hours. . . . Nil

Part IV. Observed/Forecast 10.7-cm Flux and K/Ap
The observed 10.7-cm flux for 02 Oct 94 was 074
The forecast 10.7-cm flux for 03, 04, 05 Oct 94 are 076, 077, and 077.
The observed K/Ap value for 02 Oct 94 was 02/09.
The forecast K/Ap values for 03, 04, 05 Oct 94 are 03/15, 04/25, and 04/30.
Satellite X-ray Background: A1.0 (1.0 E Minus 05 ergs/cm sq/sec).
The effective Sunspot Number for 02 Oct 94 was 20.0.

Before getting to propagation matters, it's clear, on comparing the Solar Report and Propagation Reports, that propagation forecasters underestimated the potential for magnetic activity, forecasting Ap of 15 for 03 Oct while the estimated value during 03 Oct was 65. Their only solace would be that the magnetic field was quiet, as they had forecasted, until the last 6 hours of 03 Oct 94. But even if the storming held off, it would have ruined their forecast for 04 Oct.

The only part of this report that needs explanation is where conditions are specified according to region. In that regard, the Propagation Report distinguishes between normal (N), fair (U) and poor (W) conditions. Thus, the conditions in higher latitudes were fair to normal. But there are degrees of each, 1 through 9:

1. Useless 2. Very Poor 3. Poor 4. Poor to Fair 5. Fair 6. Fair to Good 7. Good 8. Very Good 9. Excellent

and also predictions of MUF values, when 20% or more from seasonal means. Those predictions, either positive or negative, are for single-hop, 4,000-km paths with midpoints located in the relevant grid block.

With those distinctions in mind, we can go on to the update:

Secondary HF Radio Propagation Report issued at 03/1200 Z Oct 94.

Part I.	Summary	03/0600Z to 03/1200Z		Oct 94	
	Forecast	03/1200Z to 03/1800Z		Oct 94	
				Quadrant	
		I	II	III	IV
		0 to 90W	90W to 180W	180 to 90E	90E to 0
Region	Polar	U3/-20	U2/-25	U2/-25	U3/-20
	Auroral	N4/-20	U2/-30	U2/-30	N4/-20
	Middle	N5	N4/-20	N5	N5
	Low	N6	N5	N5	N6
	Equatorial	N7	N6	N7	N7

Part II. Conditions affecting HF Propagation: Geomagnetic storming which began at 03/00Z has de graded propagation, particularly in the higher latitude night sectors. Forecast: Expect little change in geomagnetic conditions over the next 24 hours. Multipathing, absorption and fading are likely for the entire period.

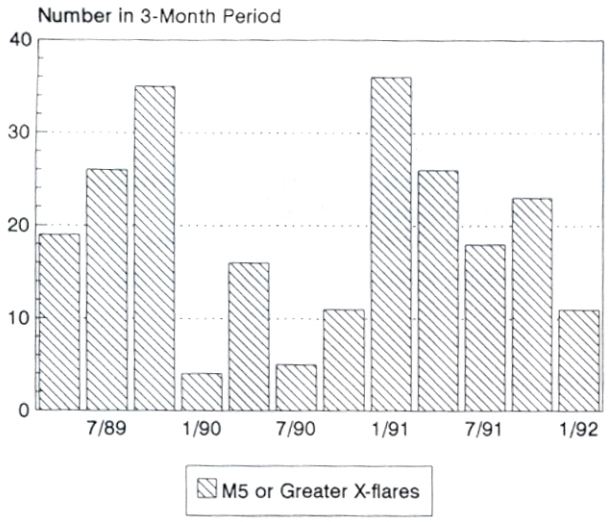

Figure 19.1 The number of M5 or greater X-flares in three-month periods, 1 April 1989 to 31 March 1992. From NOAA/SESC Report.

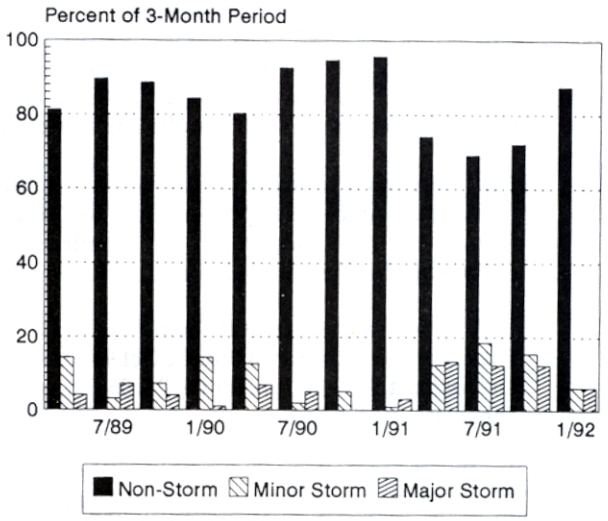

Figure 19.2 Levels of magnetic activity in three-month intervals, 1 April 1989 to 31 March 1992.

That was the bad news and one shouldn't dwell on it too long; after all, most of the time, propagation is not disrupted that much. But there are some points worth considering before going on to the good news. For example, a great deal of information was available to the forecasters, both solar and propagation, right at their fingertips, far more than the Little Pistol had. That would limit any forecasting effort by the LP if based only on the numbers from WWV. At best, the LP could plot values of the solar flux and A-index but beyond forecasting 27-day recurrences of those values and what they imply, little more could be said or done without more information. However, even 27-day recurrences are variable and uncertain, being found more frequently on the descending side of a cycle. And disruptions from energetic X-ray flares vary too, being more frequent near the peak of a cycle. That is shown by Figure 19.1 which displays variations in the number of energetic X-ray flares in three-month intervals across the peak of activity in Cycle 22. But no matter what the source, propagation disturbances are the main concern here.

In that regard, Figure 19.2 shows geomagnetic variations for the same period, the percent of days in three-month periods which would be quiet for the lack of storm conditions, and then the number of those which would be stormy with corresponding perturbations or disruptions of propagation conditions.

While the thrust so far might seem to be slanted or biased toward the bad side of propagation conditions, those figures tell another story related to the good side. For example, over the three-year period covered, the data in Figure 19.2 show that, on the average, propagation conditions were free of any sort of storm disruption 84.3% of the time. That's the good news, only tempered by the fact that variations about the average reached a promising 95.9% during the first part of '91 and a grim 69.1% in the next three-month interval during the middle of '91.

The data in Figure 19.1 indicate that there was an average of 6.7 energetic flares per month during that three-year period. Those disruptions, SWFs or SIDs, are short in duration, more of an annoyance than anything else. So the good news is still that about 84% of the time, right there during Solar Maximum when propagation is the greatest, the bands were open to the Little Pistol for DXing. That was something to celebrate at the time or to hope for in looking forward to when Cycle 23 comes around.

20: HISTORICAL FEATURES

In talking about the expectation of Cycle 23, the next in the series starting back in 1750, it's worth pausing for a bit and taking a look at what the historical record has to say about solar cycles. The Little Pistol, of course, is hoping for another humdinger, maybe even as good as Cycle 19, the greatest of all time — recorded time, that is. But what was the range of sunspot numbers in those previous cycles? That's worth looking at, even briefly, so turn to Figure 20.1; that shows the range of the maximum and minimum sunspot counts, up to the maximum of the present one, Cycle 22.

Looking at that figure, the Little Pistol can see that things have not always been the same as they are now and, as a corollary, probably won't be the same in the future. At the moment, we're on the downside of Cycle 22 with an SSN

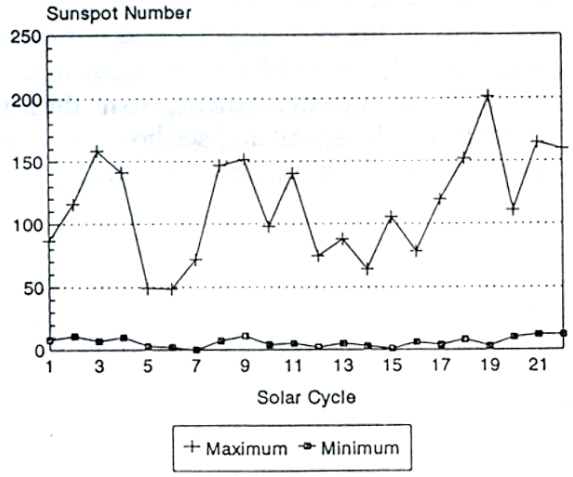

Figure 20.1 Maximum and minimum sunspot numbers for Cycles 1-22.

around 25. Back in September '93, the SSN was 50, at about the maximum level in Cycles 5 and 6, so the LP could review his DX log and see what might be expected if Cycle 23 came in with a maximum SSN of 50 or so. Grim thought.

But even worse would be another maunder minimum, a sunspot drought with SSN less than 20 that lasted about 75 years, from 1640 to 1715. Of course, there is some question about the reliability of the actual sunspot counts back in those times. After all, it was just at the very beginning, telescopes and sunspots being new on the scene. But there are other indications, say almost a total lack of auroral sightings in the period, to support the idea. So that'd be a chilling experience, radio propagation essentially carried out at minimum levels of solar activity.

But think what life would be like on the HF bands without the geomagnetic field. We curse it roundly now when magnetic storms are in progress but when things calm down, we'd be lost without it as it's the vital agent that keeps the F-region in place when the sun goes down. Without it, there'd be the D- and E-regions when the sun is up in the sky and some sort of higher region that would persist somewhat after sunset, until electron-ion recombination reduced the electron density to a low level due to just the ionization from scattered starlight and cosmic rays. As a guess, it'd probably be like the F1-region is now, present in daytime but less of a DXer's choice than the F2-region. In any event, that'd be DXing, pretty much a daytime affair.

While the geomagnetic field is not going to disappear, the Little Pistol should know that it does wander around the globe. A fascinating paper by Fraser-Smith (1987) deals with pole wandering in recent times, the North Pole in the centered-dipole approximation moving from 70° N, 263° E in 1831 to 77.4° N, 257° E in 1984. Since the earth's field controls ionospheric electrons to a large degree, it is not out of the question that, given time, the foF2 maps that we depend on now will have to be redone sometime in the next century, as the pole wandering continues its course.

Of course, there's the whole science of paleomagnetism which gives glimpses of old geomagnetic orientations from magnetism frozen into various artifacts when they solidified

in earlier geological times. Those are extremes that we need not worry about in our lifetimes but are amusing to think about. For example, what would HF propagation be like if the north-seeking pole were located on the International Date Line at the geographic equator. That places the south-seeking pole at the equator and on the Greenwich meridian. So what we now call transpolar propagation to Europe would be transequatorial propagation, geomagnetically speaking, and one can't help but wonder what the cold polar temperatures would do to the chemistry which bears on ionospheric physics. That'll take a while to figure out, maybe to be worked on during a cold, wintry day or two.

Of course, the ultimate historical moment for radio was when Marconi carried out his experiment across the Atlantic in 1901 when the SSN was only 3. That moment and others like it are interesting to contemplate but will not be recreated in real time again. About the best that can be done is to explore propagation in other times using some standardized event or touchstone, making use of what can be done with computers. In that way one wouldn't have to go at the slow pace of real time; instead, with a computer, one could have a model ionosphere to play with, almost like a toy, and satisfy oneself on how it really worked. In that regard, I use the CQ WW DX Contest format in a computer game I devised, SOLAR MAX, and can see how game scores are affected by sunspot numbers, seasons, transmitter powers or QTHs. Some use SOLAR MAX to check out band plans for contests but my interests are more historical in nature and I can make great leaps back in time and space with SOLAR MAX.

In concluding this short section, it is important that some sort of numerical comparison be put forward, a number to use in talking about historical matters. So turning to Figure 4.6, giving critical frequencies at noon and at mid-latitudes as a function of SSN, the Little Pistol could expect about a 30% drop in critical frequencies in Cycle 23 if it came in with a maximum SSN of 50, like Cycles 5 and 6. But at the moment, NOAA and others are not of that mind and are predicting that the next solar maximum will be in March 2000 with a maximum SSN of 108, with an uncertainty in SSN of +/-20. That'd be a bit below the average (111.7) of all the earlier cycles and critical frequencies only about 10% below those in Cycle 22. That's the current prediction so all the Little Pistol has to do is wait and see how accurate it is when the real thing comes around.

21: STATISTICAL CONSIDERATIONS

In the early days of radio, it was a matter of observing the various phenomena as they became evident and trying to find their origin. At the low frequencies first used, day-night effects were immediately apparent and the role of solar illumination, although not fully understood, was deemed important. With the start of ionospheric sounding, a major step forward was taken and the study of radio propagation became more of a science, measures of the ionosphere overhead taken in the course of a day rather than being observed off obliquely, across vast distances and in different directions.

And then there were disruptions — radio storms — and they soon became associated with magnetic disturbances. Since there was a long history connecting terrestrial magnetic activity and solar activity, as given by sunspot counts or measures of the area of sunspots, it should come as no surprise that aspects of radio propagation were explored too, to see whether they were associated with solar activity and if so, how they varied with it.

The critical frequencies — foFe, foF1 and foF2 — of the ionosphere are a case in point. With the introduction of the ionosonde, the vertical structure of the ionosphere was explored and daily variations of the critical frequencies soon found. But those data were not taken on a continuous basis; that would have presented a huge problem, just in the analysis of the data alone. So continuous monitoring was never really attempted and periodic sampling used instead, the critical frequencies observed every hour or sometimes more frequently, depending on the need. But that meant there were gaps in the records of the critical frequencies, nothing really known between samples or, put another way, nothing known on how the critical frequencies varied at time scales shorter than the sampling period.

If critical frequencies of the ionosphere varied little, say from day to day at a given hour, the gaps in the data record would be of little concern and no major causative agent need be found. But that proved not to be the case so there was little recourse at the time but continue with sampling, compiling a data record of critical frequencies and their limits. Causative agents would have to wait until more was known about how the ionosphere worked. Nowadays, we have big words and phrases for that sort of undertaking, building a database, and the contents of the database are described with the language of statistics.

And therein lies a problem as many people are not familiar with that language nor what it means. True, there seems to be a universal feeling for an average, like a batting average in baseball, but outside of that context, there seems to be little appreciation of what goes into an averaging process or other measures of performance, especially what they suggest about the range of variability for future events based on past performance.

There's a worry here and to see what it is for the ionospheric situation, consider the geomagnetic data shown earlier in Figure 19.2. People might take those results for propagation disruptions due to magnetic storminess during Cycle 22 and expect the same to apply in Cycle 23. That would not be unreasonable if they took the larger view and accepted the idea that variations about the average are all part of the picture. But to expect that HF propagation will be the same from one three-month period (the sampling interval) to the next, only disrupted by magnetic storms about 15% of the time, is unrealistic considering the database from which the result was originally derived. There were variations about the average, storminess for as much as 31% or as little as 5% of the time in the three-month periods that made up the record. Those have to be reckoned with.

Critical frequencies foF2 and MUFs are

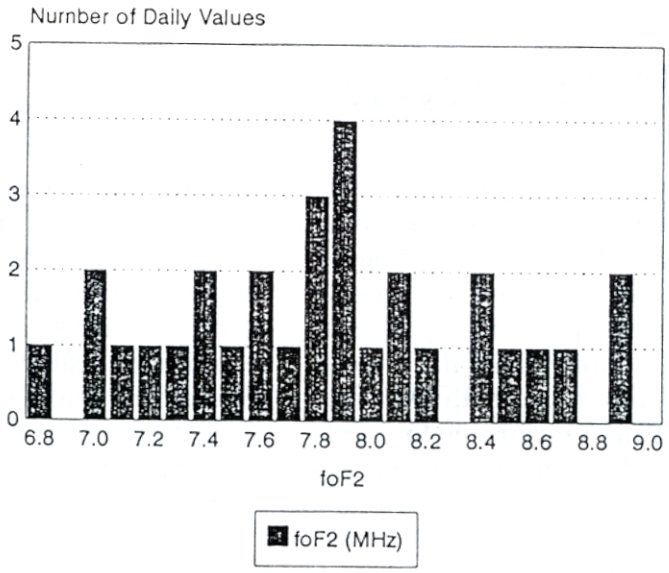

Figure 21.1 Typical foF2 values for a given hour in the 30 days of a month.

other cases in point, discussed earlier in connection with Figure 12.5. To illustrate that idea again, consider the data in Figure 21.1, foF2 values measured at a given hour in the 30 days of a month. The data make up a fairly simple distribution of foF2 values and its median (50%) value is 7.85 MHz. That means that half the data points lie above that value and half lie below it. If that data were used in connection with propagation along a path and the oblique geometry of the path called for the vertical value foF2 to be increased by a factor of 3.5, the median value of the maximum useable frequency (MUF) would be 27.5 MHz. Thus, 50% of the time, the MUF for the path would be above 27.5 MHz and 50% of the time it would be below 27.5 MHz.

The two decile values, marking the top and bottom 10% of the foF2 distribution, are 8.7 MHz, the upper decile value, and 7.0 MHz, the lower decile value. On that basis, 10% of the time the maximum useable frequency for the path would be 30.5 MHz or greater and 10% of the time the maximum useable frequency would be 24.5 MHz or lower in frequency. Another way of saying the same thing might be that for 80% of the time, the maximum useable frequency for the path would lie above 24.5 MHz and below 30.5 MHz.

All that seems fairly straightforward as long as one has the data in sight or in mind. But when it comes to MUF calculations with a propagation program, the Little Pistol does not see the data, much less even think that there was a distribution of foF2 values in the database which the computer uses to predict the MUF value. And therein lies a problem, even two or three.

Taking first things first, say the Little Pistol's propagation program came up with an MUF of 15 MHz for a path to Timbuktu and to his great disappointment, he found the path was closed. What's the problem? If the solar/geophysical scene were quiet, it'd probably just be a case of statistics, the LP not coming to grips with the fact that MUF values are not always the same and have some statistical variation of their own. So chances were that his disappointment was due to the fact that he tried to operate at a time when the real time foF2 value along the path to Timbuktu was significantly below the median value in the propagation program's database.

But there's a nagging question — just how did the Little Pistol come up with the MUF value that was so disappointing? Was his MUF calculation on firm ground or maybe, just maybe, the Little Pistol got a questionable result as he took a 10.7-cm flux value from the daily WWV broadcast and put that in his

propagation program. That'd be a silly thing to do as propagation programs are supposed to convert smoothed 10.7-cm flux values to corresponding smoothed sunspot numbers before making any calculations.

If LP thought about it, a smoothed value involves 13 months of data so the use of a single, daily value of 10.7-cm flux would be a very poor substitute for a smoothed average of 395 separate values. So maybe the LP was disappointed for two reasons, the first for not understanding that any prediction is founded on data with a statistical spread in values, and second, and possibly more importantly, that individual data entries will never give reliable results when smoothed data input is called for.

If the Little Pistol made that mistake, one wonders what prompted him to do it in the first place, a change in the 10.7-cm flux value from one day to the next? But as discussed back in the section on solar data, the 10.7-cm radiation is far from energetic enough itself to affect the ionosphere; it's merely an indicator of active regions on the solar disk so any small changes are of no particular importance. But large changes have meaning, say those shown in Figure 5.1, showing the appearance and disappearance of active regions or real hot spots on the solar disk.

So propagation conditions become a matter of degree, the general level of the solar activity and the sort of conditions to expect being obtained from smoothed indicators, but after that the Little Pistol should think in terms of statistical fluctuations rather than looking for changes in propagation due to any short-term variations.

Looking back now to the beginning of this section and the start of the discussion of statistical aspects of propagation, you'll notice it all started in connection with magnetic disturbances during Cycle 22. That's not exactly big news as it's been known since back in 1937. However, only in the last thirty years or so has it been understood how magnetic activity can influence propagation through changes in the electron populations held on field lines, particularly at the higher latitudes. That's one of the major contributions to propagation studies from the plasma-and-fields era, when the new model of the geomagnetic field came on the scene and took on an important role in understanding more of the relationship between the dynamics of the field and the ionosphere.

The rest of the statistical discussion given above dealt with propagation just as if it were still a matter from the photochemical era, speaking of variations in the critical frequencies foF2 as though changes in solar UV, from active regions coming and going across the solar disk, were all that mattered. As for the other important side of ionospheric matters, the geomagnetic field, while recognized as a causative agent, it is not treated as one nor given the status of a parameter in the database.

That's another way of saying that the solar UV database remains intact and individual critical frequencies used in MUF predictions are not modified because of magnetic activity, whether forecast or in progress. Even if an attempt were made to include it, one of the problems with measures of magnetic activity is that they vary to some extent according to latitude and longitude. Thus, variations of the magnetic elements are much greater in magnitude and more frequent at auroral zone latitudes than middle latitudes. And their algebraic signs may differ, negative excursions in the horizontal component at auroral latitudes at the same time as positive changes at middle latitudes. Thus, while it would be desirable to add magnetic activity as a variable in MUF calculations, the actual choice to be used is not clear; as a result the foF2 databases currently used in MUF work are essentially those for quiet magnetic conditions.

So the scheme largely used now in HF propagation matters is to consider any significant level of magnetic activity as a threat to propagation, affecting it in minor ways until the K-index reaches 4. Any increase in K-index beyond that takes on more serious proportions, depending on whether a minor or major storm is in the offing. For minor storms, propagation would probably be affected adversely for a day or so on the highest HF bands, 21 and 28 MHz, but a major storm could take out the higher bands completely on all but transequatorial

paths for the better part of a week and even have an impact on the 7-MHz band. That being the case, alternatives are sought by transferring activity to the lower bands until the magnetic activity has subsided.

Harking back to the control-point method of calculating MUF values, the threat or possibility of magnetic activity affecting propagation can be added, after the fact, by using a measure like the K-index from a nearby observatory to adjust an overall MUF value. In essence, that approach would add magnetic activity to propagation considerations, not directly as a parameter like sunspot number but as a correction factor, the magnitude approaching a local veto for situations of storm proportion.

Presently, that approach is used by the most recent versions of the MINIPROP PLUS and CAPMAN programs to modify the MUF for a path, stations in the USA using the K-index from the magnetic observatory at Boulder, CO, as broadcast by WWV. Since the K-index changes every three hours, the method is strictly short term when it comes to any changes in MUF predictions. Unfortunately, the details of the method are not well known as the original publication was in a laboratory technical report rather than in the scientific literature.

There is another physical variable which plays a role in HF propagation, the electric field E. In our everyday experience, we are aware of electric fields from meteorological circumstances, static discharges during dry weather or thunderstorm activity. In that setting, charge separation can give rise to potential differences greater than 100,000 Volts. The situation is different in the case of the magnetosphere as it resembles a dynamo, where a moving conductor goes across a magnetic field and drives a current by virtue of its motion. For the earth's magnetosphere, the conducting material is plasma coming from the sun and it moves across the earth's field, giving rise to a potential difference the order of 300,000 Volts across the magnetosphere. In turn, that drives electrical currents which circulate and dissipate energy within the magnetosphere.

While magnetospheric electric fields are mapped along magnetic field lines holding highly conducting material, such fields are not strong enough to be detected near ground level in the presence of fields of meteorological origin. But they are not without their influence, the most notable case being electron bombardment of the atmosphere at auroral latitudes, producing visual displays showing the particle influx and significant ionization above the 100-km level. While not fully understood at the moment, auroral electrons apparently are accelerated by electric fields parallel to geomagnetic field lines, taking them from low energies the order of 1 eV up to tens of keV.

As far as propagation is concerned, the obvious effect would be signal absorption as a result of the additional ionization deposited by the incoming electrons. Since magnetospheric electric fields are not found at ground level, they can hardly be included as parameters in making primary MUF calculations; instead, they play a secondary role in propagation by increasing the absorption of signals going across the auroral zones.

As for a statistical side, there are variations in the occurrence of aurora, the latitude limits of the auroral zone with local time, magnetic activity and the phase of a solar cycle. In that regard, the polar cap is inside the auroral oval and is in the range of latitudes where proton bombardment is fairly uniform during PCA events. Across auroral latitudes, there is a falloff of D-region ionization during PCAs and except for severe geomagnetic disturbances, it does not reach into the middle latitudes.

Polar cap absorption (PCA) is another phenomenon that plays a secondary role in HF propagation. Before getting to its statistical side, we should note that the origin of energetic solar protons is on the sun but when they reach the earth's orbit, their impact on the atmosphere is determined by the state of the geomagnetic field at the time. For example, if a large solar flare accelerates protons to the MeV energy range and they cross interplanetary space to finally arrive at the earth, they are guided, according to energy or momentum, by the earth's magnetic field. If the field were quiet

when the first protons arrived, their impact would be inside a small auroral oval. But later, with a magnetic storm of some severity then in progress, the incoming protons would find a polar cap that's open wider and thus affect the D-region at lower latitudes than before.

Statistically PCA events are not numerous, an event or so per month at solar maximum, but AA events are found frequently during magnetic storms throughout a solar cycle. Both those particle influxes reach the atmosphere and give rise to ionospheric absorption for passing signals but there are differences, protons events going deeper into the atmosphere and producing larger absorption effects, in tens of dB in the HF range, and infrequent in comparison to AA events which produce only a few dB of absorption at the same frequency.

And transpolar paths are rarely able to go across the entire polar cap without a ground reflection and thus, during a PCA event, signal strength may suffer severely because of the absorption along the path coming down to a reflection and rising again through the D-region. That is not the case for AA events as the absorbing region is more narrow and ring-like at auroral latitudes so it is possible for a path to skip over it, the signal being at F-region altitudes in crossing the auroral zone, thus escaping the absorption effects at E-region altitudes.

All in all, there's little reason to think PCA events could be factored into the primary propagation calculations; as a result, they are more like threats to propagation, if predicted, and a grim reality if actually present. Auroral events are less of a problem from the absorption standpoint but may occur during magnetic activity and thus affect critical frequencies rather than signal strength.

The one bright side of PCA events for HF propagation is that they show day/night effects in the ionospheric absorption they produce. That has to do with the fact that, in darkness, ionospheric electrons form negative ions with oxygen molecules and because of having a greater mass, they are far less effective in absorption processes. By way of contrast, auroral absorption does not show a day/night effect as negative ion formation is much less probable above the 100 km level where auroral ionization is deposited.

Everything considered, the two forms of particle influx into the high-latitude ionosphere result in absorption effects, PCA events lasting for days at a time, covering the polar cap, and offer a major obstacle to propagation across high latitude regions. On the other hand, AA events are more frequent but rather restricted in latitude and duration, lasting for hours, and giving rise to absorption events of about 1/4 the magnitude of that for an average PCA event.

While auroral absorption events, originating within the magnetosphere, are found with comparable absorption levels at conjugate regions in the two hemispheres, solar protons which produce PCA events originate from outside the magnetosphere and do not enjoy equal access to the two polar regions. So, in addition, along with their day-night effects, they have a different impact on propagation in the two hemispheres.

By way of example, consider the PCA event of 11 June 1991. It was a major event and produced some 17 dB of absorption of cosmic radio noise on 30 MHz at Thule, Greenland but only 1.5-dB absorption at the Amundsen-Scott Base (South Pole). At the time, Thule was in full sunlight while the South Pole was in darkness. The difference in D-region absorption may be due to differences in access of solar protons to the polar caps via the magnetic field as well as the day/night effect mentioned above. In any event, the difference in absorption between the two hemispheres is striking and, if nothing else intervened, the southern polar cap might have been workable for HF propagation but paths going across the northern polar cap were definitely closed by the PCA event.

22: SOLAR/TERRESTRIAL ENVIRONMENT

The discussion so far has pointed to the factors which affect propagation, the magnitude and variability of their effects. Of necessity, it has been a piecemeal approach, one item discussed at a time. At this point, let's stand back and look at the big picture, as shown in Figure 22.1. Of course, that amounts to something like a snapshot of the solar / terrestrial environment and for that reason, it gives only a two-dimensional representation of the situation and as a snapshot, it only represents one moment in time.

The Little Pistol, on viewing that figure, might be intimidated, thinking that all the forces of Nature are in conspiracy against him in his quest for DX. But those forces are seldom out all at one time. In fact, it took years of work to develop that picture and DXing was going strong all the time. Moreover, it was found that the cast of players was constantly changing, a burst of X-rays this day or a blast in the solar wind that day, and only in direst of circumstances would all those forces be arrayed at once. So even though the Little Pistol knows what lurks out there, he shouldn't approach DXing with any fear or trepidation.

For example, the discussion of magnetic storminess, shown in Figure 19.2, suggested that not only would propagation be good at the peak of a solar cycle, like it was in Cycle 22, but also relatively undisturbed, on average, something like 85% of the time. That might be a bit too optimistic, maybe 75% is a more conservative figure to work with, but it represents a starting point in singling out the cast of players on scene during reasonable propagation conditions.

So for those times and circumstances, a more appropriate version of Figure 22.1 would not show either energetic particles and bursts of X-rays. As a matter of fact, a version of that figure based on the understanding of propagation before WWII would only show the sun, emitting UV radiation, and an atmosphere immersed in a dipole field out at the earth's orbit. The rest of the cast came on stage later.

With time the solar wind and the interplanetary field were found to be constantly "in the act" but with a more complicated geometry than the spirals shown in Figure 22.1. In that regard, the interplanetary field has its origin on the sun and is dragged out by the solar wind, as it evaporates from the sun's corona. Thus, field lines extend out on one side of an

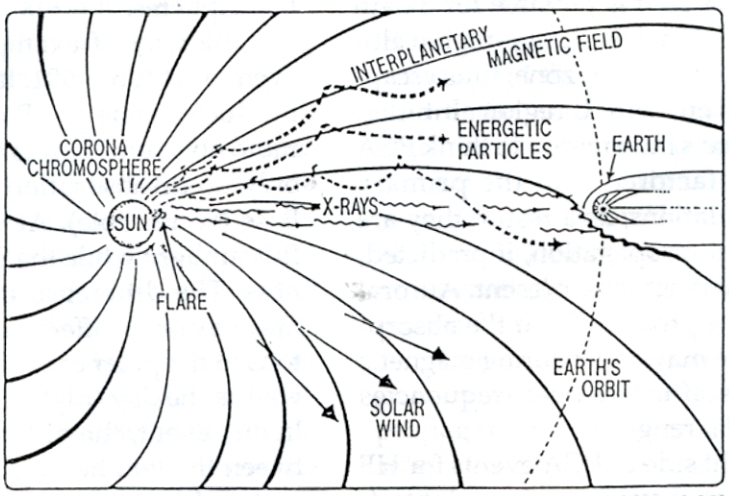

Figure 22.1 Solar/terrestrial environment. From Rosenthal and Hirman [1990]

equatorial surface and return to the sun on the other side, like a simple dipole field.

But with the 27-day solar rotation and variations in the pressure of the solar wind, the equatorial surface is not flat but more like a ballerina's skirt during a pirouette. On that basis, the vector direction of the interplanetary field observed at the earth's orbit depends on whether the earth is above or below the equatorial surface as well as the undulations or waviness of field lines and the surface, as shown in Figure 22.2.

In any event, in that scenario, the pressure of the solar wind compresses the geomagnetic field and the level of ionization in the ionosphere is determined by the solar UV reaching the earth's orbit. The electrons released in the ionosphere are held on magnetic field lines and their spatial organization depends on the spread of UV across the sunlit hemisphere and details of the earth's magnetic field.

For ionospheric purposes, solar UV is global in scope and the primary variable to be concerned about, with activity or the average magnitude of its effects described by the smoothed sunspot number. And for something like 75% of the time, HF communications could be dealt with effectively just by using the smoothed sunspot number, in conjunction with a good foF2 database, in a propagation program.

Other players of solar origin may come on stage from time to time. Those would include bursts of solar X-rays and energetic protons, both in connection with the flare process which takes place above active regions. The flare X-rays are global in scope, just like solar UV, but since the additional ionization they produce then disappears quickly when the flare ends, they are only bit players in the drama. So even though having a global coverage and capable of giving rise to rather dramatic effects, the fact that they are so transient relegates them to a minor status, not even as a secondary variable in radio propagation.

The effects of energetic particles, namely solar protons, have been known for a long time, even before WWII when their terrestrial effects were termed "polar radio blackouts." While the energies of solar X-rays are in the keV range and solar protons in the MeV range, they both penetrate as far as the D-region where ionospheric absorption efficiency is the greatest. The X-rays suffer exponential attenuation by the atmosphere in reaching the D-region while solar protons are lost mainly because of ionizing collisions with atoms and molecules along their range in the atmosphere.

The effects of energetic particles, PCA events, are not global in scope, important only for propagation paths across the polar caps. But while infrequent, the fact their effects may be large in magnitude, reducing HF signals by many dB, and of considerable duration, say days at a time, makes them something to be reckoned with when it comes to propagation, but only at the status of a secondary factor.

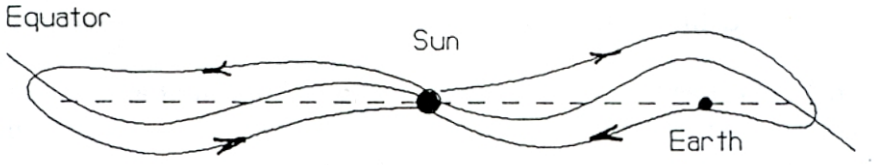

Figure 22.2 Interplanetary field lines near the earth's orbit.

In Figure 22.1, the spiral trajectories of the energetic particles about interplanetary field lines are shown in projection. The size of the spirals depends on the momentum or energy of the particles, less energetic particles following field lines closely. Those circumstances represent possible motions when the interplanetary field is organized or well ordered. During some PCA events, energetic particles arrive promptly at the earth after a flare. That usually takes place when the flare site is located west of the central meridian and the earth is

well connected to the sun by the interplanetary field.

On other occasions, when flare sites are off to the east of central meridian, the flux of energetic particles at the earth's orbit increases more slowly and may give rise to terrestrial effects of longer duration. Those circumstances suggest interplanetary field lines have a waviness or small-scale structure to them and that some energetic particles diffuse or stagger across the field lines. Either way, energetic particles coming from the sun have to be reckoned with but at the secondary disturbance level, not as primary factors in HF propagation.

At this point, it should be noted that both solar X-ray bursts and proton events involve energetic radiation, in the keV and MeV energy range, only minor magnetic effects, if any, result from the ionization created. That is in sharp contrast with geomagnetic disturbances which result from low energy solar plasma, in the eV energy range, reaching the earth's orbit from fast streams out of coronal holes or plasma emerging from coronal mass ejections. The solar plasma from those origins arrives at the earth over a broad region, 10-15 Re across, and may represent a sudden, large power input to the magnetosphere. The ensuing interactions will then start a magnetic storm, modifying the configuration of field lines throughout the magnetosphere.

But the main effect as far as propagation is concerned is ionospheric storming, from critical frequencies foF2 falling sharply because of F-region ionization being carried away into the magnetotail. Another effect would be the further opening of the polar cap, giving greater access to any solar protons coming from the sun and thus expanding the region where a PCA event is in effect. Of course there is also the matter of energization of magnetospheric electrons to auroral energies, up to tens of keV, and their less frequent effects at E-region altitudes, ionization which results in additional refraction and absorption of signals.

All in all, the effects which accompany a magnetic storm are the most important as far as propagation is concerned. They are major effects in that they disrupt the ionosphere at the F-region altitudes instead of down at D-region altitudes, as with solar X-rays or energetic protons. From an operator's standpoint, magnetic storms are a threat to propagation and represent something that must be accepted and worked around when they occur.

Finally, to pull all the discussion together, the Little Pistol would help his cause, DXing to greater fame and glory, by not only being keenly aware of the current solar/terrestrial environment but also following the predictions of professional forecasters, say at NOAA, who have a wide range of current observations to draw on. While the numbers from WWV broadcasts, or log charts from them, make good conversation, they really won't help much without additional input. So the Little Pistol needs to know where he is in the solar cycle, something of the recent solar and geophysical activity, even about disturbances, and what is predicted for the immediate future.

A first step in that direction would be to follow the information published by NOAA/SESC in the weekly Boulder Report. That does include weekly updates of the twenty-seven day outlook for magnetic activity, an important item, but more often than not, the report is held up in the mail for several days, reducing the immediate value of that information. Of course the narrative text, giving highlights and forecasts of solar and geomagnetic activity, is important and valuable, too, especially any mention of effects from coronal holes or coronal mass ejections.

But the very best thing for the Little Pistol to do is check in with the NOAA PBBS and download both the Solar and Propagation Reports. As mentioned earlier, it is relatively inexpensive to obtain all that data on a daily basis and that makes for more effective planning when it comes to DXing, either new ones or DXpeditions coming on station.

Of course a full-service propagation program is a must for primary planning purposes. The information from Boulder will give the secondary information needed to anticipate magnetic disturbances. A graphic aid, with a map display and terminator, is of great help, especially in seeing where a path goes and if it

would be in harm's way during any type of solar/terrestrial disturbance.

With the above approach, the Little Pistol will surely advance on the ladder toward the DXCC Honor Roll, hopefully at a more rapid pace from his better understanding of the solar/terrestrial environment and with all the aids at his disposal. But the Little Pistol should not forget that solar activity and all that goes with it are renewable resources, coming back again every 11 years. We don't even have to recycle solar activity; it cycles itself, again and again. If the Little Pistol wants to play that game, it's in his best interest to understand how it works and then play with all the skill he can muster. But the good part is that if he doesn't make the DXCC Honor Roll during this solar cycle, there'll surely be another one before too long and he can pick up where he left off.

So the fact that the sun renews itself and, in the process, it can reinvigorate us is exciting to contemplate. I'd hope that the Little Pistol would see the marvel and mystery in it all. More than anything else, however, I'd hope that he understands DXing is an intellectual pursuit, worth thinking hard about and working at just for the pure joy of it. If he does that, all the time and effort I've put in this book will be worth it.

23: HF PROPAGATION IN A NUTSHELL

This chapter is for those readers who want to hear the "answer" before thinking about the "question." Either they're devoted to detective stories or the popular "answer and question show" on TV, Jeopardy. So in what follows will be a summary, terse statements without too much in the way of explanation, just what's important and how propagation really works. It can be read with amusement, puzzlement and profit by all.

But first, we have to lay the groundwork. So to begin, it all goes back to the sun emitting ultraviolet light and X-rays while spewing out streams of ionized matter, largely protons and electrons. The UV and X-rays make it to Earth in 500 seconds flight time and come more or less continuously while the streams of charged matter, solar plasma, may vary considerably in their flow but travel at about 400 km/sec instead of 300,000 km/sec, as is the case for the UV and X-rays. And all that, solar photons and plasma, reach earth at a distance of 150,000,000 km from the sun.

The earth is one of the terrestrial planets, with an atmosphere and a magnetic field. The atmosphere is well mixed up to an altitude of about 90 km, consisting mainly of nitrogen and oxygen molecules. While solar X-rays penetrate below 90 km and ionize some of those molecules, at higher altitudes solar UV modifies the chemical nature of the atmosphere by photodissociation. Thus, oxygen atoms begin to appear above 90 km from the dissociation of oxygen molecules and solar UV ionizes them as well as the oxygen and nitrogen molecules. The positive ions and electrons released in that fashion go to make the ionosphere.

The flux of ionizing radiation from the sun varies slowly with solar activity and ionization of the earth's atmosphere takes place continuously, the distribution of ionizing processes over the sunlit portion of the earth essentially fixed along the earth/sun line. But atmosphere close to the earth, being thin and without tremendous inertia like the oceans, co-rotates with the earth. As a result, fresh atmospheric material rotates into solar view at dawn, then is carried past the noon meridian and finally out of solar view at dusk.

The electron density which results at ionospheric heights is due to a competition between production, mainly from photoionization by solar UV, and loss of ionization, by recombination of electrons with positive ions and transport processes. The electron density shows some structure from chemical changes with increasing altitude, distinct regions and finally a peak, before disappearing slowly at great altitudes.

The D-region is the lowest, having an electron density on the order of a thousand electrons per cubic centimeter in the range 60-90 km during the day and vanishing at night. The E-region is something like a ledge, with an electron density on the order of 50,000 electrons per cubic centimeter during daytime and remaining fairly constant for several kilometers around 110 km height. This is the region where atomic oxygen and its positive ion start to become important. The F-region, on the other hand, up around 300 km, contains on the order of a million electrons per cubic centimeter and decays slowly at night.

The spatial distribution of ionization is controlled by the earth's magnetic field as electrons, on being released by solar UV, are constrained in their motion, gyrating around the field lines instead of flying off freely on ballistic trajectories. Thus, ionospheric data is better organized in terms of geomagnetic coordinates than geographic coordinates. In addition, there are significant features of geomagnetic origin in the global distribution of electrons over the ionosphere as well as temporary distortions of the distribution from the effects of geomagnetic storms.

That's a fairly concise summary of what the quiet ionosphere is like and how it is being

created constantly by solar UV. Just how it really works and what disturbs it are other subjects. Unfortunately, not everybody in Amateur Radio is interested in those matters, being willing to bumble along without much understanding. In some ways they're like joggers who suit up, go to the front door and dash out into the elements, not even paying attention to the season or the weather. Of course there are better ways of doing things and that's what this discussion is all about.

First it should be understood that the ionosphere is a three-dimensional distribution of ionization, electrons and positive ions. At the outset the details of how the ionization is distributed are really not so important for us, merely that it is possible to map it out across the globe and then use those ionospheric maps as well as some basic knowledge to understand, even predict, propagation.

On that subject, radio propagation is nothing but the paths followed by electromagnetic waves that are trapped below the peak of the ionosphere. But with high enough frequency or launch angle above the horizon, radio waves can penetrate the F-region peak and pass through the top side of the F-region. That can lead to positive results when a satellite is on the receiving end, or a negative result, when the radio waves are simply lost into space and nothing is accomplished.

During daytime the lowest parts of the ionosphere (D- and E-region) limit propagation of waves with frequencies below 10 MHz to local contacts and those bands are used then largely for ragchewing and local emergency traffic. In short, the lower bands are not very useful for DXing when paths are sunlit.

In the absence of solar illumination, the D- and E-regions disappear and nighttime propagation on the lower bands, say 3.5 MHz and 7 MHz is limited primarily by band congestion and noise, of atmospheric origin or from man-made sources. Put another way, even at solar minimum there will be enough ionization in the F-region to support DXing on those bands as long as no portion of a path is in sunlight. But the ugly villain, noise, propagates across dark paths, too, and must be reckoned with.

At the top of the HF spectrum, say on the 24-MHz or 28-MHz bands, propagation depends more on the level of solar activity as ionospheric absorption is much less there, varying as the inverse square of the frequency. As a result, at high levels of solar activity, the pursuit of DX on those frequencies is quite feasible on paths which are sunlit and then it becomes a question of finding when the MUF on a path is above the chosen operating frequency. And in going from 3.5 MHz to 28 MHz, man-made noise falls by 25 dB so that is less of a factor than on the lowest band. But at low levels of solar activity, toward solar minimum, DXing on those bands is limited largely to low-latitude and transequatorial paths.

The middle of the HF spectrum, say from 10 MHz to 21 MHz, is what might be termed a "transition region" as all three factors which make for success in DXing —open bands, strong signals, weak noise —are at risk. In short, for frequencies in the middle of the HF spectrum, DX paths must be less exposed to solar illumination and that means in the course of a day, MUFs on paths of interest may fall below the operating frequency more often. Of course, noise is always a concern, at one end of a path or the other.

The 14-MHz and 21-MHz bands seem to have the greatest activity when it comes to DXing, especially before and after solar maximum, and support the full range of paths across the globe. Given the degree of congestion on those bands, success in DXing requires that operating times be chosen carefully, especially with regard to solar/terrestrial conditions and the sociological factors which make the bands more congested.

All of that discussion was more specific as far as how the ionosphere works but rather qualitative in other respects, just a few of the relevant quantities given, say ionospheric heights and some typical electron densities. And nothing was mentioned as to how it would be disturbed although it should come as no surprise that the sun will be tracked down ultimately as the origin of the disturbances. That

makes for an interesting situation where the source of the ionosphere and its disturbing agent are one and the same.

In proceeding in the discussion of how the ionosphere is formed and disturbed (or deformed), questions and distinctions involving energy come up — first, solar UV photons with about 10 electron-Volts or 10 eV of energy creating the ionosphere by ionizing the atoms and molecules in the atmosphere and then disturbances of the ionosphere resulting from bursts of solar X-rays with energies around 1,000 eV, (1 keV), or solar protons with energies greater than 1,000,000 eV, (1 MeV).

But instead of those energetic bursts being the most frequent factors in ionospheric disturbances, it turns out the puffs and blasts of plasma in the solar wind give rise to the greatest problems in propagation. On those occasions, the dynamic interaction of solar plasma with the geomagnetic field reshapes the field, effectively removing ionization from the lower ionosphere and then inhibiting propagation. In terms of energy, the power input of solar plasma to the earth is huge and leads to a mechanism, still not fully understood, by which electrons of solar origin, with about 1 eV in energy, are raised to energies like 10 keV in auroral displays, all within the confines of the geomagnetic field.

While propagation can be characterized as good or bad, with all shades in between, it is better described as being normal (N), fair (U) or poor (W), as done in Propagation Reports from the NOAA PBBS. At this QTH, the last two abbreviations are taken to mean "Ugly" and "Wretched," typical of conditions found during minor and major magnetic storms, respectively. But for practical purposes, the question is not so much about how bad propagation conditions can become but how often are they in bad shape or how long the disturbances will last. In that regard, the good news is that normal propagation conditions can be expected 75%-85% of the time. But there are variations within events, some major storms disrupting the upper bands for days at a time while minor storms can be brief, lasting a day or less.

It's in those normal, calmer periods that most amateurs do their DXing and the problem then becomes one of finding the most efficient or effective way of going about it. But, residing in the USA, even a casual glance at an azimuthal equidistant map should make it clear to any operator that a good part of the time DXing will involve trying to get signals across the polar cap to DX stations on the other side of the globe.

Given that, whether one can chase DX on a given day or not depends on the state of affairs at high magnetic latitudes. So a weather eye should be cocked in the direction of the sun, watching for signs of trouble. Light, traveling faster than solar plasma, can give optical signatures which signal or warn of solar disturbances to come. Knowing what to expect and when to expect it turn out to be factors which contribute to greater effectiveness in amateur operations, in general, and DXing, in particular, minimizing time wasted on dead or dying bands. That's where the information in the Solar and Propagation Reports from NOAA PBBS is extremely helpful.

Now having said that about avoiding times of disturbance, the question becomes how to make the most of normal conditions. For that operations must be supported by several things: (1) a global database for critical frequencies, by smoothed sunspot number, seasons and time, (2) a full-service computer program to use the database, giving information on MUFs, signal strengths (easily converted to S-Units) and noise, atmospheric or manmade, (3) a source of reliable data and current information on solar/terrestrial conditions, and (4) an understanding of the various aspects of HF propagation, say paths across the polar regions or the geomagnetic equator as well as long-path propagation.

The first two supporting items are fairly easy to come by and the third one is a matter of choice, either basing one's operations on a minimal input of information and trusting to luck or using the options available from NOAA to make a more refined approach to propagation and DXing. In any event, it is important to have an awareness of the general level of solar activity and recent solar/

terrestrial events and conditions.

The last item on that list takes time and is obtained largely by on-the-air experience, supplemented by output from the propagation program in use. Thus, everyone has some feeling when the JAs are coming through but what about the JTs? That'll take a bit of study, looking for times when those signals would be readable, over the local noise level.

And then there's the matter of sharpshooting, getting ready for a rare one like the 3Y0PI operation in February '94. There are several ways of preparing for operations like that, DX well off the beaten track. First there's the matter of beam heading. That's easy. Then there's the matter of the MUF, also known as "mode availability." That can be obtained from knowledge of the E- and F-regions but has nothing to do with signal strength or signal/noise ratios. Both those are determined, in part, by absorption processes in the D-region and can be obtained by calculations of "path reliability." That's interesting but to plan times for operation would require going back and forth between them, availability and reliability, keeping track of which is high and which is low, etc. It's easier to work out a new quantity that's termed "DX feasibility," which simply combines the two probabilities into one; from that probability, a plan of action becomes pretty obvious. Of course, a quick review of mob psychology would help too.

Since the possibilities are infinite when it comes to DX and propagation, this discussion could go on forever. But one thing would be missing, figures or curves which illustrate the ideas and carry far greater meaning than just a few words. In that regard, the chapters of this book contain more than 80 figures. So maybe it's time to add music to the words of this theme, starting at the beginning and working through the fuller discussion that has been put together for the benefit of your friend and mine, the Little Pistol. So turn to it!

REFERENCES

Akasofu, S.I., Dynamics of the Magnetosphere, Proceedings of the Chapman Conference, D. Reidel Publishing Co., Dordrect, Holland, 1978.

Anari, Z.A., The Aurorally Associated Absorption of Cosmic Radio Noise at College, Alaska, J. Geophys. Res. Vol. 69, p. 4493, 1964.

ARRL Handbook for Radio Amateurs, American Radio Relay League, Newington, CT, 1994.

ASAPS, Advanced Stand Alone Prediction System, IPS Radio and Space Services, Australia, 1992.

Basler, R., Radio Wave Propagation in the Auroral Ionosphere, J. Geophys. Res. Vol. 68, p. 4665, 1963.

Brown, R.R., Long-Path Propagation, A Study of Long-Path Propagation in Solar Cycle 22, Anacortes, WA, 1992.

Brown, R.R. and J.R. Barcus, Day-Night Ratio for Auroral Absorption Events Associated with Negative Magnetic Bays, J. Geophys. Res. Vol. 68, p. 4175, 1963.

Chapman, S. and J. Bartels, Geomagnetism, Vols. 1 and 2, Oxford University Press, New York, 1940.

Davies, K., Ionospheric Radio Propagation, U.S. Department of Commerce U.S. National Bureau of Standards, Monograph 80, Washington, D.C., 1965.

Davies, K., Ionospheric Radio, Peter Perigrinus Ltd., London, 1990.

Davies, K. and C.M. Rush, High-Frequency Ray Paths for Ionospheric Layers with Horizontal Gradients, Radio Sci., 20, p. 95-110, 1985.

Fraser-Smith, A.C., Centered; and Eccentric Geomagnetic Dipoles, 1600-1985, J. Geophys. Res. Vol. 25, No. 1, p. 1-16, 1987.

Fricker, R., H.F. Propagation, A Microcomputer Method for Predicting the Field Strength of H.F. Broadcast Transmissions, BBC External Services, Engineering, London, England, 1988.

Handwerker, J., IONSOUND, An Ionospheric Propagation Prediction Program for IBM PC's and Compatibles, Lexington, MA, 1994.

Leftin, M., Ionospheric Predictions, Telecommunications Research and Engineering Report, Vol. 1-4, Institute of Telecommunications Sciences, Boulder, CO, 1971.

Leinbach, H. and R.P. Basler, Ionospheric Absorption of Cosmic Radio Noise at Magnetically Conjugate Auroral Zone Locations, J. Geophys. Res. Vol. 68, p. 3375, 1963.

Lucas, D., CAPMAN, Computer Assisted Prediction Manager, Boulder, CO, 1994.

McNamara, L. F., Radio Amateurs Guide to the Ionosphere, Krieger Publishing Co., Melbourne, FL, 1994.

Norton, R.B., The Middle-Latitude F-region during Some Severe Ionospheric Storms, Proc. IEEE, Vol. 57, p. 1147, 1969.

Oler, C., SKYCOM, High Frequency Ionospheric Signal Analyst, Solar Terrestrial Dispatch, Stirling, Alberta, Canada, 1994.

Piggott, W.R. and K. Rawer, URSI Handbook of Ionogram Interpretation and Reduction, Report UAG-50, World Data Center A for Solar-Terrestrial Physics, Boulder, CO, 1975.

Rosenthal, D.A. and J.W. Hirman, A Radio-Frequency Users Guide to the Space Environment Services Geophysical Alert Broadcasts, NOAA Technical Memorandum, ERL SEL-80, Space Environment Laboratory, Boulder, CO, June 1990.

Shallon, S., MINIPROP, An HF Propagation Prediction Program, Los Angeles, CA, 1994.

Snyder, W.F. and C.L. Bragaw, Achievement in Radio, Seventy Years of Radio Science, Technology, Standards and Measurement at the National Bureau of Standards, National Bureau of Standards, Boulder, CO, October 1986.

Teters, L.R., J.L. Lloyd, G.W. Haydon and D.L. Lucas, IONCAP, Ionospheric Communications Analysis and Prediction Program, U.S. Department of Commerce, Washington, D.C., 1983.

PROPAGATION AIDS

DXAid by Peter Oldfield, 251 Chemin Beaulne, Piedmont, Quebec J0R 1K0

DX Edge from Xantek, Inc., P.O. Box 834, Madison Square Station, New York, NY 10159

Geoclock by Joseph Ahlgren, 2218 N. Tuckahoe St., Arlington, VA 22205

NEEDS TO BE RENUMBERED WHEN PAGES ARE FIXED

SUBJECT INDEX

Worldradio
BOOKS

P.O. Box 189490, Sacramento, CA 95818